REPORT DOCUMENTATION PAGE

Form Approved
OMB No. 0704-0188

1. AGENCY USE ONLY (Leave blank)	2. REPORT DATE	3. REPORT TYPE AND DATES COVERED
	1/10/95	Final - 12/1/93 - 11/30/94

4. TITLE AND SUBTITLE

Chua's Circuits: Phenomena and Applications

5. FUNDING NUMBERS

N00014-94-1-0308

6. AUTHOR(S)

Professor Leon O. Chua

7. PERFORMING ORGANIZATION NAME(S) AND ADDRESS(ES)

Regents of the University of California
c/o Sponsored Projects Office
336 Sproul Hall
Berkeley, CA 94720-5940

8. PERFORMING ORGANIZATION REPORT NUMBER

442427-25832

9. SPONSORING/MONITORING AGENCY NAME(S) AND ADDRESS(ES)

Office of Naval Research
Ballston Tower One
800 North Quincy Street
Arlington, VA 22217-5660

10. SPONSORING/MONITORING AGENCY REPORT NUMBER

11. SUPPLEMENTARY NOTES

n/a

12a. DISTRIBUTION/AVAILABILITY STATEMENT

Approved for Public Release
Distribution Unlimited

12b. DISTRIBUTION CODE

13. ABSTRACT *(Maximum 200 words)*

A workshop on Chua's Circuit: Chaotic Phenomena and Applications was held December 7, 1993 in conjunction with the 1993 International Symposium on Nonlinear Theory and its Applications (NOLTA 93), Honolulu, Hawaii.

14. SUBJECT TERMS	15. NUMBER OF PAGES
	16. PRICE CODE

17. SECURITY CLASSIFICATION OF REPORT	18. SECURITY CLASSIFICATION OF THIS PAGE	19. SECURITY CLASSIFICATION OF ABSTRACT	20. LIMITATION OF ABSTRACT

1993 International Symposium on
Nonlinear Theory and its Applications

Sheraton Waikiki Hotel, HAWAII
December 5 - 10, 1993

PROCEEDINGS

WORKSHOPS

Organizers:
Research Society of Nonlinear Theory and its Applications, IEICE
Dept. of Elect. Engr., Univ. of Hawaii
Sponsor:
Research Society of Nonlinear Theory and its Applications, IEICE
Cosponsors:
The Telecommunications Advancement Foundation (TAF)
International Communications Foundation (ICF)
In cooperation with:
IEEE Hawaii Section
IEEE Circuits and Systems Society
IEEE Neural Networks Council
International Neural Network Society
IEEE CAS Technical Committee on Nonlinear Circuits and Systems
Technical Group of Nonlinear Problems, IEICE
Technical Group of Circuits and Systems, IEICE

PART 2

Workshop on Chua's Circuit: Chaotic Phenomena and Applications

Session Chairman
Dr. Rabinder N. Madan
U.S. Office of Naval Research
Electronics Division

December 7, 1993

MORNING SESSION

COFFEE BREAK

1993 International Symposium on Nonlinear
Theory and Its Applications (NOLTA '93)
Hawaii, U.S.A., December 5-10, 1993

Chua's Circuit: Ten Years Later

L. O. Chua

University of California, Berkeley
Department of Electrical Engineering and Computer Sciences, Berkeley, CA 94720

Abstract

More than 150 papers, two special issues (Journal of Circuits, Systems, and Computers, March, June, 1993), and a book (Edited by R. N. Madan, World Scientific, 1993) on Chua's circuit have been published since its inception a decade ago. This review paper attempts to present an overview of these publications and to identify some milestones of this very active research area.

An important milestone is the recent fabrication of a *monolithic* Chua's circuit. The robustness of this IC chip demonstrates that an array of Chua's circuits can also be fabricated into a monolithic chip, thereby opening the floodgate to many unconventional applications in information technology, synergetics, and even music.

The second milestone is the recent global unfolding of Chua's circuit by adding a linear resistor in series with the inductor to obtain a *canonical* Chua's circuit – now generally referred to as *Chua's oscillator*. This circuit is most significant because it is structurally the *simplest* (it contain only 6 circuit elements) but dynamically the *most complex* among all nonlinear circuits and systems described by a 21-parameter family of continuous odd-symmetric piecewise-linear vector fields.

The third milestone is the recent discovery of *stochastic resonance*, *chaos-chaos type intermittency*, and $\frac{1}{f}$ *noise spectrum* in Chua's circuit. These new phenomena could have far-reaching theoretical and practical significance.

The fourth milestone is the theoretical and experimental demonstration that Chua's circuit can be easily *controlled* from a chaotic regime to a prescribed periodic or constant orbit, or it can be *synchronized* with 2 or more identical Chua's circuits, operating in a chaotic regime. These recent breakthroughs have ushered in a new era where *chaos* is deliberately created and exploited for unconventional applications, e.g., secure communication.

1 BRIEF HISTORY OF EVOLUTION

Prior to 1983, no autonomous electronic circuit was known to be chaotic, in spite of numerous attempts by researchers to uncover such examples. In particular, Matsumoto and his students had struggled for years to build an electronic circuit analog of the Lorenz Equation. The history of how Matsumoto's heart-breaking failure had spurred the author to design a chaotic circuit from first principles was described vividly in[1]. Here, we only outline the chronological events, which began in the fall of 1983, where this chaotic circuit was designed by the author, using a systematic nonlinear circuit synthesis technique. After describing his design to Matsumoto and instructing him on how to choose the circuit parameters for a possible chaotic regime, the author's involvement in this circuit was abruptly interrupted for over a year due to illness.

Having no prior experimental background, Matsumoto uses computer simulation to verify that the author's circuit, which he had named *Chua's Circuit*, is indeed chaotic[2]. Meanwhile, Matsumoto and his students had followed the author's suggestion to modify Rosenthal's circuit [3] in order to obtain an active 2-terminal *nonlinear resistor* with the desired piecewise-linear characteristic. [1] Handicapped by Matsumoto's lack of experience in nonlinear electronic circuits, it took two years before his student Tokumasu finally succeeded in 1986 to adapt Rosenthal's circuit to obtain the desired nonlinearity [4]. [2]

[1] From his hospital bed in Tokyo, the author had communicated to Matsumoto on the possibility of using Rosenthal's circuit as the basis for designing the desired nonlinearity.

[2] Although neither acknowledged nor referenced in [4], the core of the resulting 2-transistor circuit is essentially Rosenthal's circuit.

Meanwhile, using the op-amp circuit synthesis technique proposed by the author, Zhong and Ayrom[5] had succeeded to build a 2 op-amp Chua's circuit where chaos was first observed *experimentally* during the winter of 1984. Their experimental confirmation of chaos was published in January 1985, one month after Matsumoto's publication in December 1984 of his *computer observation* of chaos in Chua's Circuit [2].

The most robust and economical method to hook up an experimental Chua's circuit is given in [6, 7]. In this setup, the nonlinear resistor, called *Chua's diode* by Kennedy[7], is realized by a single IC package (containing two op amps) and 6 linear resistors. The entire setup can be easily hooked up in 30 minutes for less than $ 10. Because of its low cost and robustness, Chua's circuit has become the circuit of choice in applications where an inexpensive and robust source of chaotic signals is required.

For mass applications, it would be desirable to have the Chua's diode integrated into an IC chip. This has been achieved using a 2-μm CMOS process, with 39 CMOS transistors occupying a chip area of 0.5 mm^2 [8]. More recently, the *entire* Chua's circuit has been successfully integrated into a *monolithic* chip via two different designs [9, 10], the photomicrograph of one of which is shown in Fig. 1. This latest evolution represents a milestone in the ever-widening studies and exploitation of Chua's circuits because it demonstrates that an entire array of closely matched Chua's circuits can be fabricated in monolithic form.

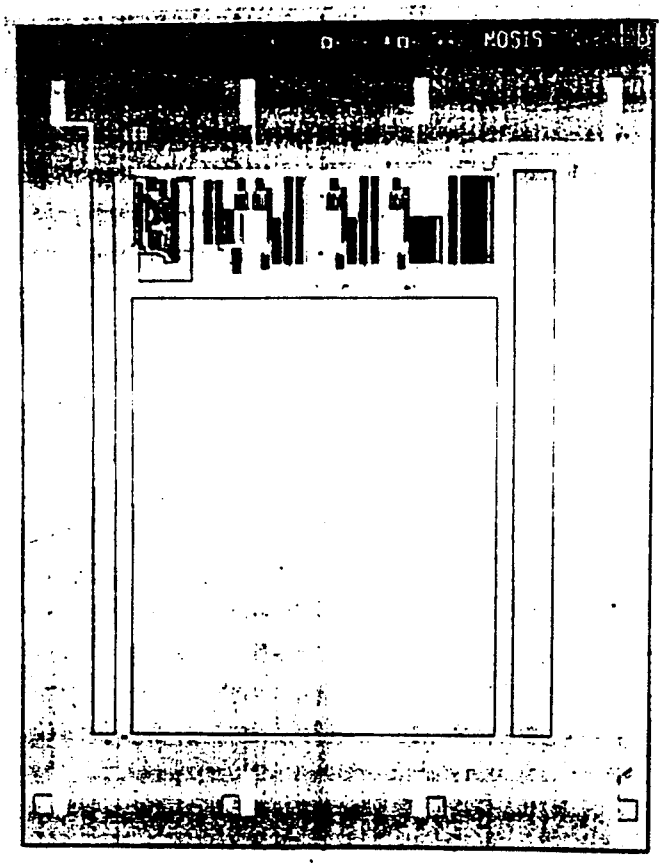

Figure 1: Photomicrograph of the monolithic Chua's circuit described in [8].

2 GENERALIZATIONS OF CHUA'S DIODE

The original piecewise-linear characteristic of Chua's diode has been generalized by many researchers to assume various different forms. For example, the original piecewise-linear function is replaced by a *discontinuous* function in [11], a C^∞ "sigmoid function" in [12], and a cubic polynomial $f(x) = c_0 x + c_1 x^3$ in [13], [14], and [15]. The main motivation for choosing a "smooth" rather than "piecewise-linear" function for Chua's diode is to obtain a smooth state equation so that analytical tools from nonlinear dynamics can be brought to bear.

In some applications, the symmetry in the Chua's diode $v-i$ characteristic is deliberately broken in order to allow nonlinear wave propagations in a chain of Chua's circuits [16], or in a Chua's circuit terminated by a transmission line [17]. The symmetry can be broken either by shifting the origin, or changing the shape, of the characteristic.

In yet another application, the number of segments of the original piecewise-linear characteristic of Chua's diode is increased in order to synthesize strange attractors with multiple scrolls [18].

3 GENERALIZATIONS TO HIGHER-DIMENSIONS

In order to investigate chaotic dynamics and new phenomena in higher-dimensional spaces, Chua's circuit has been generalized by replacing the resonant tank circuit by an RLC ladder circuit in [19], by a coaxial cable in [20], and by a lossless transmission line terminated in a short circuit in [17]. The dynamics in the latter case is described by 2 *linear* partial differential equations with a *nonlinear* boundary condition. However, in the limiting case where the capacitance C_1 across Chua's diode tends to zero, the partial differential equations reduces to a 1-dimensional map with a time delay, which makes it analytically tractable. A further generalization of Chua's circuit to a Banach Space is given in [21].

Another direction of generalization consists of a *chain* [16], [22], or an *array* [23], [24] of Chua's circuits. This generalization leads to a system of nonlinear *ordinary* differential equations which has the same form on the right hand side as that of a system of nonlinear *reaction-diffusion partial* differential equations. Consequently, the currently very active research areas of "spiral wave", "Turing patterns", and "spatio-temporal chaos" can all be studied by an array of Chua's circuits. Moreover, the signals extracted from such an array have many potential applications.

4 GENERALIZATIONS TO CHUA'S CIRCUIT FAMILY

The theory[3] developed in [25] for investigating the dynamics of Chua's circuit is actually applicable to any family $\mathcal{C}$ of *continuous, odd-symmetric piecewise-linear vector fields* in $\mathcal{R}^3$. partitioned by two parallel planes U_1 and U_{-1} (of arbitrary orientation) into an inner region D_0 and two outer regions D_1 and D_{-1}, respectively. Any member of $\mathcal{C}$ is described by[4]

$$\begin{aligned} \dot{\mathbf{x}} &= \mathbf{A}\,\mathbf{x} + \mathbf{b}, & x_1 \geq 1 \\ &= \mathbf{A}_0\,\mathbf{x}, & -1 \leq x_1 \leq 1 \\ &= \mathbf{A}\,\mathbf{x} - \mathbf{b}, & x_1 \leq -1 \end{aligned}$$

[3] As a compromise for departing from Matsumoto's previous tradition of placing his name first in all publications involving Chua's circuit, the authors in this paper have been reordered *alphabetically*. Indeed, most of the results in this paper is developed by Komuro.

[4] We would like to take this opportunity to correct the following equations in [26].

where

$$\mathbf{A} = \begin{bmatrix} a_{11} & a_{12} & a_{13} \\ a_{21} & a_{22} & a_{23} \\ a_{31} & a_{32} & a_{33} \end{bmatrix}, \qquad \mathbf{b} = \begin{bmatrix} b_1 \\ b_2 \\ b_3 \end{bmatrix}$$

defines an *affine* vector field in the outer regions D_1 and D_{-1}, and

$$\mathbf{A}_0 = \begin{bmatrix} \alpha_{11} & \alpha_{12} & \alpha_{13} \\ \alpha_{21} & \alpha_{22} & \alpha_{23} \\ \alpha_{31} & \alpha_{32} & \alpha_{33} \end{bmatrix}$$

defines a *linear* vector field in the inner region D_0.

Using the nonlinear state equation synthesis technique developed in [27, 28], any member of this 21-parameter family of vector fields can be synthesized by a circuit using one Chua's diode and linear resistive elements, including controlled sources. The basic structure of this circuit family is summarized in Fig.14, page 1031, of Wu'paper [29]. In Wu's Fig.14, the Chua's diode is fixed to be a *passive* element, made of two ideal back-to-back Zener diodes connected in parallel across a linear passive resistor. In this case, the linear resistive 4-port N must contain at least one *negative* resistor or controlled source. By using standard circuit transformation techniques, one can choose N to be passive and transfer the activity requirement into Chua's diode. Indeed, once the 21 parameters defining $\mathbf{A}$, $\mathbf{A}_0$, and $\mathbf{b}$ are given, much simpler circuits equivalent to that of Fig.14 can be synthesized. In the *simplest* case, only 4 circuit elements are needed; namely, 2 capacitors, 1 inductor, and a Chua's diode with an appropriate $v - i$ characteristic. One such circuit, [5] synthesized, built, and analyzed by Tokunaga [30], has a strange attractor which is spawned by the breakdown of a torus. A detailed analysis of this member of Chua's circuit family shows that the complicated bifurcation phenomena follows the scenarios predicted by the Afraimovich-Shil'nikov torus breakdown theorem [31].

Many other members of Chua's circuit family have been synthesized and built [32, 33, 34, 35]. Except for the circuit reported in [35], the dynamics of the above cited circuits, including the original Chua's circuit, are not sufficiently general in the sense that certain phenomenon observed from one such member of Chua's circuit family can *not* be observed from another member, regardless of the choice of circuit parameters. From the nonlinear circuit foundation point of view, it is highly desirable to synthesize the *simplest* circuit topology which is capable of reproducing the *qualitative* phenomena exhibited by *every* member of Chua's circuit family. The circuit structure provided by Fig.14 of Wu [29] has this property but it is not the *simplest* in the sense that there exist circuits with fewer number of circuit elements that are also endowed with this property. In fact, the circuit reported in [35] is one (among several others) such circuit and is therefore said to be *canonical* because no circuit having fewer number of elements has this property.

Among several equivalent *canonical* Chua's circuits, Dr. Madan, guest editor of 2 recent special issues on Chua's circuit [36, 37], has chosen the globally unfolded Chua's circuit [26] – obtained by adding a *linear resistor* R_0 in series with the inductor – as the standard bearer of the name *canonical*, and had named it *Chua's Oscillator* to distinguish it from the original Chua's circuit. Dr. Madan chose this augmented circuit as canonical not only because Chua's oscillator reduces to Chua's Circuit upon setting the linear resistor R_0 to zero, but also because all recent publications on canonical Chua's circuit are already based on the Chua's oscillator [24, 26, 38, 39, 40, 41, 42, 43, 44, 45]. From the theoretical point-of-view, the significance of Chua's oscillator is fully analyzed in [26, 44]. Here, we simply paraphrase the main result succintly as follows:

[5] The content of this paper is due almost exclusively to Tokunaga.

Significance of Chua's Oscillator
Chua's oscillator is ***structurely*** the ***simplest*** and ***dynamically*** the ***most complex*** member of the Chua's circuit family.

It is the simplest circuit because no circuit with fewer number of circuit elements is as general. It is the most complex because no circuit belonging to the Chua's circuit family exhibits more complex dynamics.

The significance of the Chua's oscillator transcends beyond nonlinear circuit theory. Indeed, there are many publications involving *systems* which are *not* circuits but which are also described by Equations (1)-(4), e.g., [46, 47, 48, 49, 50]

No longer is it necessary for beginners in nonlinear dynamics to study all of these seemingly unrelated papers, along with their diverse notations and jargons. Instead, since *nothing* new can be learned that is not already included as special cases of the dynamics endowed upon Chua's oscillator, the researchers need only obtain an in-depth understanding of the nonlinear dynamics and bifurcation phenomena of this single circuit. In short, Chua's oscillator has unified the nonlinear dynamics of the entire 21-parameter family of piecewise-linear vector fields into a single system defined by (1)-(4). Moreover, the dynamics of many non-piecewise-linear systems can also be understood and explained by the dynamics of Chua's oscillator, as illustrated in [51, 52, 53].

5 SOME RECENT PHENOMENA OBSERVED FROM CHUA'S CIRCUIT

In addition to the various standard routes to chaos (e.g., period doubling, torus breakdown) that are now well known for Chua's circuit, several interesting new phenomena have been discovered recently which we now briefly summarized.

5.1 Stochastic Resonance

It is well known that when two spiral Chua's attractors (similar in structure to the Rossler attractor) collide in a *crisis* biburcation, they merge into a single attractor; namely, the double-scroll Chua's attractor. For a narrow "band" along this bifurcation boundary in the $\alpha - \beta$ parameter space, a *chaos-chaos type* of intermittency phenomena is observed. If a small sinusoidal signal with the appropriate frequency close to some "natural frequency" of the circuit is applied, a significantly amplified version of this signal is observed. The power gain seems to come at the expense of the energy previously distributed over the entire chaotic power spectrum. Moreover, under certain conditions, the *signal-to-noise ratio* of the amplified output signal is observed to be greater than the signal-to-noise ratio of the input signal – a novel phenomenon which can not be achieved with a *linear* amplifier. This phenomenon is called *stochastic resonance* [54], and is currently an active research area being pursued by many scientists, specially physicists and biologists.

5.2 Signal Amplification via Chaos

Apart from the stochastic resonance phenomenon described above, another mechanism for achieving voltage gain (up to 50 dB has been demonstrated experimentally) from Chua's circuit has been discovered recently [55]. The mechanism of this voltage gain is different from that of stochastic resonance because the effect is observed even when Chua's circuit is operating in a spiral attractor regime far from the bifurcation boundary where stochastic resonance takes place.

5.3 $1/f$ Noise Phenomenon

In addition to the chaos-chaos type intermittency one observes near the bifurcation boundary from a spiral Chua's attractor regime to a double-scroll Chua's attractor regime, extensive numerical simulations of Chua's circuit have shown that the associated power spectrum is characterized by a $\frac{1}{f}$ divergence in the low-frequency region. This phenomenon can be used as a $\frac{1}{f}$ noise generator, and can lead to a better understanding of the ubiquitous yet still poorly understood $\frac{1}{f}$ phenomenon.

5.4 Antimonotonicity phenomenon

Yorke and his co-workers have predicted that antimonotonicity – i.e., inevitable reversal of period - doubling cascades, is a fundmental phenomenon for a large class of nonlinear systems [56]. Recent experiments on Chua's circuit have provided the first *experimental* confirmation of this phenomenon [57].

5.5 Period-Adding Phenomenon

Most readers of chaos are familiar with the *period-doubling* phenomenon, where the oscillation period doubles at a geometric rate in accordance with the Feigenbaum number. Another phenomenon rarely observed in autonomous system is that of *period adding*, where the oscillation period increases by consecutive integers, while interspersed between chaotic regimes. Such a phenomenon has been observed in Chua's oscillator [58] and is in fact the basis for designing a bassoon-like musical instrument [45]. The same phenomenon has been observed and rigorously proved by Sharkovsky et al for the Chua's circuit characterized by a 1-D map with a time delay [17].

5.6 Autowave Phenomenon

A 1-dimensional chain or 2-dimensional array of identical Chua's circuits with resistive couplings has been shown to support stable *autowave* solutions for a wide range of coupling resistances [16, 22, 23, 59]. Below a certain diffusion coefficient, however, the autowave suddenly ceases to propagate. This propagation failure mechanism is similar to that observed in diseased nerve fibers, such as multiple sclerosis. Such a phenomenon has baffled biologist for many years because no such phenomenon has been observed from simulations of the various associated nonlinear *partial differential* equation models. Indeed, it can be proved mathematically that no such propagation phenomenon can occur in any 1-dimensional active medium modeled by a partial differential equation. Consequently, our observation of this phenomenon from a chain of Chua's circuits implies that a "discrete" chain of Chua's circuits(described by *ordinary* differential equations) is richer in dynamics, and that it can predict certain phenomenon which its limiting partial differential equation model can not [23].

5.7 Spiral Wave Phenomenon

Spiral waves are special cases of autowaves that are widely observed in active chemical media – e.g., the classic Belousov-Zhabotinski reaction. Such media are modeled by nonlinear reaction - diffusion partial differential equations. It has been shown recently that an array of Chua's oscillators can also support a stable spiral wave solution [24], an example of which is shown in Fig. 2 . This is the first spiral wave phenomenon that has been observed in Electrical Engineering, and could lead to novel applications.

5.8 Universality and Self-Similarity

The observation that the $\alpha - \beta$ plane bifurcation patterns contain *self-similar* features resembling that of "swallow tails" has been pointed out in [25] and [60] . A recent in-depth analysis of this phenomenon using

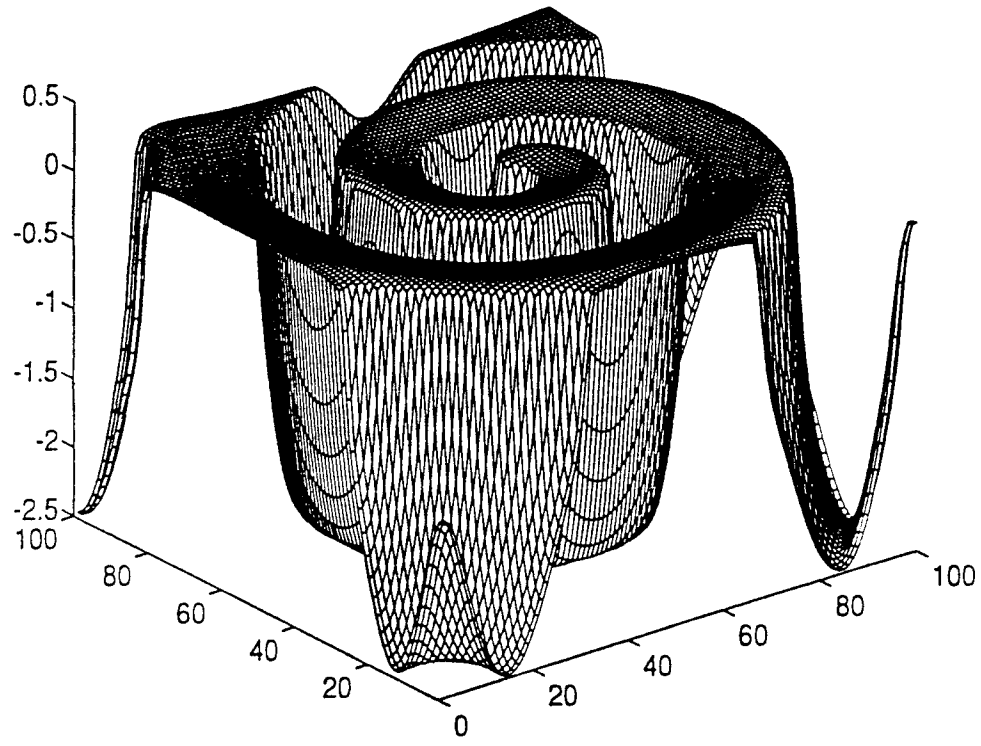

Figure 2: Example of a *spiral wave* generated from a 100 × 100 array of identical Chua's oscillator.

renormalization group analysis [61] has resulted in a definitive characterization of the geometry of this self-similarity phenomenon. In particular, the complex fine structure in the topography of regions of different dynamical behavior near the onset of chaos has been investigated in a 2-parameter 1-D map which describes approximately the dynamics of Chua's circuit. Besides the typical piecewise-smooth Feigenbaum critical lines, the boundary of chaos contains an infinite set of codimension-two critical points, which may be coded by itineraries on a binary tree. In regions nearby critical points having periodic codes, the infinite topography of the parameter plane reveals a property of self-similarity. Moreover, the well-known "Feigenbaum number" for 1-parameter 1-D maps has been generalized to ***two universal numbers*** for 2-parameter 1-D maps [61] .

6 RECENT ANALYTICAL INVESTIGATIONS OF CHUA'S CIRCUIT

Many deep mathematical analysis, and their generalizations, of Chua's circuit have been published during the past two years. We now summarized some of these *analytical* results:

6.1 The double-hook attractor

For certain parameters in the $\alpha - \beta$ plane, all eigenvalues associated with the origin of Chua's equation are *real* numbers. The strange attractor associated with this chaotic regime is called a ***double-hook*** attractor in [62]. An in-depth analytical study of this regime has been made by Silva [62, 63, 64].

6.2 One-dimensional Chua's map

The original Chua's 1-D map presented in [25] has been extensively investigated numerically [65, 66] and analytically [17, 12, 67, 68]. Using the generalized framework developed by Brown [12], Misiurewicz investigated maps of the real line into itself obtained from the modified Chua's equation [67]. For a large range of parameters, Misiurewicz found the existence of *invariant* intervals as well as invariant sub-intervals on which the associated Chua's circuit is *unimodal* and resembles the well-known *logistic* map. Moreover, this map is found to have a negative Schwarzian derivative, implying the existence of at most one attracting period orbit. Moreover, Misiurewicz proved that there is a set of parameters of positive measure for which chaos occurs.

6.3 Universality in cycles of chaotic intervals

The order of the bifurcation sequence in piecewise-linear maps is different from that of smooth maps. In the case of the piecewise-linear map associated with the Chua's circuit with time - delay [17], Maistrenko et al have found that when a period-n *point cycle* loses its stability, a "rigid" period-doubling bifurcation occurs which leads to the emergence of *not* point cycles but *interval cycles* of double period having chaotic trajectories [69]. This is followed by an inverse period-doubling bifurcation, i.e., interval cycles of period 2n are merged pairwise, giving birth to a period - n interval cycle. Finally, in the next bifurcation all intervals of interval cycles will merge into the full *interval* cycle $I = [0, 1]$. In this case, there are no subintervals of I which recur periodically under the map of f. Among many elegant mathematical properties concerning interval cycles, Maistrenko et al derived two *universal* constants analytically, and in explicit form [69].

6.4 Global Stability and Instability of Chua's Oscillator

Recently, Leonov et al investigated Chua's oscillators as a feedback control system and derived frequency-domain criterion for global stability and instability [70]. This analytical study has led to a new version of the generalized Kalman's conjecture.

6.5 The Double-Horseshoe Theorem

Using a new geometric model of Chua's circuit, Belykh and Chua have presented an analytical study of a new type of strange attractors generated by an odd-symmetric three-dimensional orbit at the origin. This type of attractor is intimately related to the double-scroll Chua's attractor. They have proved rigorously that the chaotic nature of this attractor is different from that of a Lorenz-type attractor, or a quasi-attractor. In particular, this attractor has the geometry of a *double horseshoe*. For certain nonempty intervals of parameters, this strange attractor has no stable orbits. Unlike other known attractors, the double horseshoe attractor contains not only a Cantor set structure of hyperbolic points typical of horseshoe maps, but unstable points (i.e., stable in reverse time) as well. This inplies that the points from the stable manifolds of the hyperbolic points must necessarily attract the unstable points.

6.6 Synchronization, Trigger Wave, and Spatial Chaos

Several criteria for synchronizing two *mutually-coupled* Chua's circuits operating under chaotic regimes are derived in [71]. For a chain of Chua's oscillators, analytical results couched in terms of a moving coordinate system have been derived which guarantee the existence of *heteroclinic* orbits [72]. This analytical study is highly significant because it proves, among other things, the presence of a trigger wave along the chain. The proof of the existence of heteroclinic orbits represents a major breakthrough since it is generally extremely difficult if not impossible to derive such analytical results. In addition to trigger waves, this investigation also proves the existence of *Spatial Chaos* along a finite chain of Chua's oscillators.

6.7 Fine Structure of the Double-scroll Chua's Attractors

Using the theory of *confinors* [73, 74, 75], Lozi and Ushiki have developed an *analytical* approach, in sharp contrast to numerical integration methods, for examing the fine features of Chua's attractors. The keystone of the original definition of confinors is that very often, changes in the shape of experimentally observed signals are more significant in characterizing the phase portrait, than any topological change between chaotic attractors. The theory of confinor takes into account the "shape" of the signals, and is capable of modeling both transient and asymptotic regimes. Applying this unique approach to Chua's equation, Lozi and Ushiki had discovered the co-existence of 3 *distinct* double-scroll Chua's attractors in close proximity of each other for *the same value* of parameters [75]. Without a precise knowledge of initial conditions, which only the confinor theory can supply, it would be virtually impossible to pick these 3 attractors apart. This explains why in spite of the rather extensive numerical and experimental works of many researchers on Chua's circuit over the last 10 years, no one has ever observed the simultaneous existence of 3 chaotic attractors.

In addition to ths discovery, Lozi and Ushiki have also provided the most precise characterizations of the structure of the double-scroll Chua's attractors via an exact 2-dimensional Poincare map. Moreover, they have discovered some very unusual bifurcation phenomena which are distinct from the usual period-doubling cascades [74]. Since these results are all highly original and robust, they can be used as a guide for characterizing strange attractors of other chaotic systems, thereby demonstrating yet another application of Chua's Circuit as a universal paradigm for chaos.

7 SOME RECENT APPLICATIONS OF CHAOS FROM CHUA'S CIRCUIT

During the last 20 years, many researches have begun to control and exploit chaos from various dynamical systems for novel applications. In this final section, we summarize some recent results in this area which have been applied to Chua's circuit.

7.1 Controlling chaos in Chua's circuit

To control chaos in Chua's circuit means to influence its normal chaotic regime and transform it into some "desired" dynamic operation, such as a fixed point, or a periodic orbit. Many different techniques have been developed successfully to control chaos in Chua's circuit [76, 77, 78, 79, 80, 14, 81, 82, 83, 84, 85]. Some of the control techniques involve varying the circuit parameters, stabilizing some unstable orbits embedded in a strange attractor, absorbing the chaotic dynamics by a controlling circuit, etc. Since different controlling techniques have their advantages and drawbacks, the best approach will depend on specific applications.

7.2 Secure Communication via Chua's circuit

One of the most intriguing applications of chaos is to "hide" the small information - bearing signal within a much larger chaotic signal. Such a signal cannot be recovered unless the receiver is tuned to the exact circuit parameters – the *decoding* key – of the transmitter (Chua's circuit). Several secure communication systems based on Chua's circuit have been proposed [86, 87, 88, 89, 90]. So far, the approaches proposed in [89, 90] appear to be the most secure and accurate.

7.3 Trajectory Recognition via Array of Chua's Circuits

Recently, Altman uses the center manifold and normal form theory to relate the local behavior of Chua's circuit to some input trajectory to be recognized [91]. This mathematical problem arises in the recognition of hand gestures where the hand position as a function of time is used to drive Chua's circuit to an attracting surface. Since Chua's circuit is known to undergo a series of bifurcations from fixed points, to limit cycles, to a cascade of period-doubling oscillations leading to chaotic oscillations in the vicinity of the center manifold surface, the rapid entrainment of the chaotic system to an external signal having a trajectory near the center manifold surface provides the basic mechanism for trajectory recognition. The recognition of many trajectories can be achieved by using a 2-dimensional array of Chua's circuits. In this case, the variation of responses to the common input trajectory creates a *spatial pattern* which can be used to recognize the input trajectory. The above approach to trajectory recognition is both novel and fascinating.

7.4 Handwritten Character Recognition Using Chua's Oscillator

A neural network architecture and learning algorithm for associative memory storage of analog patterns, continuous sequences, and chaotic attractors via a network of Chua's oscillators has recently been designed by Baird and Hirsch [92]. Their design is used in the application to the problem of real-time handwritten digit recognition. They have demonstrated that several of the attractors from Chua's oscillator have out-performed the previously studied Lorenz attractor system in terms of both accuracy and speed of convergence.

7.5 Applications of Chua's Circuit to Music

Perhaps the most fascinating application to date of Chua's circuit and its generalizations is in music. Recently, Mayer-Kress et al [45] have discovered that in the $\alpha - \beta - \gamma$ parameter space of Chua's Oscillator, there is a manifold which gives rise to novel musical sounds. For example, a point on this manifold gives rise to a consecutive sequence of bassoon-like musical tones. This research project is presently conducted by a multidisciplinary team at the university of Illinois, Urbana, and consists of Professors G. Mayer-Kress and A. Hubler from the Physics department, Robin Bargar, project leader of sonification research and development at the National Center for supercomputing Applications, and Insook Choi, a doctoral candidate in musical arts. Their music-making method may herald an attractive alternative to the time-consuming pre-mixing of the audio frequencies, an essential step for electronic synthesizers of musical sounds. By varying the circuit element values from Chua's Oscillator, frequencies and overtones characteristic of musical instruments can be easily generated without the necessity of separately programming each frequency. Already these researchers

have generated unharmonious sound and created music in overtones never heard before because no instrument exists that can make them. In fact by exploiting these unusual musical tones, choi has composed some truly *avant-garde* music via Chua's oscillator for a recent concert at Expo'93 in Seoul and Taejeoun, Korea in October 1993.

Independent of the research group from the university of Illinois, Professor Xavier Rodet from the Institute de Recherche et de coordination Acoustique/Musique (IRCAM) in Paris, and the university of Paris has used a time-delay version of Chua's circuit, not only to generate musical sounds, but also as a unified model of an interesting class of musical instruments, including those (e.g., clarinet) consisting of a massless reed coupled to a passive linear system. The surprisingly rich and novel family of periodic and chaotic musical sounds generated by Rodet has already enriched the sound synthesis repertoire of tools for researchers in computer music [93].

8 CONCLUDING REMARKS

Although first conceived only 10 years ago, more than 150 papers, two special issues (Journal of Circuits, Systems, and Computers, vol.3, no.1 and no.2, 1993), and a book (Edited by R. N. Madan, World Scientific, 1042 pages, 1993) have been published on all aspects of bifurcation and chaos of Chua's Circuit and its recent global unfolding, the Chua's oscillator. Yet, our understanding of this simplest among all chaotic circuits is still far from complete. Indeed, what has been published on Chua's circuit represents only the tip of an iceberg [94], specially when viewed from the broader perspective of an array of driven Chua's oscillators, as well as other higher-dimensional generalizations of Chua's circuit. This yet uncharted territory will no doubt be systematically explored and exploited for novel applications in the next decade.

References

[1] L. O. Chua. The Genesis of Chua's Circuit. *Archiv fur Elektronik und Ubertragungstechnik*, 46(4):250–257, 1992.

[2] T. Matsumoto. A chaotic attractor from Chua's circuit. *IEEE Transactions on Circuits and Systems*, 31(12):1055–1058, 1984.

[3] L.S. Rosenthal. Inductively tuned astable multivibrator. *IEEE Transactions on Circuits and Systems*, 27(10):963–964, 1980.

[4] T. Matsumoto, L. O. Chua, and K. Tokumasu. Double Scroll via a two-transistor circuit. *IEEE Transactions on Circuits and Systems*, 33(8):828–835, 1986.

[5] G. Q. Zhong and F. Ayrom. Experimental confirmation of chaos from Chua's circuit. *International Journal of Circuit Theory and Applications*, 13(1):93–98, 1985.

[6] M. P. Kennedy. Experimental chaos via Chua's circuit. In *Proceedings of the 1st Experimental Chaos Conference, eds. S.Vobra, M.Spano, M.Shlesinger, L.Pecora, and W.Ditto*, pages 340–351, World Scientific, Singapore, 1992.

[7] M. P. Kennedy. Robust op amp realization of Chua's circuit. *Frequenz*, 46(3–4):66–80, 1992.

[8] J. M. Cruz and L. O. Chua. A CMOS IC Nonlinear Resistor for Chua's Circuit. *IEEE Transactions on Circuits and Systems*, 12(39):985–995, December 1992.

[9] A. Rodriquez-Vazquez and M. Delgado-Restituto. CMOS design of chaotic oscillators using state variables: a monolithic Chua's circuit. *IEEE Transactions on Circuits and Systems-II: Analog and Digital*

Signal Processing, 10(40), October 1993. Special Issue on Chaos in Nonlinear Electronic Circuits, Part C.

[10] J. M. Cruz and L. O. Chua. An IC Chip of Chua's Circuit. *IEEE Transactions on Circuits and Systems-II: Analog and Digital Signal Processing*, 10(40), October 1993. Special Issue on Chaos in Nonlinear Electronic Circuits, Part C.

[11] A. I. Mahla and A. G. Badan Palhares. Chua's Circuit with a discontinuous non-linearity. *Journal of Circuits, Systems, and Computers*, 3(1):231–237, March 1993.

[12] R. Brown. From the Chua circuit to the generalized Chua map. *Journal of Circuits, Systems, and Computers*, 3(1):11–32, 1993.

[13] E. J. Altman. Bifurcation analysis of Chua's Circuit with applications for low-level visual sensing. *Journal of Circuits, Systems, and Computers*, 3(1):63–92, March 1993. Special issue on Chua's circuit: A Paradigm for chaos.

[14] T. T. Hartley and F. Mossayebi. Control of Chua's Circuit. *Journal of Circuits, Systems, and Computers*, 3(1):173–194, March 1993.

[15] A. J. Khibnik, D. Roose, and L. O. Chua. On Periodic Orbits and Homoclinic Bifurcation in Chua's Circuit with Smooth Nonlinearity. *International Journal of Bifurcation and Chaos*, 3(2):363–384, April 1993.

[16] V. Perez-Munuzuri, V. Perez-Villar, and L.O. Chua. Propagation Failure in Linear Arrays of Chua's Circuits. *Int. Journal of Bifurcation and Chaos*, 2(2):403–406, June 1992.

[17] A. N. Sharkovsky, Yu Maistrenko, P. Deregel, and L. O. Chua. Dry Turbulence from a Time-Delayed Chua's Circuit. *Journal of Circuits, Systems, and Computers*, 3(2):645–668, June 1993.

[18] J. A. K. Suykens and J. Vandewalle. Generation of n-double scrolls ($n = 1, 2, 3, 4, \cdots$). *IEEE Transactions on Circuits and Systems-I: Fundamental Theory and Applications*, 11(40), November 1993. Special Issue on Chaos in Nonlinear Electronic Circuits.

[19] Lj. Kocarev, Lj. Karadzinov, and L. O. Chua. N-dimensional Canonical Chua's Circuit. *Journal of Circuits, Systems, and Computers*, 3(1):239–258, March 1993.

[20] K. A. Lukin. High frequency oscillations from Chua's Circuit. *Journal of Circuits, Systems, and Computers*, 3(2):627–643, June 1993.

[21] C. M. Blazquez and E. Tuma. Dynamics of Chua's Circuit in a Banach space. *Journal of Circuits, Systems, and Computers*, 3(2):613–626, June 1993.

[22] V. Perez-Munuzuri, V Gomez-Gesteira, V. Perez-Villar, and L. O. Chua. Travelling Wave propagation in a one-dimensional fluctuating medium. *International Journal of Bifurcation and Chaos*, 3(1):211–215, March 1993.

[23] V. Perez-Munuzuri, V. Perez-Villar, and L. O. Chua. Travelling Wave Front and Its Failure in a One-Dimensional Array of Chua's Circuits. *Journal of Circuits, Systems, and Computers*, 3(1):215–229, March 1993.

[24] A. Perez-Munuzuri, V. Perez-Munuzuri, and V. Perez-Villar. Spiral waves on a two-dimensional array of nonlinear circuits. *IEEE Transactions on Circuits and Systems-I: Fundamental Theory and Applications*, 40(11), November 1993. Special Issue on Chaos in Nonlinear Electronic Circuits, Part B.

[25] L. O. Chua, M. Komuro, and T. Matsumoto. The Double Scroll Family, Parts I and II. *IEEE Transactions on Circuits and Systems*, 33(11):1073–1118, 1986.

[26] L. O. Chua. Global unfolding of Chua's circuits. *IEICE Transactions on Fundamentals of Electronics, Communications and Computer Sciences*, E76-A:704–734, 1993.

[27] L. O. Chua. *Introduction to Nonlinear Network Theory.* McGraw-Hill Book Co., New York, 1970.

[28] L. O. Chua. Device modeling via basic nonlinear circuit elements. *IEEE Transactions on Circuits and Systems*, 27(11):1014–1044, 1980.

[29] S. Wu. Chua's circuit family. *Proc. IEEE*, 75(8):1022–1032, 1987.

[30] T. Matsumoto, L. O. Chua, and R. Tokunaga. Chaos via torus breakdown. *IEEE Transactions on Circuits and Systems*, 34(3):240–253, 1987.

[31] V. S. Anishchenko, M. A. Safonova, and L. O. Chua. Confirmation of the Afraimovich-Shil'nikov torus breakdown theorem via a torus circuit. *IEEE Transactions on Circuits and Systems-I: Fundamental Theory and Applications*, 11(40), November 1993. Special Issue on Chaos in Electronic Circuits, Part B.

[32] P. Bartissol and L. O. Chua. The Double Hook. *IEEE Transactions on Circuits and Systems*, 35(12):1512–1522, 1988.

[33] A. Huang. A study of the chaotic phenomena in Chua's circuit. In *Proceedings of the ISCAS*, pages 273–276, Helsinki, 1988.

[34] Y. Nishio, N. Inaba, and S. Mori. Chaotic phenomena in an autonomous circuit with nonlinear inductor. In *Proceedings of the ISCAS*, 1990.

[35] L. O. Chua and G. N. Lin. Canonical Realization of Chua's Circuit Family. *IEEE Transactions on Circuits and Systems*, 37(7):885–902, 1990.

[36] R. N. Madan, editor. *Chua's circuit: A paradigm for chaos.* World Scientific, Singapore, 1993.

[37] R. N. Madan. Observing and learning chaotic phenomena from Chua's circuit. In *Proceedings of the 35th Midwest Symposium on Circuits and Systems*, pages 736–745, 1992.

[38] L. O. Chua. A Zoo of Strange Attractors from Chua's Circuit. In *Proc. of the 35th Midwest Symposium on Circuits and Systems, Washington DC*, pages 916–926, August 9-12 1992.

[39] L. O. Chua. A simple ODE with more than 20 strange attractors. In *Proceedings of the World congress of Nonlinear Analysis*, pages 19–26, Tampa, Florida, August 1992.

[40] P. Deregel. Chua's Oscillator: A zoo of attractors. *Journal of Circuits, Systems, and Computers*, 3(2):309–359, June 1993.

[41] F. Bohme and W. Schwarz. Transformations of circuits belonging to Chua's Circuit family into nonlinear feedback loops made of passive RC-filter and active memoryless non-linearity. *Journal of Circuits, Systems, and Computers*, 3(2):293–308, June 1993.

[42] M. J. Ogorzalek and J. Galias. Characterization of Chaos in Chua's Oscillator in terms of unstable periodic orbits. *Journal of Circuits, Systems, and Computers*, 3(2):411–430, June 1993.

[43] V. Spany and L. Pivka. Boundary surfaces in sequential circuits. *International Journal of Circuit Theory and Applications*, 18(4):349–360, 1990.

[44] L. O. Chua, C. W. Wu, A. Huang, and G. Q. Zhong. A Universal Circuit for Studying and Generating Chaos, part II: Strange Attractors. *IEEE Transactions on Circuits and Systems-I: Fundamental Theory and Applications*, 10(40), October 1993. Special Issue on Chaos in Nonlinear Electronic Circuits.

[45] G. Mayer-Kress, I. Choi, N. Weber, R. Bargar, and A. Hubler. Musical signals from Chua's circuit. *IEEE Transactions on Circuits and Systems-II: Analog and Digital Signal Processing*, 40(10):63–92, October 1993. special Issue on Chaos in Nonlinear Electronic Circuits, Part C.

[46] R. W. Brockett. On conditions leading to chaos in feedback systems. *Proc. CDC*, pages 932–936, December 1982.

[47] C. T. Sparrow. Chaos in three-dimensional single loop feedback systems with a piecewise-linear feedback function. *Journal of mathematical analysis and applications*, 83(1):275–291, 1981.

[48] P. Coullet, C. Tresser, and A. Arneodo. Transition to stochasticity for a class of forced oscillators. *Physics Letters*, 72A(4,5):268–270, 1979.

[49] A. Arneodo, P. Coullet, and C. Tresser. Possible new strange attractors with spiral structure. *Communications in Mathematical Physics*, 79:573–579, 1981.

[50] A. Arneodo, P. Coullet, and E. A. Spiegel. Chaos in a finite macroscopic system. *Physics Letters*, 92A(8):369–373, 1982.

[51] M. Shinriki, M Yamamoto, and S. Mori. Multi mode oscillations in a modified van der pol oscillator containing a positive nonlinear conductance. *Proceedings of IEEE*, 69(3):394–395, 1981.

[52] E. Freire, L. G. Franquelo, and J. Aracil. Periodicity and chaos in an autonomous electronic system. *IEEE Transactions on Circuits and Systems*, 31(3):237–247, March 1984.

[53] A. S. Dmitriev and V. Y. Kislov. Stochastic oscillations in a self-excited oscillator with a first-order inertial delay. *Radiotekhnika i electronika*, 29:2389, 1984.

[54] V.S. Anishchenko, M.A. Safonova, and L.O. Chua. Stochastic Resonance in Chua's Circuit. *Int. J. of Bifurcation and Chaos*, 2(2):397–401, June 1992.

[55] K. S. Halle, L. O. Chua, V. S. Anishchenko, and M. A. Safonova. Signal Amplification via Chaos: Experimental Evidence. *International Journal of Bifurcation and Chaos*, 2(4):1011–1020, December 1992.

[56] P. S. Dawson, C. Grebogy, J. A. Yorke, I. Kan, and H. Kocak. Antimonotonicity – inevitable reversal of period-doubling cascades. *Phys. Letter A*, 162:249–254, 1992.

[57] L. Kocarev, K. S. Halle, K. Eckert, and L. O. Chua. Experimental observation of antimonotonicity in Chua's circut. *International Journal of Bifurcation and Chaos*, 3(4), 1993.

[58] L. Pivka and V. Spany. Boundary surfaces and basin bifurcations in Chua's Circuit. *Journal of Circuits, Systems, and Computers*, 3(2):441–470, June 1993.

[59] V. Perez-Munuzuri, V. Perez-Viller, and L. O. Chua. Autowaves for image processing on a two-dimensional CNN Array of Excitable Nonlinear Circuits: Flat and Wrinkled Labyrinths. *IEEE Transactions on Circuits and Systems*, 40(3):174–193, March 1993.

[60] L. Yang and Y. L. Liao. Self-similar structures from Chua's circuit. *International Journal of Circuit Theory and Applications*, 15:189–192, 1987.

[61] A. P. Kuznetsov, S. P. Kuznetsov, I. R. Sataev, and L. O. Chua. Two-Parameter Study of Transition to Chaos in Chua's Circuit: Renormalization Group, Universality and Scaling. *International Journal of Bifurcation and Chaos*, 3(4), August 1993.

[62] C. P. Silva. The double hook attractor in Chua's circuit: Some analytical results. In R. N. Madan, editor, *in Chua's circuit: A paradigm for chaos*, pages 671–710. World Scientific, Singapore, 1993.

[63] C. P. Silva and L. O. Chua. The Overdamped Double Scroll Family. *International Journal of Circuit Theory and Applications*, 1(7):223—302, 1988.

[64] C. P. Silva. Shil'nikov's theorem. *IEEE Transactions on Circuits and Systems-I: Fundamental Theory and Applications*, 10(40), October 1993. Special Issue on Chaos in Electronic Circuits, Part A.

[65] L. O. Chua and I. Tichonicky. 1-D Map for the Double Scroll Family. *IEEE Transactions on Circuits and Systems*, 38(3):233–243, March 1991.

[66] Marc Genot. Applications of 1-D map from Chua's circuit: A pictorial guide. *Journal of Circuits, Systems, and Computers*, 3(2), June 1993.

[67] M. Misiurewicz. Unimodal interval maps obtained from the modified Chua's equations. *International Journal of Bifurcation and Chaos*, 3(2):323–332, April 1993.

[68] Yu. L. Maistrenko, V. L. Maistrenko, and L. O. Chua. Cycles of chaotic intervals in a time-delayed Chua's circuit. *International Journal of Bifurcation and Chaos*, 3(6), December 1993.

[69] Yu. L. Maistrenko, V. L. Maistrenko, and L. O. Chua. Cycles of chaotic intervals in a time-delayed Chua's circuit. In R. N. Madan, editor, *Chua's circuit: A paradigm for chaos*, pages 993–1017. World Scientific Publishing Co., Singapore, 1993.

[70] G. A. Leonov, D. V. Ponomarenko, V. B. Smirnova, and L. O. Chua. Global stability and instability of canonical Chua's circuit. In R. N. Madan, editor, *Chua's circuit: A paradigm for chaos*, pages 725–739. World Scientific Publishing Co., Singapore, 1993.

[71] V. N. Belykh, N. N. Verichev, Lj. Kocarev, and L. O. Chua. On Chaotic Synchronization in a Linear Array of Chua's Circuits. *Journal of Circuits, Systems, and Computers*, 3(2):579–589, June 1993.

[72] V. I. Nekorkin and L. O. Chua. Spatial disorder and wave fronts in a chain of coupled Chua's circuit. *International Journal of Bifurcation and Chaos*, 3(6), 1993.

[73] R. Lozi and S. Ushiki. Confinors and bounded time-patterns in Chua's circuit and the double scroll family. *International Journal of Bifurcation and Chaos*, 1(1):119–138, 1991.

[74] R. Lozi and S. Ushiki. The theory of confinors in Chua's circuit: accurate analysis of bifurcation and attractors. *International Journal of Bifurcation and Chaos*, 3(2):333–361, 1993.

[75] R. Lozi and S. Ushiki. Co-existing attractors in Chua's circuit. *International Journal of Bifurcation and Chaos*, 1(4):923–926, 1991.

[76] G. A. Johnson, T. E. Tigner, and E. R. Hunt. Controlling chaos in Chua's Circuit. *Journal of Circuits, Systems, and Computers*, 3(1):109–117, March 1993.

[77] G. A. Johnson and E. R. Hunt. Maintaining stability in Chua's Circuit driven into regions of oscillation and chaos. *Journal of Circuits, Systems, and Computers*, 3(1):119–123, March 1993.

[78] K. Murali and Lakshmanan. Controlling of chaos in the driven Chua's Circuit. *Journal of Circuits, Systems, and Computers*, 3(1):125–137, March 1993.

[79] G. Chen and X. Dong. Controlling Chua's circuit. *Journal of Circuits, Systems, and Computers*, 3(1):139–149, March 1993.

[80] R Genesio and A Tesi. Distortion control of chaotic systems: The Chua's Circuit. *Journal of Circuits, Systems, and Computers*, 3(1):151–171, March 1993.

[81] T. Kapitaniak. Targeting unstable stationary states of Chua's Circuit. *Journal of Circuits, Systems, and Computers*, 3(1):195–199, March 1993.

[82] M. J. Ogorzalek. Taming chaos: Part I- synchronization. *IEEE Transactions on Circuits and Systems-I: Fundamental Theory and Applications*, 10(40), October 1993. Special Issue on Chaos in Nonlinear Electronic Circuits, Part A.

[83] G. Chen. Controlling Chua's Global Unfolding Family. *IEEE Transactions on Circuits and Systems-I: Fundamental Theory and Applications*, 11(40), November 1993. Special Issue on Chaos in Nonlinear Electronic Circuits, Part B.

[84] G. A. Johnson and E. R. Hunt. Derivative Control of the Steady State in Chua's Circuit Driven in the Chaotic Region. *IEEE Transactions on Circuits and Systems-I: Fundamental Theory and Applications*, 11(40), November 1993. Special Issue on Chaos in Nonlinear Electronic Circuits, Part B.

[85] T. Kapitaniak, Lj. Kocarev, and L. O. Chua. Controlling Chaos without Feedback and Control Signals. *International Journal of Bifurcation and Chaos*, 3(2):459–468, April 1993.

[86] Lj. Kocarev, K. S. Halle, K. Eckert, L. O. Chua, and U. Parlitz. Experimental Demonstration of Secure Communications via Chaotic Synchronization. *International Journal of Bifurcation and Chaos*, 2(3):709–713, September 1992.

[87] U. Parlitz, L.O. Chua, Lj. Kocarev, K.S. Halle, and A. Shang. Transmission of Digital Signals by Chaotic Synchronization. *Int. J. of Bifurcation and Chaos*, 2(4):973–977, September 1992.

[88] K. S. Halle, C. W. Wu, M. Itoh, and L. O. Chua. Spread Spectrum Communication through Modulation of Chaos. *International Journal of Bifurcation and Chaos*, 3(2):469–477, 1993.

[89] H. Dedieu, M. P. Kennedy, and M. Hasler. Chaos shift keying: Modulation and demodulation of a chaotic carrier using self-synchronizing Chua's circuits. *IEEE Transactions on Circuits and Systems-II: Analog and Digital Signal Processing*, 10(40), October 1993. Special Issue on Chaos in Nonlinear Electronic Circuits, Part C.

[90] C. W. Wu and L. O. Chua. A simple way to synchronize chaotic systems with applications to secure communication systems. *International Journal of Bifurcation and Chaos*, 3(6), December 1993.

[91] E. J. Altman. Normal form analysis of Chua's circuit with applications for trajectory recognition. *IEEE Transactions on Circuits and Systems-II: Analog and Digital Signal Processing*, 10(40), October 1993. Special Issue on Chaos in Nonlinear Electronic Circuits, Part C.

[92] B. Baird, M. Hirsch, and F. Eeckman. A neural network associative memory for handwritten character recognition using multiple Chua attractors. *IEEE Transactions on Circuits and Systems-II: Analog and Digital Signal Processing*, 10(40), October 1993. Special Issue on Chaos in Nonlinear Electronic Circuits, Part C.

[93] X. Rodet. Flexible yet controllable physical models: a nonlinear dynamics approach. *International Computer Music Conference*, September 1993.

[94] L. P. Shil'nikov. Chua's circuit: Rigorous results and future problems. *Proc. of the International Symposium in Nonlinear Theory and its Applications(NOLTA), HAWAII*, Dec. 5-9 1993.

1993 International Symposium on Nonlinear
Theory and Its Applications (NOLTA '93)
Hawaii, U.S.A., December 5-10, 1993

Chaos from a time-delayed Chua's circuit

A. N. Sharkovsky

Institute of Mathematics
Ukrainian Academy of Sciences, Kiev, Ukraine

Abstract

By replacing the parallel LC "resonator" in Chua's circuit by a lossless transmission line, terminated by a short circuit, we obtain a "time-delayed Chua's circuit" whose time evolution is described by a pair of *linear partial* differential equations with a *nonlinear* boundary condition. If we neglect the capacitance across the Chua's diode, described by a non-symmetric piecewise-linear $v_R - i_R$ characteristic, the resulting idealized 'time-delayed Chua's circuit is described *exactly* by a *scalar nonlinear difference equation* with continuous time, which makes it possible to characterize its associated nonlinear dynamics and spatial chaotic phenomena.

From a mathematical view point, circuits described by *ordinary* differential equations can generate only *temporal* chaos, while the time-delayed Chua's circuit can generate *spatial-temporal* chaos. Except for stepwise periodic oscillations, the *typical solutions* of the idealized time-delayed Chua's circuit consist of either *weak turbulence*, or *strong turbulence*, which are examples of "ideal" (or "dry") turbulence. In both cases, we can observe infinite processes of spatial-temporal coherent formations.

Under *weak turbulence*, the graphs of the solution tend to limit sets which are *fractals* with a Hausdorff dimension between 1 and 2, and is therefore larger than the topological dimension(of sets).

Under *strong turbulence*, the "limit" oscillations are oscillations whose amplitudes are *random functions*. This means that the attractor of the idealized time-delayed Chua's circuit already contains random functions, and spatial self-stochasticity phenomenon can be observed.

1 GENERALIZING CHUA'S CIRCUIT TO INFINITE DIMENSIONS

The original Chua's circuit [1] consists of a *linear passive* resonator (parallel LC tune circuit) connected across a *nonlinear active* circuit composed of a Chua's diode [2], a linear capacitor C_1, and a linear resistor R, as shown in Fig. 1.

In most publications, [3] Chua's diode is characterized by a *continuous odd-symmetric* 3-segment piecewise-linear function. In this paper, we consider an "infinite-dimensional" generalization of Chua's circuit, obtained by replacing the LC resonant circuit by a *lossless* transmission line of length l, terminated on its left ($x = 0$) by a *short circuit*, as shown in Fig. 2(a).

Since the effect of the transmission line is to provide a "time delay" in the dynamics of Chua's circuit, we will henceforth call this circuit the "time-delayed Chua's circuit". Our main objective in this paper is to investigate the asymptotic behaviors of $v(x,t)$ and $i(x,t)$ at all points along the transmission line ($0 \leq x \leq l$). Since the most interesting and complex "turbulent-like" dynamical behaviors occurs when the $v_R - i_R$ characteristic of Chua's diode is *not* symmetric with respect to the origin, we have chosen the 3-segment piecewise-linear function shown in Fig. 2(b), where $i_R = G(v_R - E)$.

2 TIME EVOLUTION EQUATIONS

The lossless transmission line in Fig.2(a) is defined by the following linear partial differential equations:

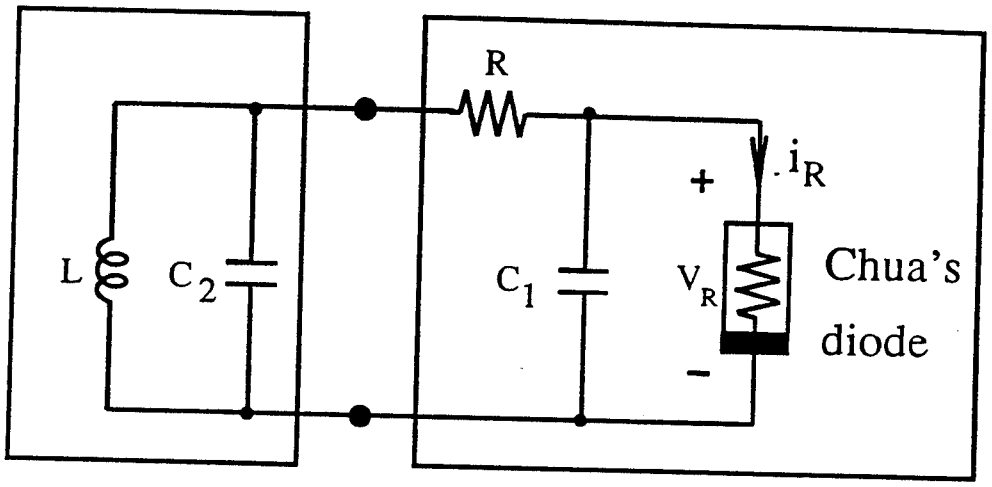

Figure 1: Decomposition of Chua's circuit into a passive linear sub-circuit on the left and an active nonlinear subcircuit on the right.

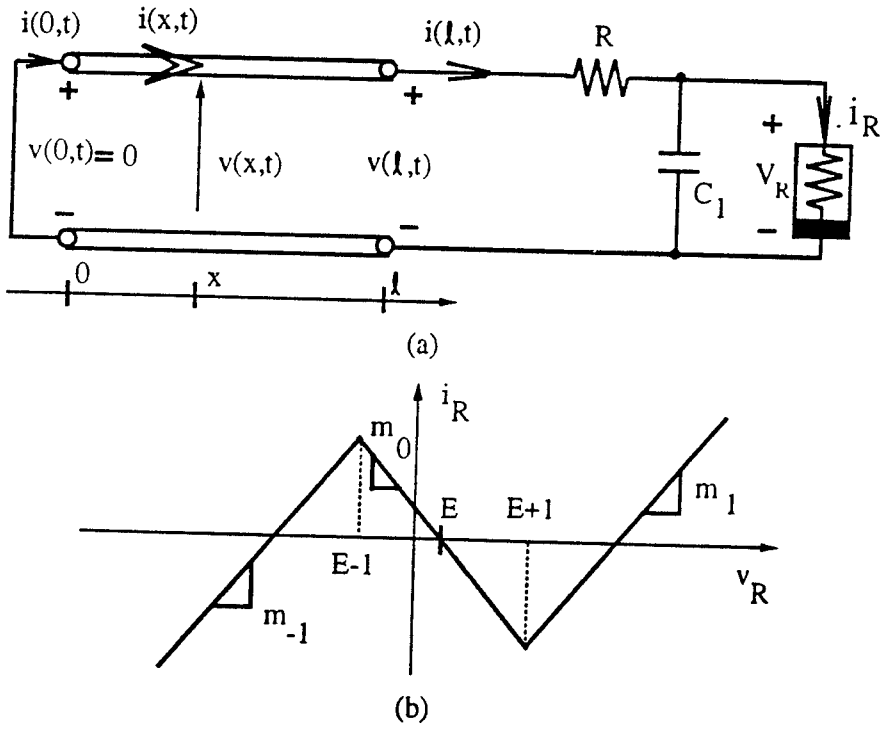

Figure 2: (a) The time-delayed Chua's circuit. (b) The $v_R - i_R$ characteristic of Chua's diode is chosen to be a 3-segment piecewise-linear function, symmetric ($m_{-1} = m_1$) with respect to the point $v_R = \mathrm{E} > 0$.

$$\frac{\partial v(x,t)}{\partial x} = -L\frac{\partial i(x,t)}{\partial t} \quad (1)$$

$$\frac{\partial i(x,t)}{\partial x} = -C\frac{\partial v(x,t)}{\partial t} \quad (2)$$

where L and C denote the inductance and capacitance per unit length of the transmission line. The boundary conditions are given respectively at $x = 0$, and $x = l$ by:

$$v(0,t) = 0 \quad (3)$$

$$i(l,t) = G(v(l,t) - E - Ri(l,t)) + C_1\frac{\partial(v(l,t) - Ri(l,t))}{\partial t} \quad (4)$$

where $G(\cdot)$ is defined by

$$G(u) = \begin{cases} m_0 u, & |u| \leq 1 \\ m_1 u - (m_1 - m_0)sgn\ u, & |u| \geq 1 \end{cases} \quad (5)$$

and $u = v_R - E$.

The general solution of Eqs.(1)-(2) has the form

$$v(x,t) = \alpha(t - \frac{x}{\nu}) - \alpha(t + \frac{x}{\nu}) \quad (6)$$

$$i(x,t) = \frac{1}{Z}[\alpha(t - \frac{x}{\nu}) + \alpha(t + \frac{x}{\nu})] \quad (7)$$

where $\nu = \sqrt{LC}$ is the velocity of the incident and reflected waves, and $Z = \sqrt{\frac{L}{C}}$ is the characteristic impedance of the transmission line.

Note that Eqs.(1)-(4) constitute a system of *linear* partial differential equations with a *nonlinear* boundary condition (at $x = l$). Since this problem is presently analytically intractable, we will investigate here only the limiting case where the capacitance C_1 in Fig. 2(a) is replaced by an open circuit, i.e., $C_1 \to 0$. Under this assumption, we can substitute Eqs.(6)-(7) into Eq.(4) with $C_1 = 0$, and introduce the new variables

$$\tau = \frac{\nu}{2l}t - \frac{1}{2}, \qquad \beta(\tau) = \alpha\left(\frac{2l}{\nu}\tau\right) \quad (8)$$

to obtain the following *difference equation*

$$\beta(\tau + 1) = f(\beta(\tau)) \quad (9)$$

The symbol $f(\cdot)$ denotes a piecewise-linear (single-valued or multivalued) function defined by

$$f(\beta) = A_k\beta - B_k, \qquad \text{where } \beta \in I_k, \quad k = 0, \pm 1 \quad (10)$$

$$
\begin{aligned}
A_k &= -1 + q_k \\
B_k &= \frac{q_0}{2}\left[E + k\left(1 - \frac{m_0}{m_k}\right)\right] \\
q_k &= \frac{2Z}{\frac{1}{m_k} + R + Z} \\
m_{-1} &= m_{+1} \\
I_0 &= \{\beta : \left|\beta - \frac{E}{2}\right| \leq \delta\} \\
I_{\pm 1} &= \{\beta : \pm(\beta - \frac{E}{2}) > \delta\} \\
\delta &= \frac{m_0 Z}{q_0}
\end{aligned}
\tag{11}
$$

It follows from the above derivations that the time evolution of the "time-delayed Chua's circuit with $C_1 = 0$ is governed by a *scalar* nonlinear difference equation with a continuous argument; namely, Eq.(9). The qualitative behavior of this equation is determined by the properties of the *one-dimensional*(1-D) map

$$\boxed{\beta \mapsto f(\beta)} \tag{12}$$

where $f(\cdot)$ is defined in Eq.(10).

3 ASYMPTOTIC BEHAVIORS

To describe the behaviors of the solutions of the "time-delayed Chua's circuit with $C_1 = 0$, it will be convenient for us to use the language of dynamical systems theory. Let $X = [0, l]$ and let $C(X)$ denote the space of all smooth or continuous functions

$$\{(v(x), i(x)) \ : \ 0 \leq x \leq l\} \tag{13}$$

with some appropriate topology, e.g., uniform metric. The solution $v_t(x) = v(x,t)$ and $i_t(x) = i(x,t)$ of Eqs.(1)-(4)(assuming $C_1 = 0$) with initial condition $v_0(x) = v(x,0)$ and $i_0(x) = i(x,0)$ defines an *infinite-dimensional dynamical system*

$$\boxed{\mathcal{F}^t : (v_0(x), i_0(x)) \mapsto (v_t(x), i_t(x))} \tag{14}$$

For the class of problems defined above, it is the usual situation that the trajectories $\mathcal{F}^t[(v_0, i_0]$ have no ω-limit set in the phase space $C(X)$, and the dynamical system(14) has no attractor in the phase space $C(X)$(at least for the reason that the Lipschitz constants can grow to ∞). In order to describe the *asymptotic* (as t $\rightarrow \infty$) behavior of the infinite-dimensional system (14), it is necessary for us to *complete* the phase space $C(X)$with the help of a suitable metric. For "weak" turbulent oscillations to be described below, it is sufficient to use the *Hausdorff* metric for the function graphs. For "strong" turbulent oscillations, however, we need to introduce some specially constructed metric, such as the one given in [4] involving all finite-dimensional joint distributions in combination with the operation of averaging. We will henceforth assume that our phase space has been *completed* by compactification via some special metric. In the following, it will be useful to consider both the *one-dimensional* system (12) and the infinite-dimensional system (14), simul-

taneously.

Case 1. $R > -\frac{1}{m_0} - Z$.

In this case, the behavior of both dynamical systems are simple: In the *one-dimensional system* there exists an attracting *fixed point*, or attracting *cycle*, which attracts all, or almost all trajectories. Correspondingly, in the *infinite-dimensional* system, the oscillations either vanish as $t \to \infty$, or tend to a periodic solution, as in Witt [5] and Nagumo and Shimura [6].

Case 2. $R < -\frac{1}{m_0} - Z$.

In this case, it is possible to observe *chaotic oscillations* in the *infinite-dimensional* system. The system can also have oscillations which vanish as $t \to \infty$, as well as stable *stepwise* periodic oscillations but only with period 2 (for example, when $R = 0$, or $R \doteq 0$). In addition, the infinite-dimensional system can also have a more complicated asymptotically-stable periodic solution of period 4. The corresponding solutions for the *one-dimensional* system are as follows: the 1-D map f has an attracting fixed point, an attracting cycle of period 2, or an attracting cycle of period 4, which occurs after a period-doubling bifurcation.

If we exclude the above classes of solutions, where it is possible to derive exact estimates, then only two other types of asymptotic behaviors can exist for the infinite-dimensional system (14); namely, *weak turbulent oscillations*, or *strong turbulent oscillations* [7, 8].

The simpler case of *weak turbulence* corresponds to the case where the 1-D map $f(\cdot)$ has an attracting cycle which attracts all trajectories except those which belong to the repeller, which is a *Cantor set* K consisting of unstable trajectories. It has a zero Lebesque measure (mes K = 0) but a positive Hausdorff dimension ($dim_H > 0$). If "p" is the period of a stable cycle of the *one-dimensional* system, then almost every trajectory of the *infinite-dimensional* system(i.e., almost all solutions of Eqs.(1)-(4) with $C_1 = 0$) will be asymptotically periodic with period p, and its ω-limit set is a *periodic* trajectory in the completed phase space. Each point of the limit trajectory is a multivalued (on some Cantor set) function graph which is a fractal set with a Hausdorff dimension $dim_H > 1$. The attractor of the *infinite-dimensional* system in this case consists of such periodic orbits of the same period.

The most complicated case of *strong turbulence* corresponds to the situation where the *one-dimensional* map f(·) has no attracting cycles and its attractor consists of one or several intervals where there is a smooth invariant measure μ. In this case, if we use the special metric defined in [4], then the following asymptotic behavior applies:

The ω-limit set of almost every trajectory of the infinite-dimensional system(14) is a periodic trajectory where each point on the trajectory is a *random* function. The distribution of the values of such a random function for each x is determined by the measure μ. Hence, in this case, the *attractor of the infinite-dimensional system consists of random functions*, which form periodic orbits. This phenomenon corresponds to a very strong "spatial chaos".

References

[1] L. O. Chua. The Genesis of Chua's Circuit. *Archiv fur Elektronik und Ubertragungstechnik*, 46(4):250–257, 1992.

[2] M. P. Kennedy. Robust op amp realization of Chua's circuit. *Frequenz*, 46(3–4):66–80, 1992.

[3] R. N. Madan (Guest Editor). *Special Issue on Chua's Circuit: A Paradigm for Chaos*, volume 3 of *Journal of Circuits, Systems, and Computers*. 1993.

[4] A. N. Sharkovsky and E. Yu. Romanenko. Ideal turbulence: Attractors of deterministic systems may lie in the space of random fields. *International Journal of Bifurcation and Chaos*, 2(1):31–36, 1992.

[5] A. A. Witt. On the theory of the violin string. *J. Technical Physics*, 6:1459–1470, 1936. (in Russian).

[6] J. Nagumo and M. Shimura. Self-oscillation in a transmission line with a tunnel diode. *Proceedings of the IRE*, pages 1281–1291, 1961.

[7] A. N. Sharkovsky and E.Yu. Romanenko. Problems of turbulence theory and iteration theory. In *Proc. of the European Conference on Iteration Theory (ECIT-91)*, pages 242–252, 1992. World Scientific Publisher, Singapore.

[8] A. N. Sharkovsky and Yu. L. Maistrenko and E.Yu. Romanenko. *Difference Equations and their Applications*. Kluwer Academic Publisher, 1993.

Theory and Its Applications (NOLTA '93)
Hawaii, U.S.A., December 5-10, 1993

DYNAMICAL SYNTHESIS OF CHUA CIRCUIT PHENOMENA

Ray Brown
Department of Mathematics, Howard University, Washington D.C. 20059

Abstract

In this paper we summarize the results of [1] where we demonstrated how to dynamically synthesize Chua circuit phenomena using a two-dimensional autonomous flow as a component in a three-dimensional autonomous flow in such a way that the resulting equations will have double scroll attractors similar to those observed experimentally in Chua's circuit. The value of this generalization is that: (1) it provides a *building block* approach to the construction of chaotic circuits from simpler two-dimensional components which are not chaotic by themselves. In so doing, it provides an insight into how chaotic systems can be built up from simple non-chaotic parts; (2) it illustrates a precise relationship between three-dimensional flows and one-dimensional maps.

Our constructions also show how to dynamically synthesize attractors similar to the Lorenz and Rössler attractors using only piecewise linear vector fields. As a result we have a method of producing the Lorenz and Rössler dynamics in a circuit without the use of multipliers. These results suggests that the generalized Chua equations are in some sense fundamental in that the dynamics of the three most important autonomous three-dimensional differential equations producing chaos are seen as variations of a single class of equations whose nonlinearities are generalizations of the Chua diode.

Introduction

In [1] we presented two generalizations of Chua's equations, referred to as type-I and type-II. Refer to that paper for details, derivations, and definitions. From type-I we derive the single scroll and one-dimensional maps and from type-II we derive Lorenz, Rössler, and vortex equations [3].

Type-I Equations

The dimensionless Chua equations can be recast into the form:

$$\begin{pmatrix} \dot{x}(t) \\ \dot{y}(t) \\ \dot{z}(t) \end{pmatrix} = \begin{bmatrix} -\alpha & \alpha & 0.0 \\ 1.0 & -1.0 & 1.0 \\ 0.0 & -\beta & 0.0 \end{bmatrix} \begin{pmatrix} x \\ y \\ z \end{pmatrix} - \alpha \begin{pmatrix} f(x) \\ 0.0 \\ 0.0 \end{pmatrix} \quad (1)$$

A more compact expression for $f(x)$ is given by $bx + 0.5(a-b)(|x+1.0| - |x-1.0|)$. Using this expression Eq. (1) simplifies to:

$$\dot{\mathbf{x}} = \begin{cases} \mathbf{A}(\alpha,\beta,b)(\mathbf{x}-\mathbf{k}) & \text{for } x \geq 1 \\ \mathbf{A}(\alpha,\beta,a)\mathbf{x} & \text{for} |x| \leq 1 \\ \mathbf{A}(\alpha,\beta,b)(\mathbf{x}+\mathbf{k}) & \text{for } x \leq -1 \end{cases} \quad (2)$$

where,

By deleting the middle region and changing coordinates Eq.(2) is transformed to:

$$\begin{pmatrix} \dot{x}(t) \\ \dot{y}(t) \\ \dot{z}(t) \end{pmatrix} = \begin{bmatrix} 0.0 & -9.876 & 0.0 \\ 1.0 & 0.334 & 0.0 \\ 0.0 & 0.0 & -3.9055 \end{bmatrix} \begin{pmatrix} x - a\,\mathrm{sgn}(u) \\ y - b\,\mathrm{sgn}(u) \\ z - c\,\mathrm{sgn}(u) \end{pmatrix} \quad (3)$$

where $a = 0.4455$, $b = -0.05445$, $c = 0.984$, and $u = x - 1.287y + z$.

The single scroll

We now use the fact that the vector field defined by Eq. (3) is an odd symmetric vector field and is invariant under the flip map $\mathbf{x} \rightarrow -\mathbf{x}$. This allows us to view the double scroll in Eq.(3) as a single scroll. In particular, whenever $\mathrm{sgn}(u)$ changes sign we apply the flip map and use the linear ODE:

$$\begin{pmatrix} \dot{x}(t) \\ \dot{y}(t) \\ \dot{z}(t) \end{pmatrix} = \begin{bmatrix} 0.0 & -9.876 & 0.0 \\ 1.0 & 0.334 & 0.0 \\ 0.0 & 0.0 & -3.9055 \end{bmatrix} \begin{pmatrix} x - a \\ y - b \\ z - c \end{pmatrix} \quad (4)$$

to continue the orbit. Note that the value of a, b, and c are the same as in Eq.(3).

Doing this amounts to *factoring* Eq.(3) into the form FT where the map T is determined by selecting an initial condition $\mathbf{x}_0$, integrating the above linear ODE until the solution starting at this initial condition reaches the boundary determined by the function $\mathrm{sgn}(u)$ and using this *final* condition as the value of $\mathrm{T}(\mathbf{x}_0)$. We continue the solution by applying the flip map, F, to this final condition and using this flipped value as the initial condition for the above ODE. The effect of doing this is exactly the same as the process used in the twist-and-flip maps of [2]. In this way we are able to plot the entire double scroll of Eq.(3) on one side of the plane determined by the function $u = x - 1.287y + z = 0.0$ around only one of the fixed points, just as happens in using the twist-and-flip map.

Since we have separated out the stable manifold direction in the transformed equations we can examine the effect of increasing the contracting eigenvalue by considering the following equation instead of Eq.(3):

$$\begin{pmatrix} \dot{x}(t) \\ \dot{y}(t) \\ \dot{z}(t) \end{pmatrix} = \begin{bmatrix} 0.0 & -9.876 & 0.0 \\ 1.0 & 0.334 & 0.0 \\ 0.0 & 0.0 & -\gamma \end{bmatrix} \begin{pmatrix} x - a\,\mathrm{sgn}(u) \\ y - b\,\mathrm{sgn}(u) \\ z - c\,\mathrm{sgn}(u) \end{pmatrix} \quad (5)$$

In this equation the entry 3.9055 in Eq.(3) has been replaced by γ.

The effect of increasing γ is to flatten the scroll onto a pair of parallel planes. If we combine this with the folding operation, we get the single scroll obtained from using Eq.(5) with $u > 0$ combined with the flip. By letting $\gamma \to \infty$, the three-dimensional single scroll becomes a two-dimensional single scroll and can be studied in the plane.

The linear part of the two-dimensional single scroll is given by:

$$\begin{pmatrix} \dot{x}(t) \\ \\ \dot{y}(t) \end{pmatrix} = \begin{bmatrix} 0.0 & -9.876 \\ \\ 1.0 & 0.334 \end{bmatrix} \begin{pmatrix} x - 0.4455 \\ \\ y + 0.054 \end{pmatrix} \qquad (6)$$

The nonlinear part is supplied by the condition that we apply the flip map when $\mathrm{sgn}(x - 1.287y + 0.984) < 0.0$.

Equation (6) is solved by

$$\begin{aligned} x(t) &= \exp(\alpha t/2)\left[(x_0 - a)\cos(\omega t) + C_1 \sin(\omega t)\right] + a \\ y(t) &= \exp(\alpha t/2)\left[(y_0 - b)\cos(\omega t) + C_2 \sin(\omega t)\right] + b \end{aligned} \qquad (7)$$

where

$$\begin{aligned} C_1 &= -(0.5\alpha(x_0 - a) + \beta(y_0 - b))/\omega \\ C_2 &= -((x_0 - a) + 0.5(y_0 - b))/\omega \end{aligned}$$

and $\alpha = 0.334$, $\beta = 9.876$, $\omega = \sqrt{\beta - (0.5\alpha)^2}$, a, b are as in Eq.(3).

One-dimensional maps

The two-dimensional single scroll maps the line $y = (x - 0.984)/1.287$ to its image under the flip map. For initial conditions of the form $0.3 \leq x \leq 0.85$ and $y = (x - 0.984)/1.287$, a segment of this line is mapped into itself. There are two fixed points on this line segment: $(0.54, -0.347)$ and $(0.6876, -0.2293)$. We have now associated Eq.(2) with a one-dimensional map of a segment of the line $y = (x - 0.984)/1.287$ onto itself.

$$\begin{pmatrix} \dot{x}(t) \\ \\ \dot{y}(t) \\ \\ \dot{z}(t) \end{pmatrix} = \begin{bmatrix} s & -1.0 & 0.0 \\ \\ 1.0 & s & 0.0 \\ \\ 0.0 & 0.0 & -\gamma \end{bmatrix} \begin{pmatrix} x - a\,\mathrm{sgn}(u) \\ \\ y - b\,\mathrm{sgn}(u) \\ \\ z - \mathrm{sgn}(u) \end{pmatrix} \qquad (8)$$

where $u = z - x$, and a, b are any real constants, and s is a positive constant.

This form of the type-I generalized Chua equations based on the analysis of [6] reveals the role of the two-dimensional flow that defines the local unstable manifold located at the fixed point (a,b,1). This two-dimensional flow is given by the equation:

$$\begin{pmatrix} \dot{x}(t) \\ \\ \dot{y}(t) \end{pmatrix} = \begin{bmatrix} s & -1.0 \\ \\ 1.0 & s \end{bmatrix} \begin{pmatrix} x - a \\ \\ y - b \end{pmatrix} \qquad (9)$$

which defines a source which spirals outward from the critical point (a,b). If, as in [6], we use Eq.(9) as the two-dimensional single scroll, and in place of the line $y = (x - 0.984)/1.287$ we

use the line $x = -1$ as the line at which we apply the flip map, then we obtain a mapping of the line $x = -1$ onto itself and the entire analysis of Misiurewicz [6] is available for analyzing these equations.

The single scroll construction can be carried out with any two-dimensional flow which always crosses the line $x = 1$ given an initial condition on the line $x = -1$. Such flows are easy to construct:

EXAMPLE

We use the following variation on Duffing's equation:

$$\ddot{x} - s\dot{x} + x^3 = 0$$

where $s > 0$ rather than $s \leq 0$ which usually defines Duffing's equation. The result of choosing s positive is to make the critical point of the equation a source rather than a sink.

We rewrite Duffing's equation in a matrix form with the critical point translated to the point (a, b):

$$\begin{pmatrix} \dot{x}(t) \\ \dot{y}(t) \end{pmatrix} = \begin{bmatrix} 0.0 & -1.0 \\ (x-a)^2 & s \end{bmatrix} \begin{pmatrix} x-a \\ y-b \end{pmatrix} \qquad (10)$$

The type-I generalized Chua equation from which we may obtain a double scroll based on this variation on Duffing's equation is given by:

$$\begin{pmatrix} \dot{x}(t) \\ \dot{y}(t) \\ \dot{z}(t) \end{pmatrix} = \begin{bmatrix} 0 & -1.0 & 0.0 \\ U & s & 0.0 \\ 0.0 & 0.0 & -\gamma \end{bmatrix} \begin{pmatrix} x - a\,\mathrm{sgn}(u) \\ y - b\,\mathrm{sgn}(u) \\ z - \mathrm{sgn}(u) \end{pmatrix} \qquad (11)$$

where $U = (x - a\,\mathrm{sgn}(u))^2$, and where a, b, s, and u are the same as for Eq.(8).

Figure 1 is the double scroll produced by Eq.(11). In this figure $a = -0.5$, $b = 0.5$, $s = 0.17$, $\gamma = 100.0$. The initial conditions are $(-1.0, 0.1, 1.0)$. ■

Type-II Equations

In the previous section we have seen one method for extending the Chua equations based on using two-dimensional flows as building blocks of double scrolls. In this section we illustrate a generalization in an entirely different direction.

The Rössler dynamics

The Rössler dynamics can be obtained from a type-II generalized Chua equation as shown in [1]. Following that analysis we obtain an equation of the form

$$\dot{X} = \mathbf{A}(u)(X - F(u))$$

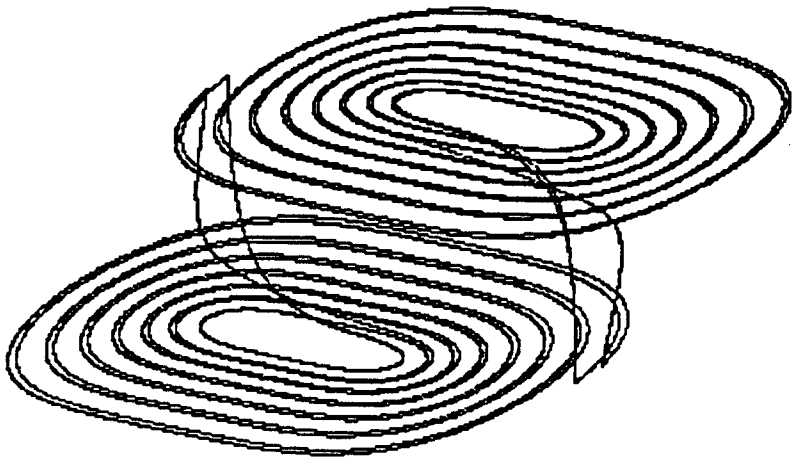

Figure 1: Double scroll for the type-I generalized Chua equation using a Duffing oscillator as the two-dimensional vector field for the two-dimensional single scroll.

where,

$$\mathbf{A} = \begin{bmatrix} 0.0 & -1.0 & -1.0 \\ 1.0 & 0.398 & 0.0 \\ (2+\lambda\, g(u))/0.398 & 0.0 & -2.0+\lambda\, g(u) \end{bmatrix}$$

and $u = x - y^2$.

Using $F(u)$ and $\mathbf{A}$ gives the desired type-II generalized Chua equation.

The Lorenz dynamics

We now illustrate that the Lorenz-like dynamics can be obtained from a type-II generalized Chua equation. The Lorenz equations are in [1].

We choose F as:

$$F(\mathbf{x}) = \begin{bmatrix} x_0\, g(x) \\ x_0\, g(x) \\ 27.0 \end{bmatrix}$$

We now generate the nonlinear matrix $\mathbf{A}$ from the linear part of the vector field:

$$\mathbf{A} = \begin{bmatrix} -10.0 & 10.0 & 0.0 \\ 1.0 & -1.0 & x_0\, g(x) \\ -x_0\, g(x) & -x_0\, g(x) & -2.7 \end{bmatrix}$$

where, as in the Rössler map, $g(x)$ is given by Eq.(7), and $\gamma = 3.0$. Figure 2 is the attractor for this map.

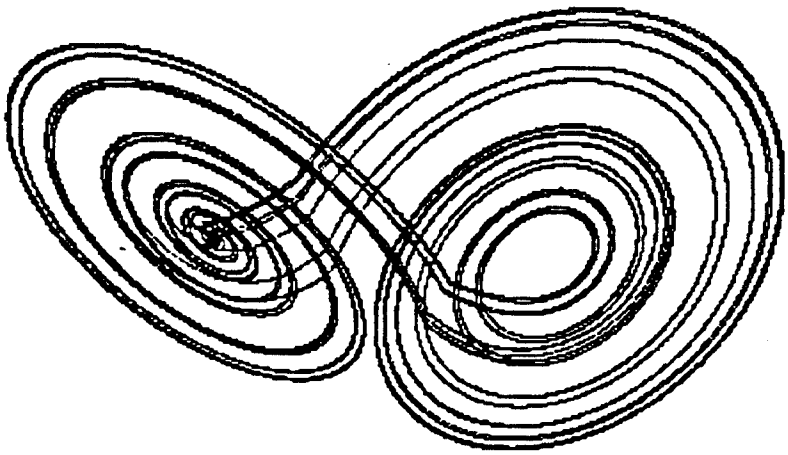

Figure 2: An attractor with Lorenz-like dynamics from a type-II generalized Chua equation.

In this case we were able to take $u = x$ since the transition from one linear region to the other takes place when $x = 0$, that is the surface of transition is the $y - z$ plane, and provides the natural surface for defining the Poincaré map.

References

[1] Brown, R. [1992] "Generalizing the Chua Equations," Int. J. Bifurcation and Chaos **2**(2).

[2] Brown, R. & Chua, L. [1991] "Generalizing the Twist and Flip Paradigm," Int. J. Bifurcation and Chaos **1**(2), 385-416.

[3] Brown, R. & Chua, L. [1991] "Chaos or Turbulence", Int. J. Bifurcation and Chaos **2**(4), 1005-1009.

[4] Chua, L. O. [1992] "The Genesis of Chua's Circuit," *Archiv für elektronik und Ubertragungstechnik*, vol. 46,no. 4, pp250-257.

[5] Chua, L. O., Komuro, M. & Matsumato, T. [1986] "The Double Scroll Family," IEEE Transactions on Circuits and Systems, Vol. CAS-33, pp.1073-1118.

[6] Misiurewicz, M. [1993] "Unimodal interval maps obtained from the modified Chua equations" Int. J. Bifurcation and Chaos **3**(2), 323-332.

1993 International Symposium on Nonlinear
Theory and Its Applications (NOLTA '93)
Hawaii, U.S.A., December 5-10, 1993

Some Analytical Results from Chua's Circuit

C. P. Silva

The Aerospace Corporation
Electronics and Sensors Division, Mail Station: M1-111
P.O. Box 92957
Los Angeles, CA 90009-2957
E-mail: silva@aerospace.aero.org (internet)

In addition to the double-scroll attractor originally found in the dynamics of Chua's circuit, we have discovered a *double-hook attractor* whose structure can be compared to that of the familiar Lorenz attractor. We have generalized the study of this attractor in Chua's circuit to a complete qualitative investigation of the *double-hook family* $\mathcal{F}_s$ of three-region, piecewise-linear, continuous vector fields on $\mathbf{R}^3$. Selected formal results and descriptions will be given concerning (1) the relationship between $\mathcal{F}_s$, the corresponding *double-scroll family* already reported in [1], and Chua's circuit; (2) the simplification techniques used, which are generic to a piecewise-linear analysis; (3) the qualitative properties of the Poincaré map that characterizes the dynamics of $\mathcal{F}_s$; (4) the existence of "horseshoe chaos" for a member of $\mathcal{F}_s$, proved using an extended heteroclinic version of Shil'nikov theory; and (5) the extension of our findings to the complementary *dual double-hook family.*

1. INTRODUCTION

1.1. Chua's circuit and the double-scroll family

Chua's circuit has become a paradigm for chaos in the field of nonlinear circuits because of its simplicity, its rich panorama of dynamical behavior, and the fact that it is amenable to a formal piecewise-linear analysis. The circuit, shown in Figure 1(a), is seen to be entirely linear except for the piecewise-linear resistor $\mathcal{R}$, whose typical odd-symmetric and locally active I-V characteristic is as in Figure 1(b).[a] The behavior of this circuit has been studied extensively on all fronts: numerically, experimentally, and analytically. The former two types of investigations, first done in [2], revealed the existence of a new *double-scroll strange attractor*, so-called because cross-sectional views displayed two rolled-up scrolls formed by the chaotic orbits. The investigators in [2] proceeded in [1] to perform a formal, qualitative piecewise-linear analysis of the general *double-scroll vector field family*, which includes the governing dynamical vector field for Chua's circuit (with appropriate circuit parameters) as a special case. This work included one of the few formal proofs of chaos that applied a piecewise-linear extension of Shil'nikov's basic theory [3].

1.2. The double-hook attractor and family

Complementing the efforts outlined above, a numerical study conducted by this author discovered a *double-hook strange attractor* [see Figure 1(c)] in Chua's circuit as well, with

[a] For practical implementations, $\mathcal{R}$ will have to be eventually passive—but for simulations of bounded chaotic behavior, this requirement can be avoided.

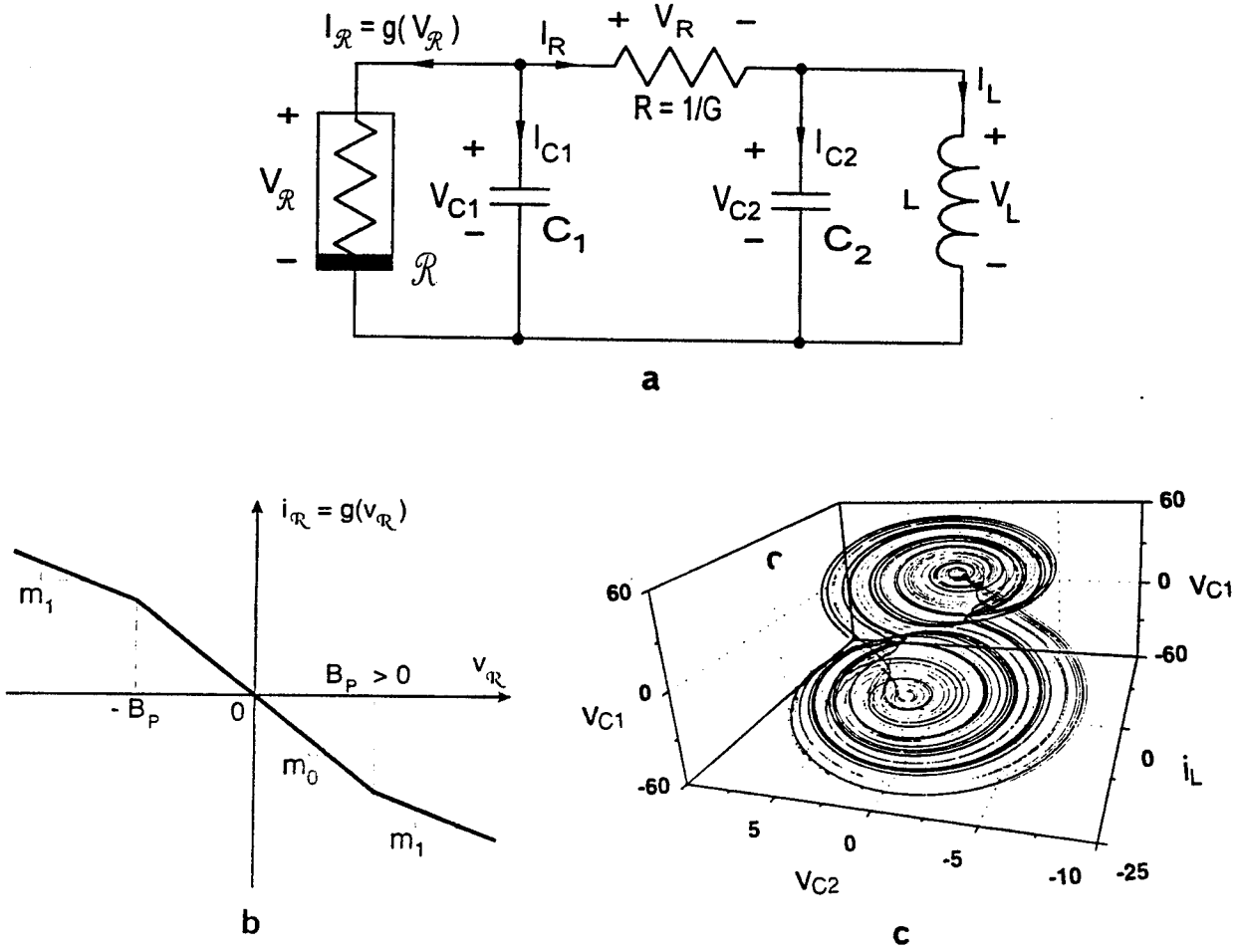

Figure 1. *Chua's circuit and its behavior. (a) Circuit topology with i_L reversed to conform to the standard associated reference convention. (b) Piecewise-linear I-V characteristic for the nonlinear resistor $\mathcal{R}$. (c) Computer simulation of the double-hook attractor in the v_{C_1}-v_{C_2}-i_L phase space.*

a characteristic cross-sectional structure made up of two "fishhooks" in tandem. Further numerical study and experimental verification can be found in [4], where the experimental work was conducted on an equivalent, but more easily realized circuit. In parallel with [1], an exhaustive qualitative treatise on the corresponding general *double-hook vector field family* $\mathcal{F}_s$ has been completed and published in [5]. An abridged form of these results is given in [6], from which the mainly descriptive discussion here is a further abstraction. Among the many findings formally demonstrated, a unique existence proof for the observed chaotic behavior was achieved using another piecewise-linear extension of Shil'nikov's basic work.

The following formal definitions establish the foundation for our presentation:

Definition 1.1 (Piecewise-linear vector field family $\mathcal{F}_s$) *Denote by $\mathcal{F}$ the family of continuous vector fields $\xi : \mathbf{R}^3 \to \mathbf{R}^3$ such that:*

(1) *ξ is odd-symmetric about the origin, that is, $\xi(-\mathbf{x}) = -\xi(\mathbf{x})$ for all $\mathbf{x} \in \mathbf{R}^3$.*

(2) *There are two distinct parallel planes U_1 and U_{-1} that are reflection-symmetric about*

the origin; these partition $\mathbf{R}^3$ *into three regions* $\mathcal{R}_i$ $(i = -1, 0, 1)$ *that include their boundary planes.*

(3) *In each region* $\mathcal{R}_i$ $(i = -1, 0, 1)$, $\boldsymbol{\xi}$ *is affine, that is,*

$$D\boldsymbol{\xi}(\mathbf{x}) = \mathsf{M}_i \ \forall \mathbf{x} \in \mathcal{R}_i, \tag{1}$$

where $D\boldsymbol{\xi}(\mathbf{x})$ *is the derivative of* $\boldsymbol{\xi}$ *at* $\mathbf{x}$, *and* M_i *is a real constant* 3×3 *matrix.*

(4) *The dynamical system*

$$\dot{\mathbf{x}} = \boldsymbol{\xi}(\mathbf{x}), \ \mathbf{x} \in \mathbf{R}^3 \tag{2}$$

possesses three distinct equilibrium points: one at the origin in $\mathrm{int}(\mathcal{R}_0)$; *one at* $P^+ \in \mathrm{int}(\mathcal{R}_1)$; *and one at* $P^- \in \mathrm{int}(\mathcal{R}_{-1})$, *which is the reflection of* P^+ *through the origin.*

(5) *The matrix* M_0 *has three real eigenvalues:* η_0, μ_0, *and* ν_0, *with* $\eta_0\mu_0 > 0$ *and* $\eta_0\nu_0 < 0$. *The matrices* $\mathsf{M}_{\pm 1}$ *each have two complex conjugate eigenvalues* $\sigma_1 \pm j\omega_1$ $(\omega_1 > 0)$ *and a real eigenvalue* $\gamma_1 \neq 0$.

(6) *The eigenspaces associated with either the real or complex eigenvalues (the latter are spanned by the real and imaginary parts of the complex eigenvectors) at each equilibrium point are not parallel to* $U_{\pm 1}$.

Definition 1.2 (Double-hook family $\mathcal{F}_s$) *Let* $\mathcal{F}$ *be as in Definition 1.1. The* **double-hook family** $\mathcal{F}_s$ *is the subfamily of* $\mathcal{F}$ *such that*

$$\eta_0 < 0, \ \mu_0 < 0, \ \nu_0 > 0, \ \sigma_1 > 0, \ \textit{and} \ \gamma_1 < 0. \tag{3}$$

Figure 2 illustrates the geometry of a typical vector field in $\mathcal{F}$, where $E^r(P^{\pm})$ denotes the eigenlines passing through $P^{\pm}$ associated with the eigenvalue γ_1; $E_1^r(0)$ $[E_2^r(0)]$ is the eigenline (eigenplane) passing through $\mathbf{0}$ associated with the eigenvalues ν_0 (η_0 and μ_0), respectively; and $E^c(P^{\pm})$ denotes the eigenplane passing through $P^{\pm}$ associated with the eigenvalues $\sigma_1 \pm j\omega_1$. In the case of $\mathcal{F}_s$, we see from (3) that $E^r(P^{\pm})$ and $E_2^r(0)$ will denote stable eigenspaces, while $E^c(P^{\pm})$ and $E_1^r(0)$ will constitute unstable ones. Recall that these eigenspaces are *invariant* to the flow of (2), thereby making the eigenplanes an impenetrable dynamical barrier that separates the phase space into *orbit cells.* (The other features presented in the figure will be discussed below.) In contrast to the double-scroll family, the equilibrium point for $\mathcal{F}_s$ at the origin is a saddle-stable node instead of a saddle-stable focus. This gives $\mathcal{F}_s$ an eigenvalue distribution (and stability) that matches the one for the Lorenz system in its chaotic regime of operation (see [7]); however, the symmetry of the outer two equilibria here is slightly different, in that their third coordinate switches sign—instead of remaining constant as it does in the Lorenz system.

The first important result of this study was the formal demonstration that the governing dynamical vector field for Chua's circuit can be a member of $\mathcal{F}_s$ for the appropriate circuit parameters. Indeed, we have the following result:

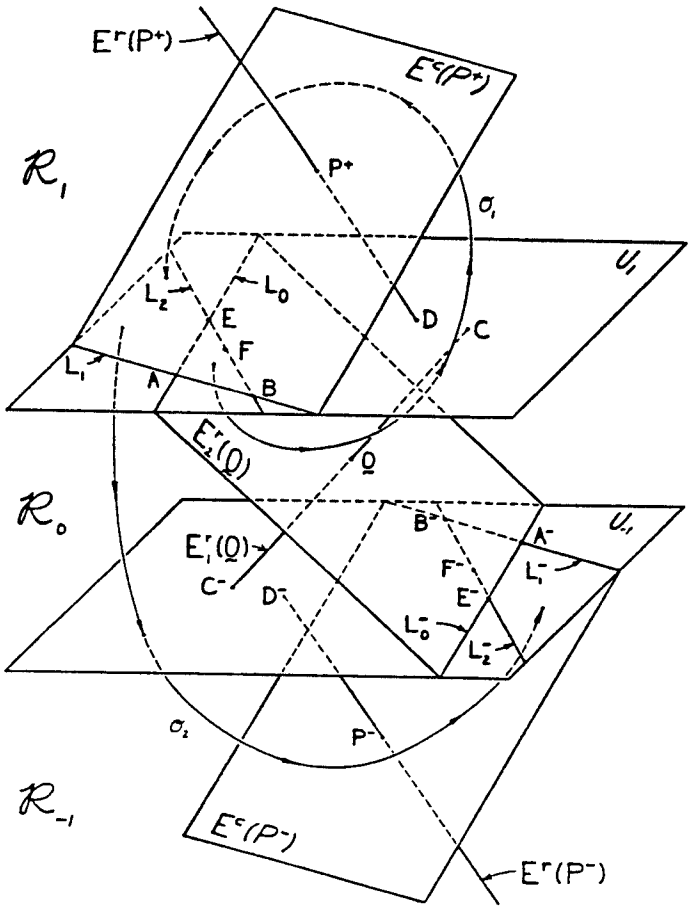

Figure 2. *Piecewise-linear geometry of a typical member $\xi \in \mathcal{F}_s$. It is the complex dynamical interplay between the three regions $\mathcal{R}_i$ $(i = -1, 0, 1)$, and their subdivision by the invariant eigenplanes, that leads to the complex behavior exhibited by the vector fields in $\mathcal{F}_s$.*

Proposition 1.1 (Chua's circuit and $\mathcal{F}_s$) *With the following circuit parameters,*[b]

$$\left.\begin{aligned} &m_0 = -1.34\,\mho,\ m_1 = -0.5\,\mho,\ B_p = 1\,\mathrm{V} \\ &C_1 = -0.067\,\mathrm{F},\ C_2 = 0.302\,\mathrm{F},\ R = \tfrac{1}{G} = 1.86\,\Omega,\ \textit{and} \\ &L \in J_L := (L_l, L_u) := (-348.2664\,\mathrm{mH}, -149.2570286\ldots\,\mathrm{mH}) \end{aligned}\right\} \qquad (4)$$

the governing vector field ξ in (2) for Chua's circuit is a member of $\mathcal{F}_s$.

2. PIECEWISE-LINEAR ANALYSIS OF $\mathcal{F}_s$

In addition to the eigenspaces already identified in Figure 2, and the obvious intersections presented in the figure, several other features are worthy of note. The special lines $L_2^{\pm}$ indicate the unique set of points where the vector field is parallel to $U_{\pm 1}$, and is thus an important boundary for the qualitative dynamics of $\mathcal{F}_s$. The points $F^{\pm}$ on $L_2^{\pm}$ mark another important delineation by representing the unique point where the vector field is parallel

[b]The negativity of L and C in (4) indicates that they must be active elements. The equivalent *double-hook circuit* in [4] would have no such element values; only one negative linear resistor is needed in addition to the usual nonlinear one.

to $L_2^{\pm}$. The sample orbits $\mathcal{O}_1$ and $\mathcal{O}_2$ indicate the two basic types of qualitative behavior possible for $\mathcal{F}_s$. Together with the crosshatched wedge-shaped region, these orbits serve as the basis for the Poincaré map presented below.

Before a full qualitative study of $\mathcal{F}_s$ could be undertaken, several simplifications and dynamical devices were used that are generic to any piecewise-linear analysis. The first feature to take advantage of here was the symmetry property (1) in Definition 1.1. This allowed the focus of our study to be restricted to regions $\mathcal{R}_0$ and $\mathcal{R}_1$ (which include the boundary planes $U_{\pm 1}$), since what occurs in region $\mathcal{R}_{-1}$ is simply the reflection through **0** of what takes place in region $\mathcal{R}_0$.

The next step was to break up $\mathcal{F}_s$ into *equivalence classes* (that is, subfamilies) whose members would be related by having qualitatively identical flows. This so-called *linear equivalence* was conveniently shown to be indicated by the equality of the following five *normalized eigenvalue parameters*, which are derived from the eigenvalues in (3):

$$\hat{\eta}_0 := \frac{\eta_0}{\mu_0} > 0,\ \hat{\nu}_0 := \frac{\nu_0}{\mu_0} < 0,\ \hat{\sigma}_1 := \frac{\sigma_1}{\omega_1} > 0,\ \hat{\gamma}_1 := \frac{\gamma_1}{\omega_1} < 0, \text{ and } k := -\frac{\nu_0}{\gamma_1} > 0. \quad (5)$$

With these linear equivalence classes defined, it was sufficient to study only one representative member of each class to know the qualitative properties of the whole class. Such a member, which required a minimum number of parameters, was constructed; that member is formally termed the *double-hook vector field.* To be more specific, the *double-hook system* is given by (2), with (i) $\boldsymbol{\xi}$ of the canonical form

$$\boldsymbol{\xi}(\mathbf{x}) = \mathsf{A}\mathbf{x} + (|z-1| + |z+1|)\mathbf{b}, \quad (6)$$

where $\mathsf{A} \in \mathbf{R}^{3\times 3}$ and $\mathbf{b} \in \mathbf{R}^3$ are functions of the eigenvalue parameters in (5); and (ii) canonical regions $\mathcal{R}_i$ $(i = -1, 0, 1)$ given by

$$\mathcal{R}_{-1} = \{\mathbf{x} \in \mathbf{R}^3 : z \le -1\},\ \mathcal{R}_0 = \{\mathbf{x} \in \mathbf{R}^3 : |z| \le 1\},\ \mathcal{R}_1 = \{\mathbf{x} \in \mathbf{R}^3 : z \ge 1\}. \quad (7)$$

The final simplification involved a time-scale change plus the linear and affine transformations of regions $\mathcal{R}_0$ and $\mathcal{R}_1$, respectively, into new coordinate settings (denoted by $\mathcal{R}_0'$ and $\mathcal{R}_1'$, respectively), so that the original vector field $\boldsymbol{\xi}$ and its associated piecewise-linear geometry were further simplified. The details of this process can be found in [6]. In essence, the resulting *canonical dynamical vector fields* $\hat{\boldsymbol{\xi}}_i'$ $(i = 0, 1)$ are of a Jordan-form structure, with elements depending on the six parameters in (5) plus the parameter $\alpha_0 := \eta_0 = \mu_0$ when $\hat{\eta}_0 = 1$. In addition, an *interconnection map* Θ is constructed that links $\mathcal{R}_0'$ and $\mathcal{R}_1'$ through their common boundary U_1 in the original coordinates. All the transformed geometry has been completely specified; the subsequent qualitative analysis focused on the following transformed dynamical systems:

$$\frac{d\mathbf{x}_i'}{d\tau_i} = \hat{\boldsymbol{\xi}}_i'(\mathbf{x}_i') \ \ (i = 0, 1);\ \tau_0 := -\mu_0 t,\ \tau_1 := \omega_1 t, \quad (8)$$

where $\mathbf{x}_i'$ represents the new coordinate system in region $\mathcal{R}_i'$.

The qualitative dynamical study of $\mathcal{F}_s$ was accomplished through the use of Poincaré maps. These maps provide a convenient means to reduce the study of the 3-D flow produced by (8) to that of a 2-D mapping between appropriate planes. Returning to Figure 2, we can define an overall Poincaré map whose cross section is the U_1-plane and whose domain $\hat{\mathcal{D}}$ is the closure of the open half-plane U_1^d, which is bounded by L_2 and denotes where $\boldsymbol{\xi}$ points

down into region $\mathcal{R}_0$ (containing the crosshatched region shown). Note that both orbits $\mathcal{O}_1$ and $\mathcal{O}_2$ denote recurrent behavior, as is needed to define this Poincaré map. Indeed, this is clear for $\mathcal{O}_1$, while the portion of $\mathcal{O}_2$ in $\mathcal{R}_{-1}$ has a symmetrically reflected portion in $\mathcal{R}_1$ that returns to $\hat{\mathcal{D}}$, as needed for recurrence. In the transformed coordinate setting, we denote the overall Poincaré map by π, consisting of two half-maps: π_0 describes the dynamics in $\mathcal{R}_0'$, and π_1 characterizes the behavior in $\mathcal{R}_1'$. The half-map π_0 further breaks down into two component half-maps: π_0^+ (π_0^-) corresponds to the orbits in $\mathcal{R}_0$ that return (transfer) to U_1 (U_{-1}) [as a result of the dynamical barrier $E_2^r(0)$], as suggested by the first part of the orbit $\mathcal{O}_1$ ($\mathcal{O}_2$) in Figure 2.

A whole host of formal properties were discovered and demonstrated for the Poincaré half-maps $\pi_0^{\pm}$ and π_1, many of which were only simulated for the double-scroll system in [1]. In particular, the findings identified and described important geometrical features for $\hat{\boldsymbol{\xi}}_i'$, identified and described transit-time properties for the flows of (8), and proved several qualitative properties for $\pi_0^{\pm}$ and π_1. Because of the limits on our current discussion, the nature and complexity of the results obtained, and our primary concern with the proof of chaos, we will again have to defer the interested reader to [6] for the details. However, we will mention the important image properties that were found for the Poincaré half-maps. Both π_0^+ and π_0^- were shown to have a *hook image property*, that is, images of appropriate lines in their domains had the qualitative shape of solution curves to a node-type equilibrium point in their ranges. This result rigorously justified the end-to-end fishhook structure found for the double-hook attractor in region $\mathcal{R}_0$. Similarly, the half-map π_1 possessed a *spiral image property*, in that the corresponding images were qualitatively like solution curves to a focus-type equilibrium point.

Before the proof of chaos can be accomplished, the overall Poincaré map π needs to be defined as follows:

$$\pi(\mathbf{x}') := \Theta \circ \pi_1^{-1} \circ \Theta^{-1} \circ \pi_0(\mathbf{x}'),\ \mathbf{x}' \in \mathcal{D} := \mathrm{cl}(V_0^d), \tag{9}$$

where V_0^d is the transformation of U_1^d and π_1^{-1} is the inverse of π_1. Finally, an extension $\tilde{\pi}^{-1}$ of π_1^{-1} must also be defined to capture all of the double-hook system's behavior (see [6] for this definition and [5] for all the qualitative features found for π and $\tilde{\pi}^{-1}$, including the relationship between their fixed points and the presence of homoclinic, heteroclinic, and periodic orbits in the original dynamics of $\mathcal{F}_s$).

3. PROOF OF CHAOS USING HETEROCLINIC SHIL'NIKOV METHOD

The basic theory of Shil'nikov provides one of the few analytical tools available to prove the existence of chaos in dynamical systems.[c] The original system studied by Shil'nikov consisted of a third-order autonomous one containing a saddle-focus-type equilibrium point $\mathbf{x}_e$ (with characteristic eigenvalues γ and $\sigma \pm j\omega_1$, where $\gamma\sigma < 0$ and $\omega_1 \neq 0$) and a trajectory $\mathcal{H}$ doubly asymptotic to it (that is, as time approaches $\pm\infty$), called a *homoclinic orbit*. For our purposes here, a piecewise-linear extension of Shil'nikov's basic result is needed (based on [3]). In this case we have a *heteroclinic loop* $\mathcal{H}_l$ connecting two distinct saddle-foci $\mathbf{x}_{ei}$ ($i = 1, 2$) made up of two *heteroclinic orbits* $\mathcal{H}_i$, each of which is time-asymptotic to both equilibria. Formally, we have the following result:

[c] A tutorial overview of basic Shil'nikov theory and its extensions can be found in [8].

Theorem 3.1 (Heteroclinic Shil'nikov method) *Given the third-order autonomous system*

$$\dot{\mathbf{x}} = \boldsymbol{\xi}(\mathbf{x}), \tag{10}$$

where $\boldsymbol{\xi}$ is a piecewise-C^2 vector field[d] on $\mathbf{R}^3$. Let $\mathbf{x}_{e1}$ and $\mathbf{x}_{e2}$ be two distinct saddle-focus-type equilibrium points for (10) that do not lie on any boundary surface of any piece. Suppose that

(i) *the characteristic eigenvalues of $\mathbf{x}_{ei}$ satisfy the* **Shil'nikov inequality**

$$|\gamma_i| > |\sigma_i| > 0 \ \ (i = 1, 2) \tag{11}$$

and the further constraint

$$\sigma_1 \sigma_2 > 0 \ \ or \ \ \gamma_1 \gamma_2 > 0; \tag{12}$$

and

(ii) *there is a heteroclinic loop $\mathcal{H}_l$ joining $\mathbf{x}_{e1}$ and $\mathbf{x}_{e2}$ that consists of two heteroclinic orbits $\mathcal{H}_i$ $(i = 1, 2)$, which are bounded away from any equilibria other than $\mathbf{x}_{ei}$ and are not tangent to any boundary surface of any piece.*

Then the system (10) will exhibit **horseshoe chaos** *that is* **structurally stable**, *that is, it remains in existence for any sufficiently small C^1-perturbation $\boldsymbol{\zeta}$ of $\boldsymbol{\xi}$.[e]*

Applying Theorem 3.1 to $\mathcal{F}_s$, we arrive at the following concluding result:

Theorem 3.2 (Horseshoe chaos in $\mathcal{F}_s$) *Given the governing vector field $\boldsymbol{\xi}$ in (2) for Chua's circuit with parameters as in (4), except that the set J_L is replaced with the subset[f]*

$$I_L := (\tilde{L}_l, \tilde{L}_u) := (-348.2664\,\mathrm{mH}, -290.222\,\mathrm{mH}). \tag{13}$$

Then there exists a small subinterval of L in I_L over which the dynamics of

$$\dot{\mathbf{x}} = \boldsymbol{\xi}(\mathbf{x}; L) \tag{14}$$

exhibits horseshoe chaos.

A discussion of the proof of Theorem 3.2 is in order. By Proposition 1.1 and the definition of I_L in (13), it follows that $\boldsymbol{\xi}$ in (14) is a member of $\mathcal{F}_s$ for all $L \in I_L$. In addition, using the monotonicity and continuity properties of the normalized eignevalues in I_L, one can show that $\boldsymbol{\xi}$ in (14) satisfies conditions (11) and (12) for all $L \in I_L$. To demonstrate the existence of the heteroclinic loop $\mathcal{H}_l$, the map $\tilde{\pi}^{-1}$ mentioned above is shown to have a first-order fixed point in an appropriate portion of L_1', the transformed version of L_1 in $\mathcal{R}_0'$. This is accomplished through a series of formal lemmas that can be found in [6]. Figure 2 dynamically represents the essential proof process: the intersection of the inverse image of the point D with the plane U_{-1} is monitored as the inductance L is varied in I_L and is shown to cross the portion of L_1' to the right of the point A^-. Under further appropriate conditions on this intersection point, which is seen to lie in the stable (with respect to reverse time) eigenplane $E^c(P^-)$, the orbit will spiral in on P^-, forming a heteroclinic orbit between P^+ and P^-. By odd symmetry, the reflection of this orbit through the origin is the other heteroclinic orbit, which

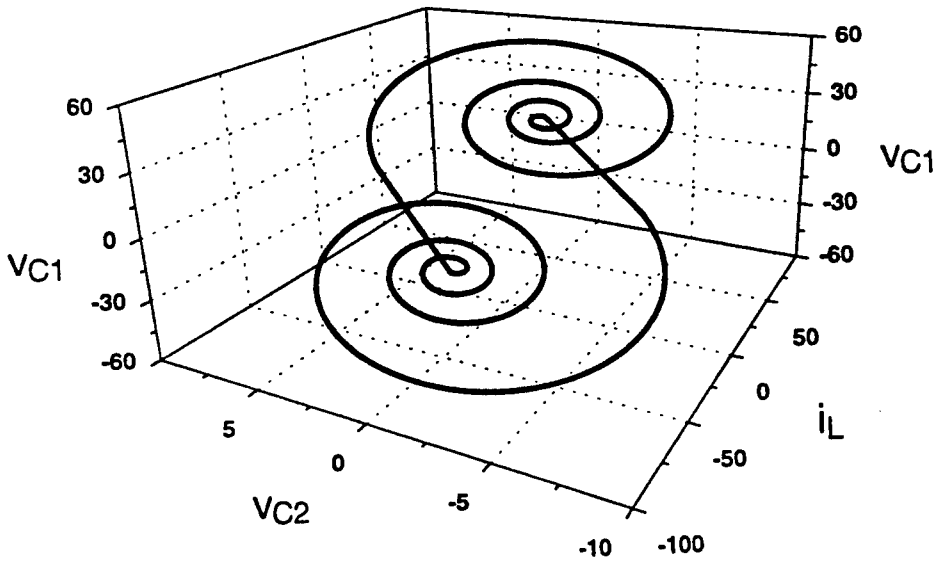

Figure 3. *Computer simulation of a heteroclinic loop $\mathcal{H}_l$ in the dynamics of Chua's circuit (when the latter is also a member of $\mathcal{F}_s$). This loop serves as the seed for the chaos exhibited in Figure 1(c), for example, and is analytically detected by means of the heteroclinic Shil'nikov method.*

completes the loop $\mathcal{H}_l$. Figure 3 gives a simulation of the heteroclinic loop $\mathcal{H}_l$ found using a value of L near $-313\,\text{mH}$, which is just a mere $2\,\text{mH}$ away from the value $-315\,\text{mH}$ used to obtain the double-hook attractor in Figure 1(c). We conjecture that all strange attractors for $\mathcal{F}_s$ share the presence of homoclinic orbits or heteroclinic loops in the dynamics of nearby systems. With this, Theorem 3.1 is satisfied and Theorem 3.2 is proved.

4. CONCLUSIONS

We have presented a descriptive summary of an extensive qualitative study of the double-hook family $\mathcal{F}_s$ of three-region, continuous, and piecewise-linear vector fields on $\mathbf{R}^3$. Our accomplishments included (1) the proof that Chua's circuit can be a member of $\mathcal{F}_s$ for the appropriate circuit parameters, (2) the discovery of the double-hook attractor in the dynamics of Chua's circuit, (3) the development and administration of an exhaustive piecewise-linear analysis for $\mathcal{F}_s$, and (4) the proof that $\mathcal{F}_s$ can exhibit chaos using an extension of Shil'nikov's basic results. In addition to all this, [5] shows that most of these results can be extended to the complementary *dual double-hook family* $\mathcal{F}_s^*$, which is the subfamily of $\mathcal{F}$ in Definition 1.1, such that [compare with (3)]

$$\eta_0 > 0,\ \mu_0 > 0,\ \nu_0 < 0,\ \sigma_1 < 0,\ \text{and}\ \gamma_1 > 0. \tag{15}$$

[d]By a piecewise-$\mathcal{C}^2$ vector field, we mean one that is $\mathcal{C}^2$ (twice differentiable with a continuous derivative) on regions whose union is $\mathbf{R}^3$.

[e]Horseshoe chaos is a formal term that guarantees certain qualitative properties normally associated with chaos, such as the existence of an uncountable number of nonperiodic orbits. By a $\mathcal{C}^1$-perturbation, we essentially mean that $\|\xi - \zeta\|$ and its first derivative are sufficiently small in a neighborhood containing $\mathcal{H}_l$.

[f]Equation (13) is a correction of (44) in [6, first printing].

We also note that vector fields in the complement of $\mathcal{F}_s \cup \mathcal{F}_s^*$ in $\mathcal{F}$ cannot exhibit chaos through the Shil'nikov mechanism, since in this case $\sigma_1\gamma_1 \geq 0$ and so $P^{\pm}$ *cannot* be saddle-foci. The study of $\mathcal{F}_s^*$ would be a good future endeavor, since Chua's circuit is known to be a member of $\mathcal{F}_s^*$ for a large set of parameter values.

ACKNOWLEDGMENTS

I thank Prof. Leon O. Chua for suggesting the submission of this paper. I also thank Michael T. Meyer of The Aerospace Corporation for lending his editorial assistance. Finally, the preparation and presentation of this conference paper was generously supported by the Aerospace Sponsored Research program.

REFERENCES

1. L. O. Chua, M. Komuro, and T. Matsumoto, *IEEE Trans. Ckts. Sys.* **CAS-33** (1986) 1072.
2. T. Matsumoto, L. O. Chua, and M. Komuro, *IEEE Trans. Ckts. Sys.* **CAS-32** (1985) 797.
3. C. Tresser, preprint, Univer. Nice, 1982. Abridged in *Annales de l'Institute Henri Poincaré* **40** (1984) 441.
4. P. Bartissol and L. O. Chua, *IEEE Trans. Ckts. Sys.* **35** (1988) 1512.
5. C. P. Silva, *Chaos in the Double-Hook Family: An Application of Shil'nikov Theory*, Ph.D. dissertation, University of California, Berkeley, 1993.
6. C. P. Silva, in *Chua's Circuit: A Paradigm for Chaos*, World Scientific, Singapore, 1993.
7. C. Sparrow, *The Lorenz Equations: Bifurcations, Chaos, and Strange Attractors*, Vol. 41, *Appl. Math. Sci.*, Springer-Verlag, New York, 1982.
8. C. P. Silva, *IEEE Trans. Ckts. Sys. I* **40** (1993), in press.

1993 International Symposium on Nonlinear
Theory and Its Applications (NOLTA '93)
Hawaii, U.S.A., December 5-10, 1993

Controlling chaos in Chua's circuit

M.J. Ogorzałek[a*]

[a]Department of Electrical Engineering,
University of Mining and Metallurgy,
al. Mickiewicza 30, 30-059 Kraków, Poland

Using the Chua's circuit, often referred to as a paradigmatic system for studying chaotic behavior, we present various techniques developed for controlling chaotic behavior. In particular several methods for suppressing chaotic oscillations and influencing the system in such a way as to achieve a desired type of goal dynamics (typically a fixed point or periodic orbit) are considered. We describe parameter variation technique, chaotic oscillation absorber, linear feedback control and stabilisation of unstable periodic orbits. Possibilities for the realization of chaos controllers are discussed.

1. INTRODUCTION

During the last five years we observed a tremendous increase of interest in possible applications of chaotic systems. In particular many research groups around the world concentrate on possibilities of controlling chaotic behavior i.e. influencing the dynamic behavior of the system to produce a desired kind of motion which could be, depending on actual needs, fixed, periodic or even another type of chaotic state [1-2], [8-15], [20–22], [24-25]. Due to very rich dynamic phenomena encountered in typical chaotic systems, there exists also a large variety of approaches to controlling such systems. Chua's circuit [3–4], [18-19] seems to be the most appropriate system for studying chaos control techniques. Exhibiting an abundance of dynamic regimes and chaotic attractors, sufficiently well understood theoretically and offering extreme flexibility in performing laboratory experiments this circuit proves to be most versatile when compared to other chaotic systems. Below we present a selection of methods developed for controlling chaos in various aspects – starting from the most primitive concepts like parameter variation, through classical controller applications (open– and closed–loop control), to quite sophisticated ones like stabilisation of unstable periodic orbits embedded within the strange attractor.

The state equations describing the dynamics of the canonical Chua's circuit read:

$$\begin{aligned} C_1\frac{dv_{C_1}}{dt} &= G(v_{C_2}-v_{C_1}) - G_b v_{C_1} - \tfrac{1}{2}(G_a-G_b)(|v_{C_1}+v_{bp}|-|v_{C_1}-v_{bp}|) \\ C_2\frac{dv_{C_2}}{dt} &= G(v_{C_1}-v_{C_2}) + i_L \\ L\frac{di_L}{dt} &= -v_{C_2} - R_0 i_L \end{aligned} \tag{1}$$

(where: v_{bp} - coordinate of the breakpoint of the piecewise linear characteristic, G_a and G_b are its inner and outer slopes respectively), or in normalised form:

$$\begin{aligned} \dot{x} &= \alpha[y-x-g(x)] \\ \dot{y} &= x-y+z \\ \dot{z} &= -\beta y+\gamma z \end{aligned} \tag{2}$$

*This research has been supported by the University of Mining and Metallurgy, grant 11.120.15

Throughout this study we use classical Chua's circuit i.e. $R_0 = 0$ ($\gamma = 0$).

2. PARAMETER VARIATION TECHNIQUES

The simplest possible but not very efficient method is parameter variation. To understand its principle one has to consider typical bifurcation diagrams showing how the circuit behavior changes when some parameter is being varied. Having a system (Chua's circuit) operating in a chaotic mode, looking at the bifurcation diagrams, it is possible to choose a new set of parameter values to cause a different type of behavior. We can do it either choosing the new values for the desired steady state from the bifurcation diagrams or by trial–and–error. The most important drawback of such a method is that a large parameter variation is usually needed and in fact we have to redesign the system. For Chua's circuit this means eg. changing one of the resistors, replacing a capacitor or fixing a different coil. This is not acceptable in many applications.

3. "OSCILLATION ABSORBER" CONCEPT

The principle of operation of this method is based on such a modification of the original chaotic system that a new stable orbit appears in a neighbourhood of the original attractor. This modification is introduced via a simple addition of the "absorber" to the existing system without major changes in the design or construction of the considered system. Kapitaniak, Kocarev and Chua [15] proposed such an "chaotic oscillation absorber" for Chua's circuit. The "absorber" could be for example a parallel RLC circuit coupled with original Chua's circuit via a resistor.

4. CONTROL ENGINEERS STRATEGIES

There exists a variety of control engineering approaches for the stabilisation of chaotic dynamical systems. Some of these methods have been tested using Chua's circuit. Hartley and Mossayebi [13] applied clasical PI and PID controllers obtaining satisfactory results. Genesio and Tesi [12] used a scheme based on the harmonic balance technique for suppression of chaos in Chua's circuit. Interesting developments are also due to Chen and Dong [2] who applied a static linear feedback controller enabling stabilisation of chaotic motion in Chua's circuit. Using the linear feedback method, Chen and Dong [2] were able to stabilise the chaotic trajectories directing them towards the saddle–type unstable limit cycle coexisting with the chaotic attractor.

5. CONTROLLING CHAOS VIA IMPULSES

A very promising method for controlling chaos has been developed recently [8], [9]. The principle of this method is based on finding a suitable forcing for a Lur'e type dynamical system to force it to follow any desired kind of periodic orbit uncovered from the chaotic attractor. The authors observed that such forcing exists and can be applied at discrete time moments only (impulse control). Using this method Dedieu and Ogorzałek were able to direct chaotic orbits in Chua's circuit towards several chosen periodic orbits of various lengths.

6. STABILIZATION OF UNSTABLE PERIODIC ORBITS

This method of controlling chaos is based on the key property of chaotic attractors namely the existence of a dense set of unstable periodic orbits in the attractor. Various aspects of the method were elaborated in a series of papers [24], [25], [11]. Some implementation aspects have been discussed in [14] and first successful application have been reported in [5], [26], [27].

Let us assume that the dynamics of the system is described by a map $\xi_{n+1} = f(\xi_n, p$ ($x_n \in R^m$, p - some accessible, variable parameter). Let ξ_F – chosen fixed point (unstable) of the map f of the system existing for the parameter value p^*. In the close vicinity of this fixed point with good accuracy we can assume that the dynamics is linear and can be expressed approximately by:

$$\xi_{n+1} - \xi_F = M(\xi_n - \xi_F) \tag{3}$$

The elements of the matrix M can be calculated using the least squares technique on the basis of measured chaotic time series and analysis of its behavior in the vicinity of the fixed point. Let λ_s, λ_u denote eigenvalues, and e_s, e_u eigenvectors of this matrix. Denoting by f_s, f_u the contravariant eigenvectors ($f_s e_s = f_u e_u = 1$, $f_s e_u = f_u e_s = 0$) we can find the linear approximation valid for small $|p_n - p^*|$:

$$\xi_{n+1} = p_n g + [\lambda_u e_u f_u + \lambda_s e_s f_s][\xi_n - p_n g] \tag{4}$$

where: $g = \frac{\partial \xi_F(p)}{\partial p}|_{p=p^*}$.

We would like to force ξ_{n+1} to fall on the stable manifold of ξ_F. This is achieved with p_n such that $f_u \xi_{n+1} = 0$:

$$p_n = \frac{\lambda_u \xi_n f_u}{(\lambda_u - 1) g f_u} \tag{5}$$

Using an application–specific software package [6] we were able to find some of the unstable periodic orbits embedded in the double scroll chaotic attractor. We have also implemented and tested the OGY method for controlling chaos in Chua's circuit [6].

7. CHAOS CONTROLLERS

7.1. Implementation of the OGY method

We have implemented the OGY method for controlling chaos in a laboratory Chua's circuit [7]. Fig. 1 shows the structure of the laboratory environment built for controlling chaos in Chua's circuit. The controller in this case consists of an interface circuitry for measuring chaotic time series, software package implemented on a personal computer and hardware for injecting the control signal back into the circuit. All the calculations needed are implemented in the software. The user can interactively choose the goal of control (one of the unstable orbits detected).

Using this kind of computerised feedback control we were able to stabilize low period orbits only. When applying the OGY method in a real physical circuit the main problem encountered was the noise associated with the inevitable noise of the circuit elements, A/D and D/A conversion of signals (quantisation), rounding operations in the computer calculations etc. The method was found to be very sensitive to the noise level – very small control signals sometimes are hiden within the noise and control is impossible. For successful implementation of this method some hardware developments specific for the purpose are needed and are currently being constructed. This includes a hardware Poincare section identifier which

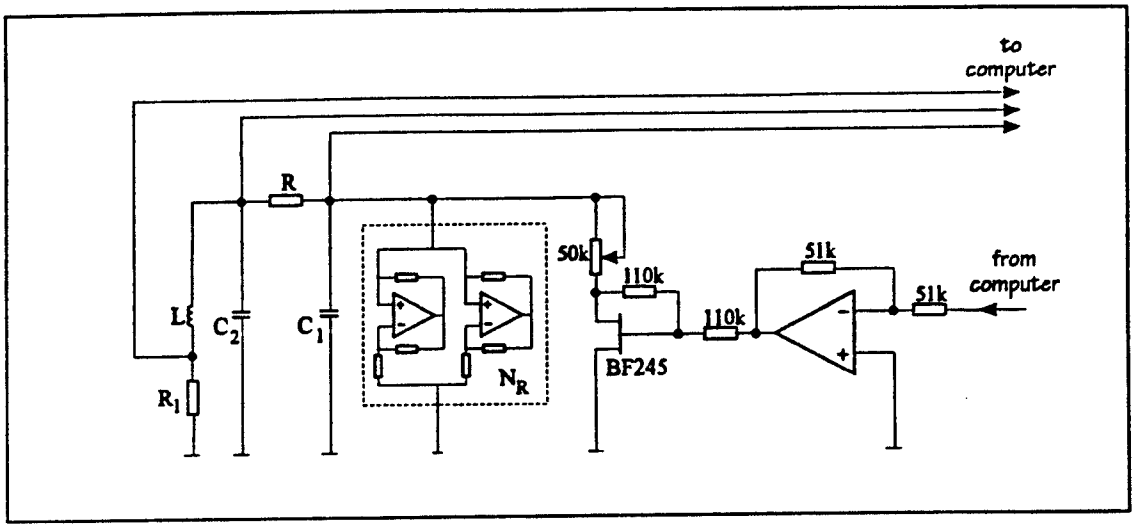

Figure 1. Diagram of the laboratory system for controlling Chua's circuit using OGY method (stabilisation of unstable periodic orbits).

will calculate the coordinates of the successive points in real time and an ϵ-comparator as the signal injection block. These hardware blocks will increase the accuracy and limit the time delays in the feedback loop.

7.2. Occasional Proportional Feedback method

Johnson and Hunt have built a simplified circuitry for controlling chaos in Chua's circuit [14]. Their method can be considered as a "one-dimensional" OGY with external synchronisation. The block diagram of the control system is shown in Fig.2. There are basically two main blocks: the Poincare section identifier (window comparator, Sample-and Hold etc.) and control signal generator (timing block, gain block, voltage-controlled resistor etc.). The external synchronising signal is provided as a reference for the desired type of periodic orbit. Using this system it is possible to stabilise many different periodic orbits in Chua's circuit [14]. This hardware implementation has however one major drawback compared to the full OGY method - it is not possible to specify beforehand the goal of the control. Stabilizable orbits are known only on the basis of trial-and-error. It should be mentioned that similar implementations were used in stabilizing chaos for example in a chaotic laser [5], [27], which enabled the performance of the laser to be raised by a factor of 10.

8. CONCLUSIONS

Using Chua's circuit as the object of investigations we have demonstrated a selection of available chaos control methods. The simplest ones are attractive because of their extremely simple principle of operation and the fact that any of the stable operating modes can be chosen. Suppression of chaotic oscillations is achieved without feedback and control signals. However usually some kind of redesign of the system is required (either in terms of large changes of parameters or building additional subsystems). In many practical situations such changes in the design are not allowed. In many cases the goal behavior must be chosen by

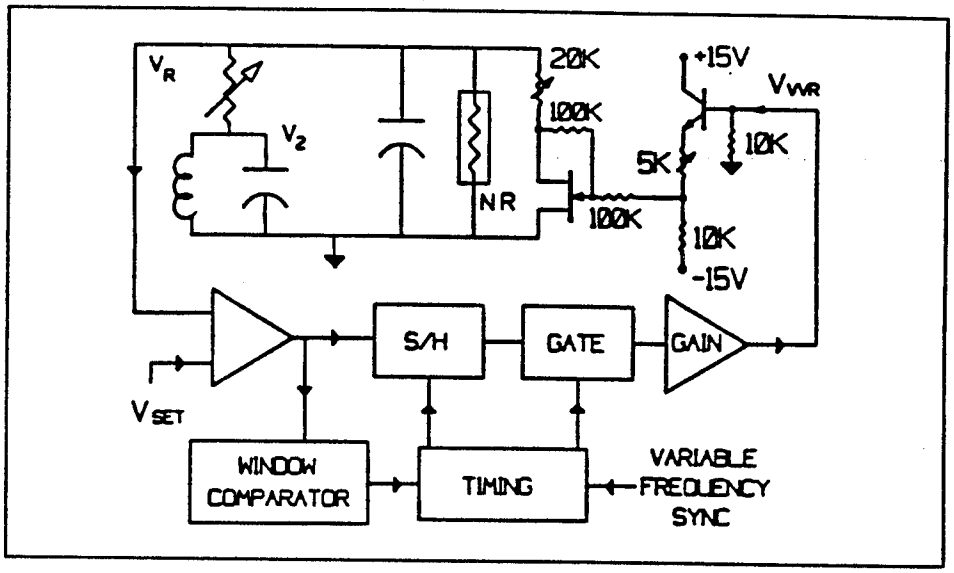

Figure 2. Electronic system for implementation of the occasional proportional feedback (OPF) for controlling chaos in Chua's circuit

trial–and–error – the bifurcation behavior in real physical systems is difficult to learn.

Several methods used by control engineers can be successfully applied to controlling chaos in Chua's circuit and other chaotic systems. The controller has typically a very simple structure and does not require any access to system parameters. The method might be difficult to apply in real systems (interactions of many system variables needed).

Among the known methods the OGY technique seems to be most attractive. It does not require any model of the system, operates on the experimental measurements only and takes advantage of the inherent property of chaotic systems - existence of an infinite number of unstable periodic orbits. Thus the goal of the control already exists in the system!! We found however that in the presence of noise and error inevitable in real applications the method is often not functional. In real applications so far the OPF method has been confirmed to be most reliable and operational despite the fact that the stabilized orbit can be chosen in an experimental way only.

Interested reader is referred to survey papers [1] and [21] for further details and extensive list of references.

REFERENCES

1. G. Chen, X. Dong, "From Chaos to Order - Perspectives and Methodologies in Controlling Chaotic Nonlinear Dynamical Systems", Int. J. Bif. Chaos, vol.3, Dec. 1993.
2. G. Chen and X. Dong, "Controlling Chua's circuit", J. Circuits, Systems and Computers, vol.3, pp.139-149, 1993.
3. L.O.Chua "The genesis of Chua's circuit". Archiv für Elektronik und Übertragungstechnik, vol.46, No.4, pp.250-257, 1992.
4. L.O. Chua, "Global unfolding of Chua's circuit". IEICE Trans. Fundamentals, Vol.E76-A, No.5, pp.704-734, 1993.

5. E. Corcoran, "Kicking Chaos out of Lasers", Scientific American, No.11, 1992, pp. 19.
6. A. Dąbrowski, Z. Galias and M.J. Ogorzałek, "A Study of Identification and Control in a Real Implementation of Chua's Circuit", System Structure and Control - 2nd IFAC Workshop, Prague 1992, pp. 278—281.
7. A. Dąbrowski, Z. Galias and M.J. Ogorzałek, L.O.Chua, "Laboratory Environment for Controlling Chaotic Electronic Circuits" Proc. ECCTD'93, H. Dedieu Ed., vol.1, pp.867-872, Elsevier, 1993.
8. H. Dedieu, M.J. Ogorzałek, "Simple and robust method for controlling chaotic systems", (preprint 1993).
9. H. Dedieu, M.J. Ogorzałek, "Controlling chaos in Chua's circuit via impulses", (preprint 1993)
10. W.L. Ditto, L.M. Pecora, "Mastering Chaos", Scientific American, No.8, 1993, pp.62-68.
11. U. Dressler and G. Nitsche, "Controlling Chaos Using Time Delay Coordinates", Phys. Rev. Letters, vol. 68, No. 1, pp. 1—49, 1992.
12. R. Genesio and A. Tesi, "Distortion Control of Chaotic Systems: The Chua's circuit", J. Circuits, Systems aand Computers, vol.3, No.1, pp.151-171, 1993.
13. T.T. Hartley and F. Mossayebi, "Control of Chua's circuit", J. Circuits, Systems and Computers, vol.3, No.1 , pp.173-194, 1993.
14. G.A. Johnson, T.E. Tigner and E.R. Hunt, "Controlling chaos in Chua's circuit", J. Circuits, Systems and Computers, vol.3, pp.109-117, 1993.
15. T. Kapitaniak, L. Kocarev and L.O. Chua, "Controlling chaos without feedback and control signals", Int. J. Bif. and Chaos, vol.3, No.2, pp.459-468, 1993.
16. R.N. Madan, (ed.), "Chua's Circuit; A Paradigm for Chaos". World Scientific 1993.
17. K. Murali and M. Lakshmanan, "Controlling of Chaos in the Driven Chua's Circuit", preprint 1992.
18. M.J.Ogorzałek: "Chaotic regions form double scroll". IEEE Transactions on Circuits and Systems, vol.CAS- 34, 1987, No.2, pp.201- 203.
19. M.J.Ogorzałek: "Bifurcations and chaos in Chua's circuit - A state- of- the- art review". World Congress of Nonlinear Analysts , Tampa 1992, (in press)
20. M.J.Ogorzałek, "Taming Chaos: Part I - Synchronisation", IEEE Trans. Circuits and Systems, vol. CAS-40, No.10, 1993.
21. M.J. Ogorzałek, "Taming Chaos: Part II - Control", IEEE Trans. Circuits and Systems, vol. CAS-40, No.10, 1993.
22. M.J. Ogorzałek, "Chaos control techniques: A study using Chua's circuit", Proc. NDES'93, Dresden, 1993.
23. M.J.Ogorzałek, Z. Galias, "Characterisation of chaos in Chua's oscillator in terms of unstable periodic orbits" J. Circuits, Systems Comput., vol.3, No.2, pp.411-429, 1993.
24. E. Ott, C. Grebogi and J.A. Yorke, "Controlling Chaos", Phys. Rev. Letters, vol. 64, No. 11, pp. 1196—1199, 1990.
25. E. Ott, C. Grebogi and J.A. Yorke, "Controlling Chaotic Dynamical Systems", in Chaos: Soviet-American Perspectives on Nonlinear Science, D.K.Campbell ed., American Institute of Physics, New York 1990,
26. I. Peterson, "Ribbon of Chaos: Researchers develop a Lab Technique for snatching Order out of Chaos", Science News, vol. 139, No. 4, pp. 60—61, 1991.
27. R. Roy, T.W. Murphy Jr., T.D. Maier, Z. Gills and E.R. Hunt, "Dynamical Control of a Chaotic Laser: Experimental Stabilization of a Globally Coupled System", Phys. Rev. Letters, vol. 68, No.9, pp. 1259—1262, 1990.

1993 International Symposium on Nonlinear
Theory and Its Applications (NOLTA '93)
Hawaii, U.S.A., December 5-10, 1993

Theory of Confinors in Chua's Circuit

R. LOZI

Laboratoire de mathématiques, U.R.A. 168,
Université de Nice-Sophia Antipolis,
Parc Valrose, B.P. 71, 06108 Nice Cedex 2, France
e.mail: lozi@math.unice.fr

1 CHUA'S CIRCUIT : A PARADOXICAL SIMPLICITY

The purpose of this joint work with S.Ushiki from the Kyoto University, is to apply the new concept of confinors and anti-confinors, initially defined for ordinary differential equations constrained on a cusp manifold [1] to the equations governing the circuit dynamics of Chua's circuit.

Chua's circuit is a *physical* electronic circuit made up of four *linear* circuit elements (one resistor, one inductor and two capacitors) and a two-terminal *nonlinear resistor* (also called Chua's diode) characterized by a five-segment v-i curve [2] or just a three-segment v-i curve [3]. Depending on the choice of the v-i characteristic for Chua's diode, Chua's circuit can exhibit many distinct forms of strange attractors.

For researchers working in the field of dynamical systems it is astonishing that Chua's circuit affords a paradoxical simplicity in different ways.

First in spite of its intrinsic simplicity it exhibits an immensely rich variety of behaviors among the regular and strange behaviors of the dynamical systems. In fact, by adding a resistor in series with the inductor in Chua's circuit , one obtains a globally unfolded circuit with an even richer bifurcation landscape [3]-[4].

Secondly, although the solution of Chua's equation (the differential equation describing Chua's circuit) is explicitly known in every subspace D_1, D_0 and D_{-1} of the (X, Y, Z) variables space [5], the global solution remains unkown and can only be approached through numerical computations. Moreover, Chua's equation is dissipative. Depending on the value of the parameters, the volume contraction ratio could be very small. This explains why on most of the pictures showing one solution of Chua's equation, either obtained by numerical integration or by the display of the values of the physical variables on the oscilloscope, it is almost impossible to infer its actual structure.

Thirdly the accurate computation of the Poincaré map $\pi = \pi_1 \circ \pi_0$ using the brute force method is so difficult that most of the time only one-dimensional approximations of this map are analysed [5]-[6], thereby occulting important bifurcation phenomena and the precise structures of its strange attractors.

As an endeavour to go beyond this paradoxical simplicity and to understand the innermost features of Chua's equation, we apply our theory of confinors to the numerical analysis of the dynamics of this circuit. We find several interesting new results on Chua's equation:

- The coexistence of 3 distinct chaotic attractors for the *same value* of the parameters.

- The precise structure of 2D strange attractors (of the Poincaré map π).
- The unusual bifurcation phenomena which are not period-doubling as they could incorrectly appear in diagrams plotted with standard and hence inaccurate methods.

2 THE THEORY OF CONFINORS

The keystone of the initial definition of confinors is that very often , changes in the shape of experimentally observed signals are more significant in characterizing the phase portrait of dynamical systems defined by systems of ordinary differential equations constrained on a cusp manifold than any topological change between attractors, especially when chaotic regimes occur.

In the scope of the numerical analysis of such systems, the classical tools used by mathematicians in order to define and study chaos, which are very often related to the topological properties of the attractors,(e.g. topological entropy, invariant measures, fractal dimensions, power spectra, invariant manifolds, homoclinic orbits ...) are not easily tractable because they do not allow the use of exact analytic computations.

Then, if computers are used to identify such structures, one has to be very cautious in their results due to the sensitive dependence upon initial conditions for the chaotic solutions versus the truncation errors usually made by computers. Moreover, transient regimes are not easily explained in such a topological way, because it is not obvious to discriminate transient regimes from asymptotic ones in actual experiments.

The confinors and anticonfinors we introduced when we decided to break off from the paradigm of ω-limit sets have the following properties:
Taking into account the "shape" of the signal, they are able to model both transient and asymptotic regimes. They are tractable even in the presence of "chaos" or an infinite number of periodic ω-limit sets, and robust with respect to the approximate computation of the solutions of ODEs.For 2-D confinors in the phase space the proof of their existence is based on inequalities and can be reliably verified with a computer. Surprisingly our attempt to apply the theory of confinors to Chua's equation in order to prove the existence of 3-D confinors[7]-[8]-[9] has led us to a very accurate numerical method for the computation of the Poincaré map, and therefore to the following new results.

3 CO-EXISTING CHAOTIC CHUA'S ATTRACTORS

Thereafter we consider the following Chua's equation [7]:

$$\begin{cases} \dot{X} &= \alpha(Y - m_1 X + \frac{1}{2}(m_0 - m_1)[\mid X+1 \mid - \mid X-1 \mid]) \\ \dot{Y} &= X - Y + Z \\ \dot{Z} &= -\beta Y \end{cases} \tag{1}$$

Patterns in the time waveforms are very easily obtained for a large range of parameter values in Chua's equation. Such patterns consist of m *successive peaks* belonging to the upper sheet of the attractors, followed by n *successive peaks* on the lower sheet. The number of peaks is linked to the number of "turns" around some axis. We can compute the time spent in going from a point to some point. Dividing this time by the time needed to make an exact turn around the axis of rotational symmetry of the linear part of the vector field, we obtain an estimate of this *real* number of "turns".

If we have an estimate for this real number of "turns" for example, if we can have t_{min} and t_{max} such that

$$t_{min} \leq t \leq t_{max}$$

holds for all t needed in going from one set (e.g some part of the separating planes) into another set, it would describe some aspect of a pattern.

Actually the Poincaré map is divided into two half map π_0 and π_1 and the consequence of the existence of their main confinor for Chua's equation based on isochronic lines is the existence of τ_{min}, τ_{max}, θ_{min}, θ_{max} which allows a very accurate and novel numerical method for the computation of both π_0 and π_1.

Using this accurate numerical method, we find that for the values $\alpha = 15.60$, $\beta = 28.58$, $m_0 = \frac{-1}{7}$, $m_1 = \frac{2}{7}$, three different chaotic attractors coexist. The initial values used to define the global solutions of Eq.(1) attracted by one of these three attractors are:

For the "red" attractor [8] of Fig.1 $(X_0, Y_0, Z_0) = (-0.005, 0.017, 0.019)$; for the "blue" attractor of Fig.2 $(X_0, Y_0, Z_0) = (-0.002, 0.014, 0.010)$; for the "cyan" attractor of Fig.3 $(X_0, Y_0, Z_0) = (-0.008, 0.020, 0.028)$.

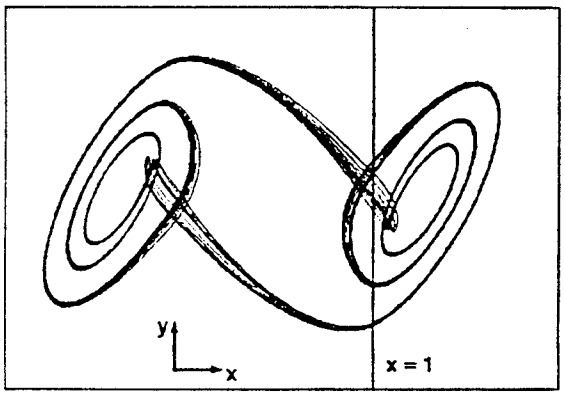

Figure 1.The "red" strange attractor.

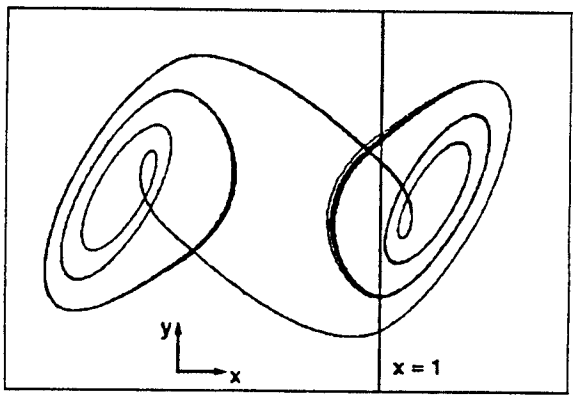

Figure 2.The "blue" strange attractor.

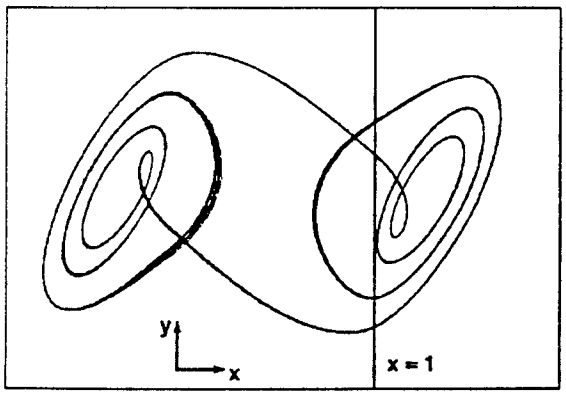

Figure 3.The "cyan" strange attractor.

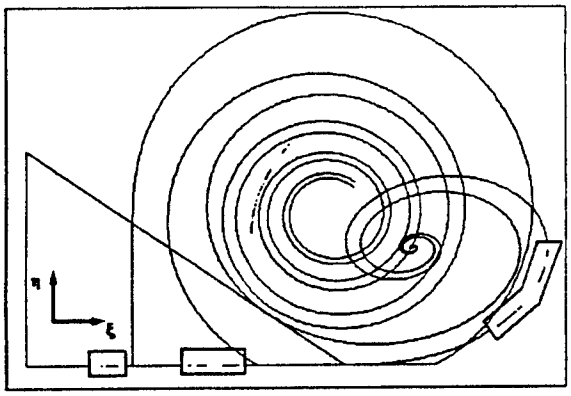

Figure 4.Poincaré map of the three attractors.

Though no mathematical proof of the existence is given, there is a strong evidence that the attractors remain distinct. This evidence is based on the computation of 60,000 iterations of the Poincaré map. We do not use integration methods which are not relevant due to their rounding errors in this case, because 60,000 iterates of π correspond to 60,000,000 steps of numerical integration.

4 PRECISE STRUCTURE OF 2-D STRANGE ATTRACTORS OF CHUA'S EQUATION

Using both the accurate numerical method for the computation of Chua's Poincaré map and a special method of a sequence of coordinate transforms based on the "Taylor expansion" of the Chua's strange attractors [9] we are able to identify the precise structures of the strange attractors of Chua's equation. In this short presentation paper it is not possible to develop the Taylor's coordinate system. Therefore we only present some results.

Figure 5 shows the projection in the (X, Y) plane of the strange attractor found for the parameter values of the normal form equation [7]: $\sigma_0 = -0.3176$, $\gamma_0 = 0.1289$, $\sigma_1 = 0.4122$, $\gamma_1 = -0.9287$, $k = 0.0960$.

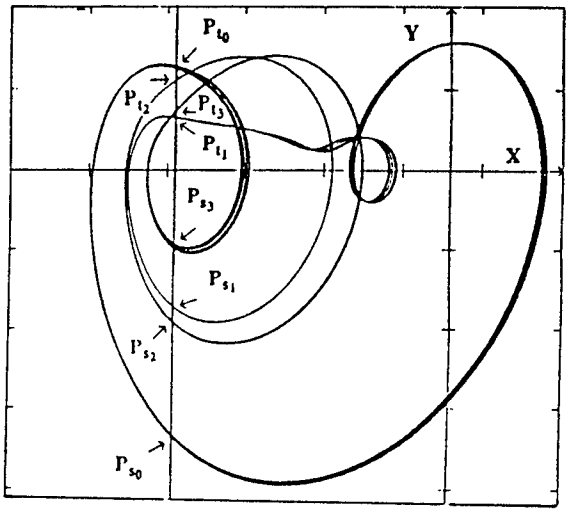

Figure 5.Projection in the (X, Y)-plane of the strange attractor.

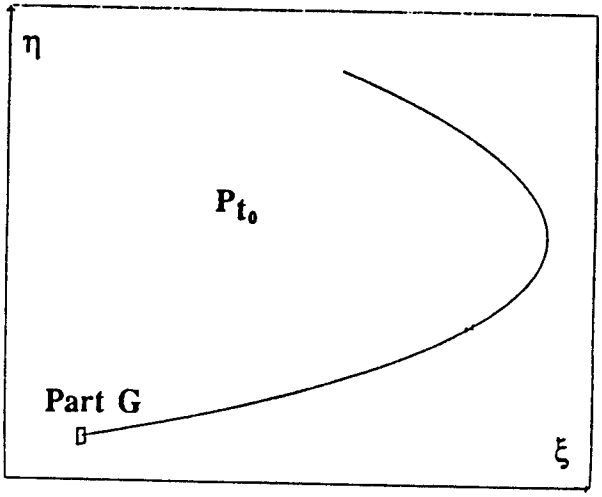

Figure 6.Magnification of the P_{t_0}.

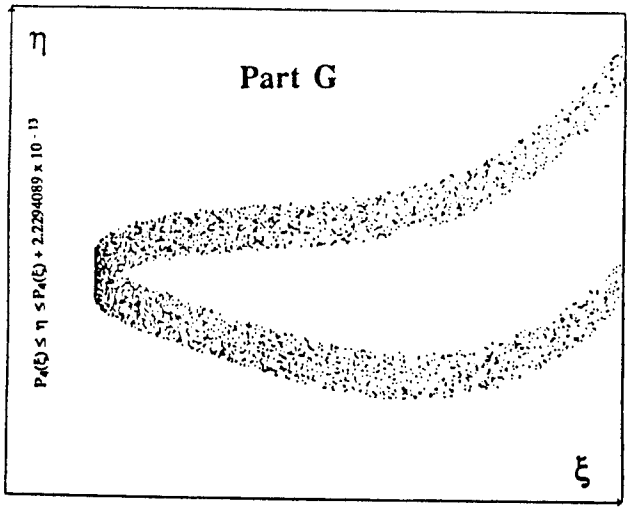

Figure 7.Enlargement of the lower left end point.

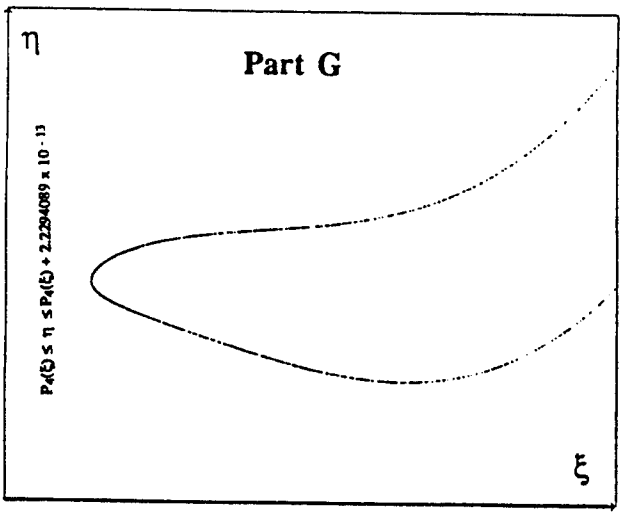

Figure 8.The same enlargement with an extended precision of order 10^{-16}.

Figure 6 shows the magnification of the Poincaré map of the piece P_{t_0}.The dissipative nature of Chua's equation gives rise to a very strong contraction such that the width of this strange attractor is about 10^{-12}. Figure 7 is an enlargement of part G of Figure 6 using our

method with a computation error of order 10^{-14}.The width of the ribbon does not reveal any particular mathematical structure but corresponds to the size of computation errors.We show in Fig.8 the same enlargement computed with a precision of order 10^{-16}.In both cases the computations are performed with extended real numbers in PASCAL for which nineteen figures are available.

These figures point out the power of our method with which it is possible to reveal for the first time the precise structure of the strange attractors of Chua's equation.

5 EXACT BIFURCATION DIAGRAMS FOR CHUA'S EQUATION

Finally, we point out unusual bifurcation phenomena for Chua's equation which are not period-doubling as they could incorrectly appear in diagrams plotted with standard and hence inaccurate methods , or using approximate one-dimensional Poincaré maps.

We show in Fig.9 the bifurcation diagram of Eq.(1).Chua's parameter values σ_0, γ_0, σ_1, k, are fixed as follows:$\sigma_0 = -0.325$, $\gamma_0 = 0.135$, $\sigma_1 = -0.3921$, $k = 0.1034$.

The abscissa of this figure represents the parameter γ_1 which varies between -0.86 and -0.83.The ordinate corresponds to ξ of the standard coordinate in the triangular region $\mathcal{T}$ [9].For each value of γ_1 we take an initial point in the triangular region and iterate the exact Poincaré map, obtained in the scope of the confinor theory, for this point to plot the ξ coordinate of the points on the orbit. In order to suppress the transient behavior, many iterations were executed before starting the plot.

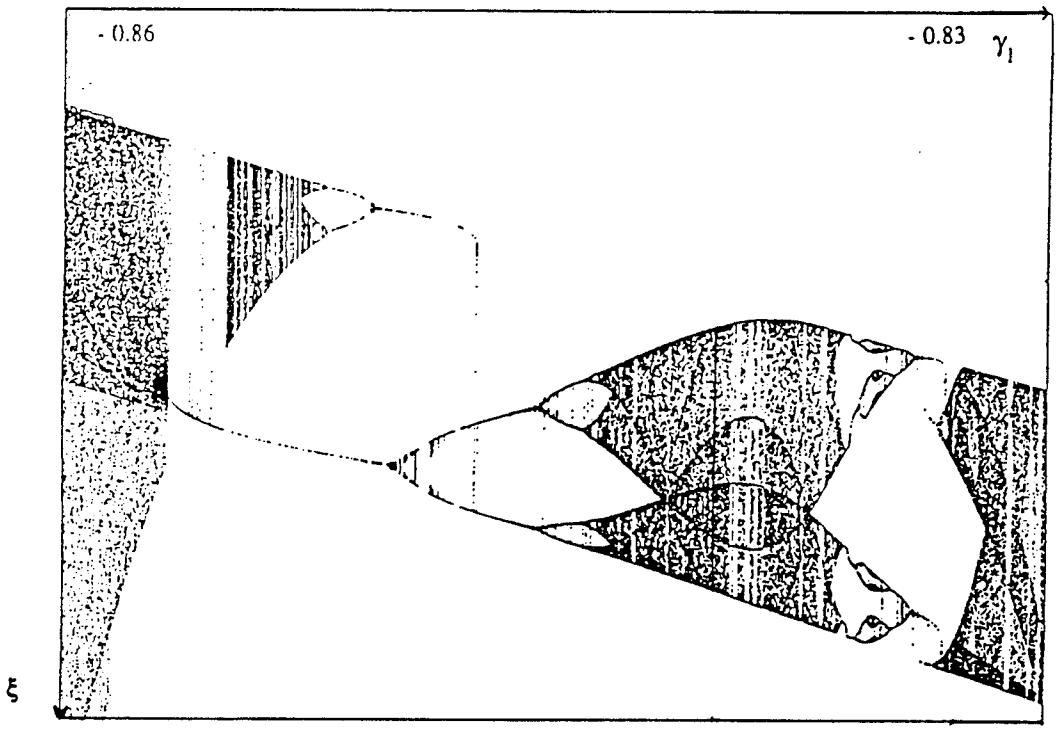

Figure 9.Exact Bifurcation Diagram of Chua's equation

In Fig.9, we observe the cascade of period-doubling sequence of bifurcations and the inverse cascade of bands of chaotic attractors which reminds us of the bifurcation of the family of unimodal maps.However the sequence of bifurcations shows some anomalies.

It is obvious that at least two attractors can coexist.The top-left corner shows a series of period-doubling cascade, while another attractor exist for the same values of parameters (the coexistence phenomenon with three attractors is explored in Sec.3).

Because the standard family of unimodal maps can have at most one attractor, it is not adequate to interpret this diagram.We need at least multimodal maps, or two-dimensional maps.

Another anomaly we observe in these figures is that the bifurcation and inverse bifurcation process is found not only in the relatively wide range interval of the parameters, but also in the small scale range.It is observed repeatedly, as we try enlargements of the bifurcation diagram, as this occurs in a *self-similar* manner.

6 CONCLUSION

Chua's equation seems surprinsingly rich in very new behaviors not yet reported even in other dynamical systems.The application of the theory of confinors to Chua's equation and the use of sequences of Taylor's coordinates could give new perspectives to the study of dynamical systems by uncovering very unusual behaviors not yet reported in the literature.The main paradox here is that the theory of confinors, which could appear as a theory of rough analysis of the phase portrait of Chua's equation, leads instead to a very accurate analysis of this phase portrait.

References

[1] Ushiki,S. and Lozi,R. [1987] *"Confinor and Anti-confinor in Constrained "Lorenz" System,"* Japan J. Appl.Math., 4(3), 433-454.

[2] Matsumoto,T.[1984] *"A chaotic attractor from Chua's circuit,"* IEEE Trans. Circuits Syst. **CAS-31**, 1055-1058.

[3] Chua,L.O.[1993] *"Global unfolding of Chua's circuit,"* I.E.I.C.E.Trans. of Electronics, Communications and Computer Sciences, E 76-A(5), 704-734.

[4] Chua,L.O.[1992] *"A zoo of strange attractors from the canonical Chua's circuits,"* Proc. of the 35th Midwest Symposium on Circuits and System, Washington D.C., August 10-12, 916-926.

[5] Chua,L.O., Komuro,M., and Matsumoto,T. [1986] *"The double scroll family,"* IEEE Trans. Circuits Syst. **CAS-33**, 1073-1118.

[6] Yang,L. and Liao,Y.L. [1987] *"Self-similar structures from Chua's circuit,"* Int.J. Circuit Theory Appl. **15**, 189-192.

[7] Lozi,R. and Ushiki,S. [1991] *"Confinors and bounded time-patterns in Chua's circuit and the double scroll family,"* Int. J. of Bifurcation and Chaos **1**(1), 119-138.

[8] Lozi,R. and Ushiki,S. [1991] *"Coexisting attractors in Chua's circuit,"* Int. J. of Bifurcation and Chaos **1**(4), 923-926.

[9] Lozi,R. and Ushiki,S. [1993] *"The theory of confinors in Chua's circuit : accurate analysis of bifurcations and attractors,"* Int. J. of Bifurcation and Chaos **3**(2), 333-361.

1993 International Symposium on Nonlinear
Theory and Its Applications (NOLTA '93)
Hawaii, U.S.A., December 5-10, 1993

Chaos-chaos intermittency and $1/f$ noise in Chua's circuit

V.S. Anishchenko, A.B. Neiman and M.A. Safonova

Physical Department, Saratov State University
Astrakhanskaya, 83, Saratov 410071, Russia

Abstract

Statistical and dynamical properties of the "chaos-chaos" type intermittency in Chua's circuit are studied by numerical simulation methods. It is shown that at the onset of this intermittency phenomenon, the power spectrum of the associated time series has the form of $1/f$ noise. The influence of external noise and computer calculation errors on the form of the spectrum and process characteristics are analyzed.

1 INTRODUCTION

Regular and chaotic limit set bifurcations of different types are realized in nonlinear quasihyperbolic systems when their parameters are varied. Among them, various phenomena arising from the interaction between attractors have been observed, including intermittency. Three typical and relatively simple intermittency mechanisms have been distinguished and classified in the theory of chaos. However, more complicated intermittency mechanisms can take place in the general case, such as the "chaos-chaos" type of intermittency [2, 1]. The intermittency is characterized by a strong sensitivity to perturbations. In addition to a purely dynamic origin, the intermittency can also occur via a mechanism similar to that of a phase transition induced by noise [3, 4].

One of the remarkable statistical properties of the chaos-chaos intermittency is the slope of its power spectrum in the low-frequency region. The power spectrum in the region near the onset of intermittency is described by the universal law $1/\omega^{\delta}$ $(0.8 < \delta < 1.4)$ [5]. Such a spectrum shape is due to a finite probability in the existence of arbitrarily long "laminar" flow near the onset of intermittency. The $1/f$ spectrum is present in many processes having different origins: e.g. fluctuations of current in electron devices, fluctuations of the Earth's rotation frequency, fluctuations of the intensity in sound and speech sources, fluctuations of the muscle rhythms in the human heart, etc.

This paper deals with the study of chaos-chaos intermittency in the Chua's circuit [6] modeled by the following autonomous system of ordinary differential equations:

$$\dot{x} = \alpha[y - h(x)], \qquad \dot{y} = x - y + z, \qquad \dot{z} = -\beta y, \tag{1}$$

where $h(x) = bx + 0.5(a - b)(|x + 1| - |x - 1|)$.

The system (1) has a number of important properties which makes it an ideal model for studying the chaos-chaos intermittency. The dynamical properties of this system and bifurcation structure of

its parameter space are well known. On the $\alpha - \beta$ parameter plane, there is a bifurcation curve corresponding to the birth of the double-scroll Chua's attractor from two symmetrical spiral Chua's attractors. On the left side of this curve two symmetrical chaotic attractors separated by unstable invariant manifold exist (Fig.1). The system can be considered as a nonlinear bistable oscillator here. Along the bifurcation curve the separatrix surface is destroyed and these two attractors merge with each other. A new chaotic double-scroll Chua's attractor exists on the right of the bifurcation curve (Fig.2). The chaos-chaos intermittency phenomenon is observed at this moment of bifurcation transition: phase trajectories evolve for a long time around each symmetrical spiral Chua's attractor, followed by relatively rare transitions between them. During a full-scale experiment, this effect is recorded as flickers in the two symmetrical double scroll components on the screen of the oscilloscope

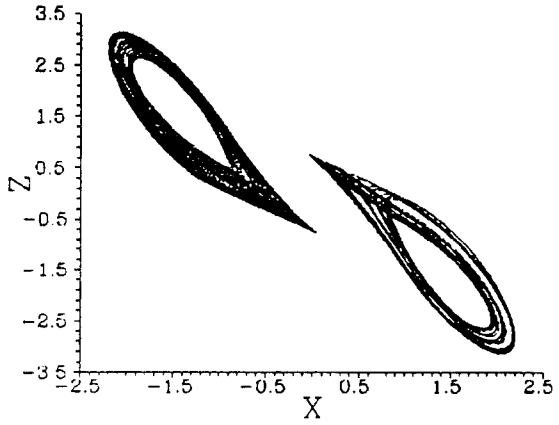

Figure 1: spiral Chua's attractor

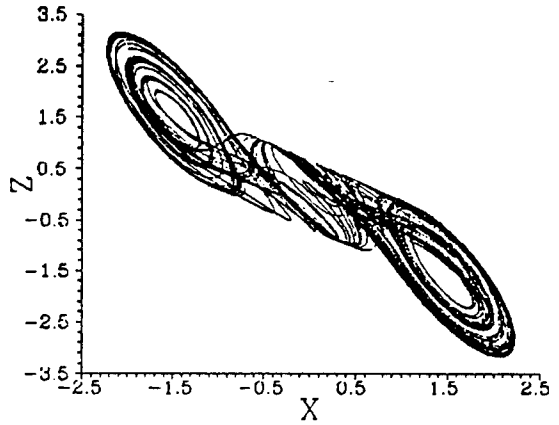

Figure 2: Double-scroll Chua's attractor

[7].

2 INTERMITTENCY PHENOMENON

In this paper, we study thoroughly the above intermittency phenomenon in Chua's circuit and investigate the influence of external noise and numerical accuracy on its statistical properties.

To analyze this intermittency phenomenon, we make use of not only such standard characterizations as Lyapunov exponents, power spectrum, and stationary probability density, but also other characteristics associated with the statistics of the "laminar" phases. Here, we mean by "laminar phase" the time period where a phase trajectory remains on one of the two symmetrical double-scroll components. In this paper, we shall dwell only on the calculation of the power spectrum and the statistics of the "laminar" phase.

In a recent paper [8], a technique for determining the main intermittency characteristics has been proposed which is based on the mean-first-passage-time theory of Markovian processes. We see that such stochastic process appears naturally in the statistics of the laminar phase associated with the chaos-chaos intermittency in Chua's circuit. A separatrix surface in the three-dimensional phase space of system (1) forms a boundary which separates the basins of attraction of the symmetric

components of the double-scroll attractor. Unfortunately, it is impossible in our case to obtain analytical results due to the difficulty of explicitly specifying the boundary separating the two basins of attraction. Therefore, all process characteristics in our study were determined by numerical simulation.

Equation (1) is integrated by a 4-*th* order Runge-Kutta method. As the numerical integration is being calculated the probability density $P(T)$ of the residence times on the two symmetrical double-scroll components and the moments of this distribution $< T^q >$ $(q = 1, 2...)$ were also calculated under the assumption that the calculated motion is ergodic. Then, the power spectrum is calculated and its shape examined.

All calculations were carried out with the fixed parameter values $(\beta, a, b) = (14.3, -1/7, 2/7)$. Only the parameter α was varied. The bifurcation value of the parameter $\alpha = \alpha^* = 8.813232... \pm 10^{-7}$ was calculated numerically to 8 digit precision by detecting the point in the α-parameter interval when the two spiral Chua's attractors suddenly merged into the double scroll Chua's attractor. By varying the parameter α, the averaged characteristics were determined as a function of the overcriticality defined by

$$\epsilon = \alpha - \alpha^*. \tag{2}$$

To investigate the effect of external noise, a δ-correlated noise source of intensity D was added to the right-hand part of the third equation of (1). The inclusion of this external noise is also particularly convenient in our full-scale experiments. The resulting system of stochastic differential equations has the form:

$$\dot{x} = \alpha[y - h(x)], \qquad \dot{y} = x - y + z, \qquad \dot{z} = -\beta y + \xi(t), \tag{3}$$

where $< \xi(t)\xi(t+s) >= 2D\delta(s)$. The extent of the noise influence on the different process characteristics was determined by varying the parameter D with fixed system parameters.

3 POWER SPECTRUM

Let us investigate the power spectrum and other statistical intermittency characteristics. When integrating Eq.(1) and Eq.(3), the integrating step was chosen automatically according to the accuracy specified. The number N of the calculated solution points in the time series $x(t)$ was fixed and can be as high as $N = 4 * 10^4$. The maximum integration time T_{max} and the discretization time ΔT were determined from the maximum frequency component ω_g in calculating the power spectrum; namely,

$$T_{max} = \frac{\pi N}{\omega_g}, \qquad \Delta = T_{max}/N. \tag{4}$$

Since the maximum frequency component ω_g in Chua's circuit is relatively small, it is possible to analyze the low-frequency region of the power spectrum $S_x(\omega)$. The power spectrum was calculated under the assumption that the motion is ergodic.

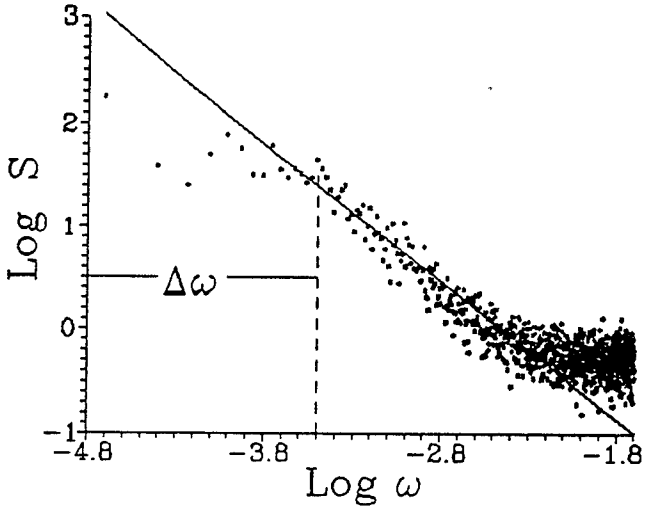

Figure 3: Power spectrum at $\alpha = \alpha^*$ (asterisks) and its approximation by the function $\omega^{-\delta}$, $\delta = 1.1$ (solid line).

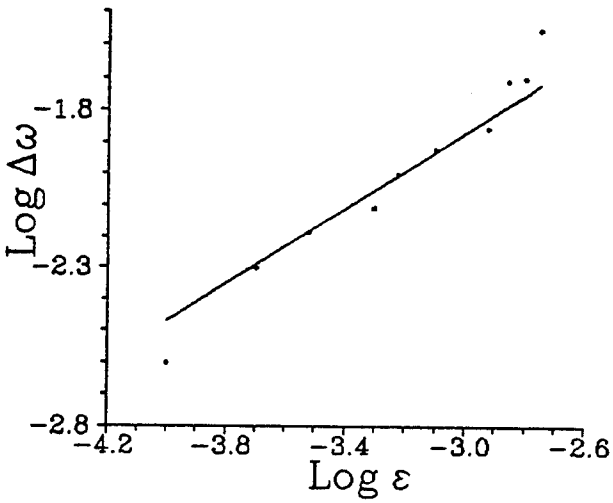

Figure 4: Width of the spectral plateau as a function of overcriticality (asterisks) and its approximation by the function ϵ^{γ}, $\gamma = 0.62$ (solid line).

Consider the power spectrum $S_x(\omega)$ at the critical parameter point $\alpha^* = 8.813232....$ The low-frequency spectrum region is shown in Fig.3, plotted on a double logarithmic scale. Observe that on the left closer to the zero frequency there is an almost constant interval $\Delta\omega \approx 10^{-3}$, henceforth referred to as the "spectral plateau". We will show later that the plateau is an artifact of numerical errors and external noise and is not a part of the actual spectrum. Beyond the plateau, however, lies the correct spectrum which follows the follow law:

$$S_x(\omega) \propto \omega^{-\delta}, \qquad \delta = 1.1 \pm 0.1. \tag{5}$$

Observe that the points cluster and cling to each side of the ideal $1/f$ line, which corresponds to points with $\delta = 1.1$.

Let us examine the dependence of those quantities which characterize the power spectrum in the low-frequency region as a function of the overcriticality $\epsilon << 1$. The plateau width $\Delta\omega$ is shown in Fig.4 as a function of ϵ on the double logarithmic scale. Observe that the $\Delta\omega(\epsilon)$ dependence can be approximated by the following degree function:

$$\Delta\omega(\epsilon) \propto \epsilon^{\gamma}, \qquad \gamma = 0.62 \pm 0.02 \tag{6}$$

As we increase the parameter α from α^* to higher values, the plateau is seen to extend closer to the zero frequency. This observation can be explained by the fact that the mean length of the laminar

phase is finite, and it decreases as ϵ increases [5]. As for the index δ in (5), it maintains its value within our limits of calculation accuracy for all small overcriticality variations $\epsilon \leq 10^{-4}$.

As we increase the parameter α farther beyond the critical value α^*, the form of the power spectrum in the low-frequency region follows approximately a Lorentzian law:

$$S_x(\omega) \propto \frac{< T >}{(\omega < T >)^2 + 1}. \tag{7}$$

This relationship is shown in Fig.5 for α=8.84.

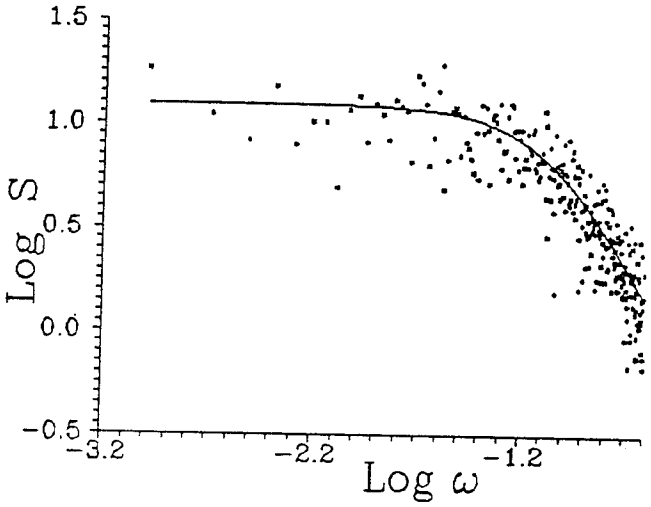

Figure 5: Power spectrum at $\alpha = 8.84$ (asterisks) and its approximation by the Lorentzian law (7) (solid line).

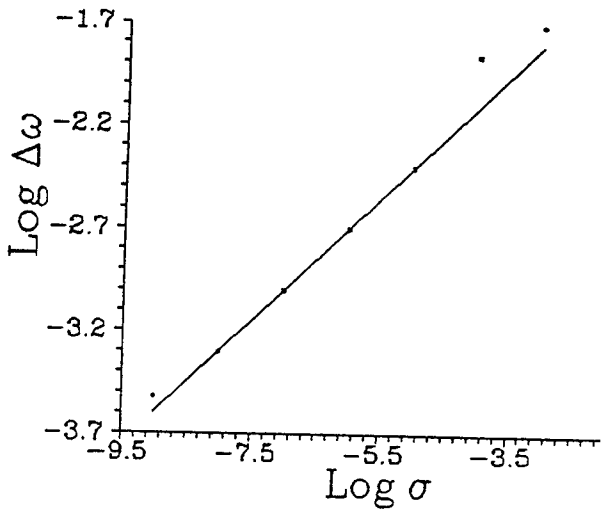

Figure 6: Width of the spectral plateau as a function of integration accuracy and its approximation by the function σ^μ, $\mu = 0.32$.

Our numerical experiments have shown that the power spectrum near the zero frequency always has a plateau whose width $\Delta\omega$ increases with ϵ. In other words, the experimental $1/f$ noise characteristic is obtained only to the right of the plateau. This low-frequency experimental limitation is due to the unavoidable perturbations in all physical systems. These perturbations are caused by the numerical integration and round-off errors. To illustrate this problem, our calculations of the statistical characteristics as a function of the integration accuracy σ are presented below. In Fig.6, the width of plateau (flat portion) $\Delta\omega$ is shown as a function of calculation accuracy σ in the double logarithmic scales. Observe that this relationship follows approximately a degree law:

$$\Delta\omega \propto \sigma^\mu, \qquad \mu = 0.32 \pm 0.02. \tag{8}$$

Again, the index δ in the spectral dependence in Eq.(5) is found to be independent of the integration accuracy, relative to the accuracy of our numerical methods.

Observe that as we increase our calculation accuracy (decreasing σ), the width $\Delta\omega$ of the plateau decreases in accordance with that given by Eq.(8). Since rounding errors are inevitable, so too is the plateau which limits the range of our measurable $1/f$ power spectrum in the low-frequency region. In fact, the formula given by Eq.(8) can be considered as a fluctuation-dissipation relation [9] for the dynamical system defined by Eq.(1) which takes into account the calculation errors.

The results of our investigation of the effect of the external noise (stochastic equations (3)) shows approximately the same dependency as Eq.(8); namely, as we increase the noise intensity D, the plateau width in the power spectrum also increases.

As a result of our numerical investigations, we have confirmed that near the bifurcation point $\alpha = \alpha^*$ which gives birth to the double scroll Chua's attractor, a chaos-chaos type intermittency is realized in Chua's circuit. This intermittency phenomenon is caused by two dynamically interacting symmetrical spiral Chua's attractors. The power spectrum associated with this chaos-chaos type intermittency is characterized by a $1/f$ divergence in the low- frequency region. Nearer to the zero frequency, however, there is a flat plateau in the power spectrum whose width depends on the overcriticality measure ϵ via Eq.(6), on the calculation accuracy σ via Eq.(8), and on the external noise intensity D which also follows from Eq.(8).

References

[1] F.T.Arecci, R.Badii, A.Politi. "Low-frequency phenomena in dynamical systems with many attractors", *Phys.Rev.* **A29**, (1984) 1006-1009.

[2] V.S.Anishchenko. "Interaction of strange attractors and chaos-chaos intermittency", *Sov. Tech. Phys. Lett.* **10**, (1984) 226-270.

[3] A.B.Neiman. "Bifurcation, chaos and noise in nonlinear dissipative systems" *in Proc. Intern. Seminar "Nonlinear circuitsand systems"*, Moscow, **2** (1992) 155-164.

[4] R.Ecke, H.Haucke. "Noise-induced intermittency in the quasiperiodic regime of Rayleigh-Benard convection", *J.Stat.Phys.* **54** (1989) 1153-1172.

[5] H.G.Schuster, *Deterministic chaos*, Physik-Verlag, Weinheim, 1984.

[6] L.O.Chua, M.Komuro, T.Matsumoto. "The double scroll family", *IEEE Trans. Circuits and Systems* **33** (1986) 1073-1118.

[7] V.S.Anishchenko, M.A.Safonova, L.O.Chua. "Stochastic resonance in Chua's circuit", *Int.J. Bif. and Chaos* **2** (1992) 397-401.

[8] V.S.Anishchenko, A.B.Neiman. "Statistical properties of intermittency in quasihyperbolic systems", *J. Tech. Phys.* **17** (1990) 3-14.

[9] Yu.L.Klimontovich, *Statistical Physics*, Hardwood Academic Publishers, 1986.

1993 International Symposium on Nonlinear
Theory and Its Applications (NOLTA '93)
Hawaii, U.S.A., December 5-10, 1993

Sound Synthesis and Music Composition using Chua's Oscillator

G. Mayer-Kress*, I. Choi†, and R. Bargar§

*Center for Complex Systems Research, Beckman Institute, Department of Physics, University of Illinois at Urbana-Champaign, 405 N. Mathews, Urbana, Il 61801, gmk@pegasos.ccsr.uiuc.edu
† School of Music, University of Illinois at Urbana-Champaign and
Center for New Music and Audio Technologies, University of California at Berkeley
§National Center for Supercomputing Applications, University of Illinois at Urbana-Champaign

We describe simulations of Chua's oscillator and its implementation in a circuit with seven computer-controlled parameters. We discuss its properties with regard to sound synthesis and composition.

1 Introduction

In recent years a number of composers have recognized that chaotic systems with their richness of dynamic behavior (see e.g., [1] for an introduction) can be used as tools for the generation of complex sounds and for the composition of music (see e.g., [2] - [10]). We investigate the properties of a non-linear system with an extremely rich repertoire of dynamical properties, the Chua oscillator [11]- [13]. Our investigation incorporates both numerical simulation as well as experiments with an analog Chua circuit with fast computer control of the relevant systems parameters. For the exploration of the parameter space both in simulation and in the analog circuit we have developed appropriate graphical interfaces.

We discuss the properties of the Chua circuit both as (self-excited) sound-generator as well as its properties as complex reverberator. In the latter case we study the transformations that a sound undergoes when it is used to modulate some of the systems parameters of the Chua circuit. Finally we discuss aspects of the Chua circuit as an electronic musical instrument that contains broadband generators as well as resonators that selectively amplify specific harmonic sounds that are requested by the musical applications. The resonator part of the circuit is implemented by a delayed feedback control method recently introduced [14]. A challenging task consists in an efficient mapping between the space of physical parameters of the circuit (values for resistances, capacitances, inductances etc.) to the space of musical perception (timbre, pitch, etc.). Preliminary efforts to have a neural network learn this mapping show that the complex structure of the physical parameter space of the Chua circuit, together with the coexistence of several attractors for the same value of the parameter make this a difficult problem [15]. Therefore a special emphasis in our work has been devoted to the development of computational tools that facilitate the exploration of the multi-dimensional space of control parameters of the Chua oscillator.

2 Chua's Oscillator and Sound Synthesis

The Chua oscillator exhibits a very large variety of attractors of different sonic properties ranging from almost sinusoidal to stochastic. A number of them have been categorized and described in [8]. Each of those sounds is generated as a solution to a nonlinear differential equation at a given parameter configuration. The dynamical equations for the Chua oscillator that we used for all simulations are in their dimensionless form given by [11]: $\frac{dx}{dt} = \alpha(y - x - g(x))$, $\frac{dy}{dt} = x - y + z$, $\frac{dz}{dt} = -\beta y - \gamma z$, where the variables x, y, z correspond to v_1, v_2, i_3 in fig. 1. The dimensionless bifurcation parameters α, β, γ are connected to the physical parameters of the circuit via the relations: $\alpha = \frac{C_2}{C_1}$, $\beta = \frac{C_2 R^2}{L}$, $\gamma = \frac{C_2 R R_o}{L}$. Here $g(x)$ defines the nonlinear resistor function (see fig.1) for which we have computer control over the location of the break points V_{BP+}, V_{BP-} as well as over the slope m_0. Typical numerical values for the circuit parameters are: $(C_1, C_2, R, R_o, L) = (4.9\,nF, 103\,nF, 1605\Omega, 11.2\,\Omega, 5.74\,mH)$.

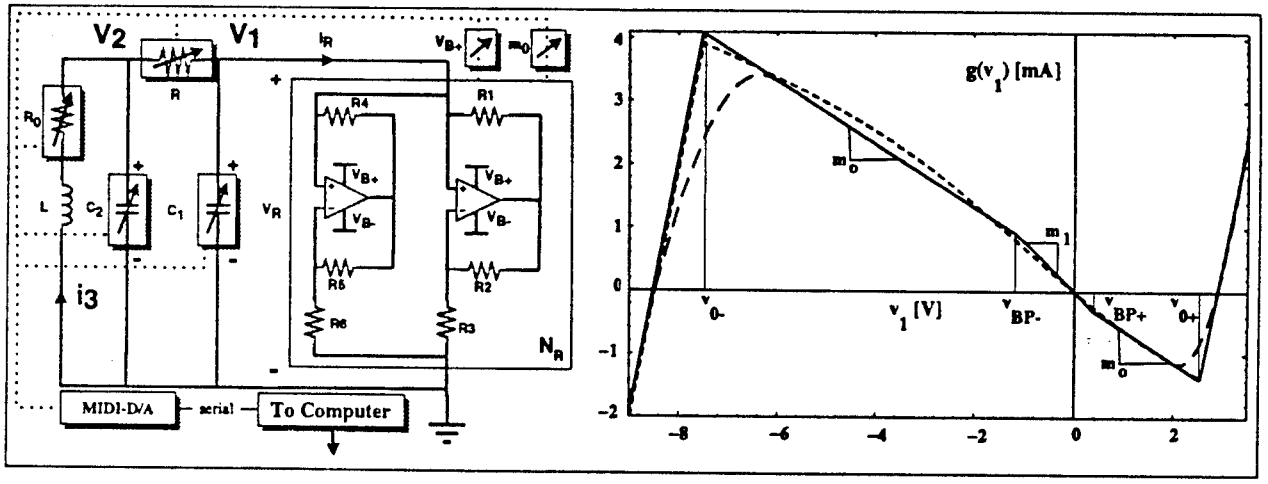

Figure 1: Schematic diagram of the unfolded Chua circuit (left). Six of the parameters of the Chua circuit (indicated by boxes with arrows) are computer-controlled via MIDI protocol and serial line. The $i-v$-characteristic of the non-linear resistor NR is shown on the right (solid line). We obtained significant variations in the timbre if we use smooth perturbations of the piecewise linear function such as a hyperbolic tangent (short-dashed line) or quadratic smoothing curves (long-dashed line). The asymmetric form of g is essential for the generation of bassoon-like sounds [8], whereas in a simplified, discrete model, a symmetric response function produced clarinet-like sounds [16].

We consider several numerical quantifiers that should describe specific audible properties. Among those properties are the variance of the signal,[1] its maximal amplitude, and the ratio r between maximal amplitude and variance (see fig.2). The first two characteristics are related to the loudness of the sounds and can also be used to mark regions in parameter space for which the system has a fixed point attractor (silence) or undergoes transitions to the large limit cycle "LLC", an (acoustically) especially unpleasant, ubiquitous solution.

[1] We typically record the signal from the voltage $v_1(t)$ across the capacitor C_1 as indicated in fig. 1.

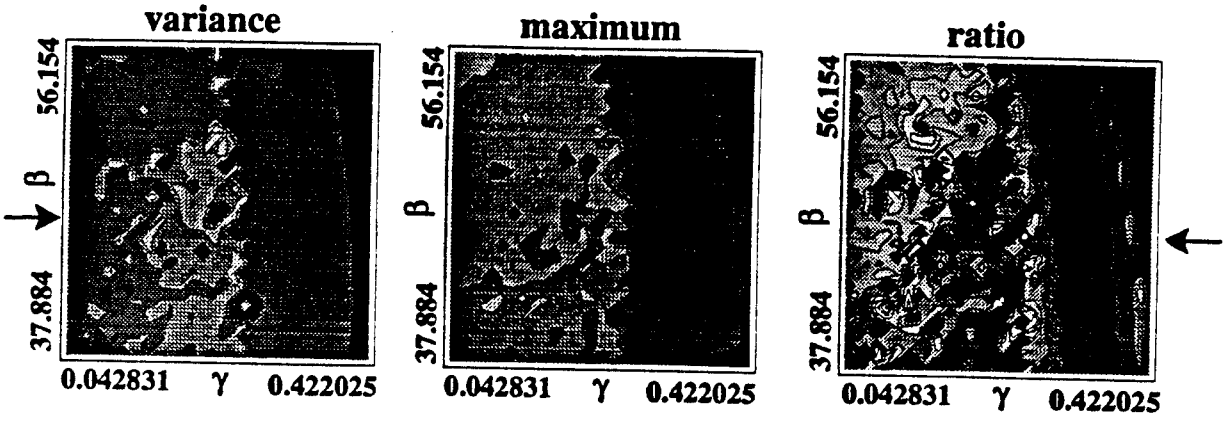

Figure 2: Contour plot of variance Δs^2 (left), maximal amplitude s_{max} (center), and ratio $r = s_{max}/(0.01 + \Delta s^2)$ (right) as a function of the bifurcation parameters β and γ for $\alpha = 21.02$ (see text). Larger values of the variables are displayed in brighter shades.

We also compute the ratio between maxima and variance which characterizes the content of intermittent excursions in the signal. An example of a time series where transitions between chaotic attractors of different size and intermittency characteristics occur is shown in fig. 3. Note that the transitions in the left part of the figure are mainly reflected in the ratio r of fig.2. We also investigate characteristics like the dominant frequency content of the signal (pitch) and degree of chaos in the signal (Lyapunov exponents) which is perceived as degree of noisiness.

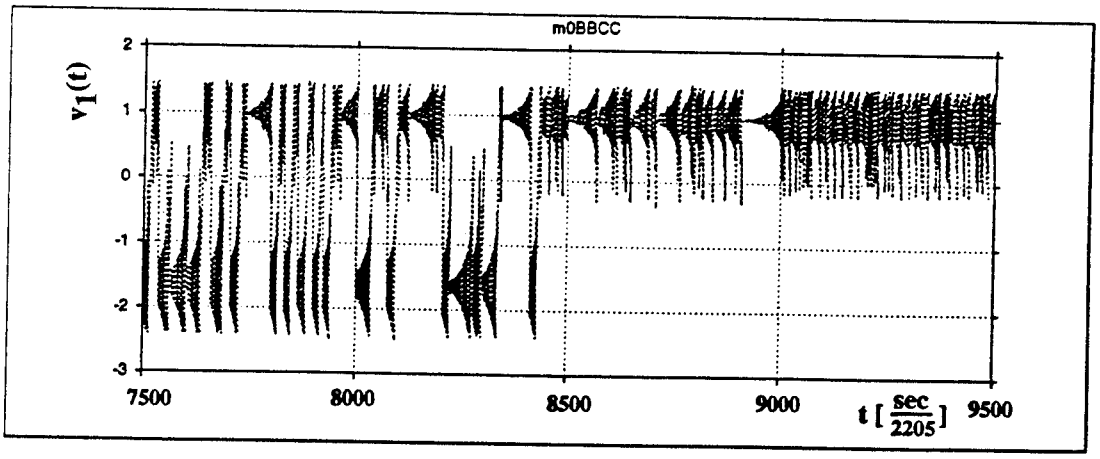

Figure 3: Time-series of the x-component of the Chua oscillator during a change of γ (γ is kept constant for 5000 time-steps). This sequence corresponds to a horizontal cut through the graphs in the previous figure at $\beta = 46.704$ (see arrows).

If the system is close to a Hopf bifurcation, external perturbations, for example from a sound source, will create damped oscillations of a shape determined by the global properties of the circuit. Especially in combination with delayed feedback can we generate a large variety of

acoustical effects depending on the real and imaginary parts of the eigenvalues of the fixed point. The external modulation can be applied to each of the parameters of the system or directly to one of its state variables[2]. In fig.4 we have applied the sound of a piano to the parameter R of the nonlinear resistor (see fig.1), which is directly related to the stability of the fixed point. Note that the pure piano sound appears much more chaotic than the distorted sound that is generally perceived as noisy. This is especially the case when *clipping* occurs in regions of strong, positive slopes of $g(v_1)$.

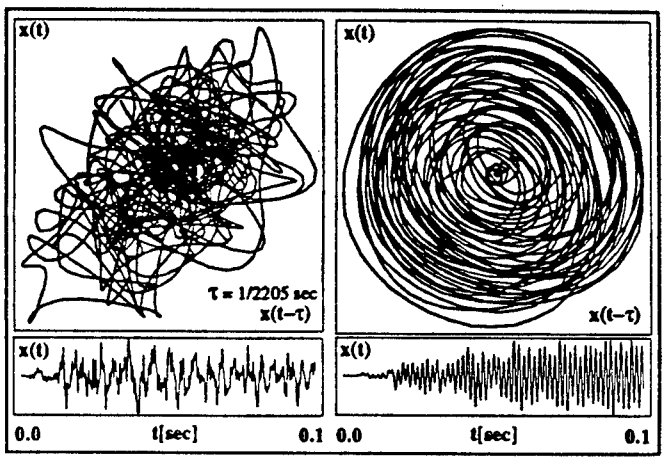

Figure 4: Time-delay reconstruction (see [1] for definitions) of attractors from the sound of a piano (left) that is used to modulate the parameter R of the circuit (see fig.1). The response from the analog Chua circuit close to a Hopf-bifurcation is shown on the right. The rate of distortions depends on the amplitude of the input as well as on the distance to the bifurcation point in parameter space. The time-series are displayed at the bottom; the sound is sampled at 22.05 kHz.

3 Transitions Between Musical Notes and External Control

A major problem in musical applications of the Chua oscillator is the predictable and reproducible transition between attractors corresponding to different parameters. Because of the complex nature of the parameter and state space, one cannot assume that a simple change to a new parameter configuration will induce a transition to the desired new attractor. In many cases the attractor to which the system will evolve will depend on its history. Thus it would be necessary to prescribe a specific path in parameter space leading from one attractor to the next. In doing so, it is also essential that the rate at which the parameters are changed are sufficiently quasi-adiabatic such that during the transition no accidental excursion occurs into basins of attractions of unwanted attractors like the notorious LLC.

Preliminary tests indicate that transitions between attractors can be induced within a time interval as short as $\Delta t = 10ms$. Close to bifurcations this time can be significantly larger (known as *critical slowing down*). In our experimental set-up the parameters are controlled via the MIDI protocol and a serial line (see fig. 1). It appears that these transition rates are still an order of magnitude below the limits that would be imposed by our configuration. One effect that one can notice during these transitions is the appearance of transient frequency

[2]The first case would be referred to as parametric perturbation, the second case as additive perturbation.

shifts, reminiscent of glissando effects of string instruments. The transient frequencies could be in principle controlled by simultaneous compensation in other parameters. For the design of an optimal transition path between different attractors, a method using convex sums of vector-fields has been introduced in [17].

For musical applications it is desirable to be able to prescribe specific goal dynamics that the system will approach or approximate. Several methods have been developed to achieve different types of goal dynamics. With an open loop control method (see e.g., [18], [19]) one can entrain the dynamics of the system to goals that can be very different from the intrinsic dynamics of the system as long as certain convergence properties are satisfied. For the Chua oscillator this control has been successfully achieved for goal dynamics that are in the convergent regions for which the nonlinear resistor has positive values, for instance, in the region of the LLC [20].

A different type of control strategy has been used to stabilize unstable periodic solutions close to a chaotic attractor. The basic idea is that the difference between a signal $x(t)$ and the time-delayed signal $x(t-\tau)$ is used as a negative feedback control force [14]. It vanishes for periodic solutions of period τ. In the context of musical sounds this method has a similar effect as coupling a noisy sound source to a resonator: resonating modes will be amplified and others will be suppressed. The result is a *pure* tone. We verified that this method works very effectively in simulations and could significantly enhance the musical applications for the Chua circuit.

Acknowledgements: We are deeply indebted to G. Zhong and N. Weber for their generous support with the electronic circuit. We would like to thank L. Chua, A. Hübler, A. Jackson, D. Pines, X. Rodet, and D. Wessel for their support and stimulating discussions and K. Alblinger for help with manuscript preparation. Finally, we would like to thank D.Cox for hardware support and E. Erwin, C. Goudesuene, J. Hardin, B. Sanderson for software support.

References

[1] H. Peitgen, H. Jurgens, D. Saupe, "Chaos and Fractals : New Frontiers of Science",Corr. 2nd print. New York, Springer-Verlag, 1993

[2] B.Truax, "Chaotic Non-linear Systems and Digital Synthesis: an Exploratory Study", In *Proceedings of the 1990 International Computer Music Conference*, San Francisco: International Computer Music Association, 100-103, 1990.

[3] X. Rodet, "Sound and Music from Chua's Circuit", J. of Circuits, Systems and Computers, vol. 3, no. 2, 49-61, March, 1992

[4] C. Ames, "A Catalogue of Sequence Generators: Accounting for Proximity, Pattern, Exclusion, Balance, and/or Randomness", Leonardo Music Journal, V.2 No.1, Hayward, MA, MIT Press, 55-72, 1992

[5] P. Beyls, "The Musical Universe of Cellular Automata", Proceedings of the International Computer Music Conference, Columbus, OH, 34-41, 1989

[6] R. Bidlack, "Chaotic Systems as Simple (but Complex) Compositional Algorithms", Computer Music Journal, V.16 No.3, Hayward, MA, MIT Press, 33-47, 1993

[7] G. Mayer-Kress, R. Bargar, I. Choi, "Musical Structures in Data From Chaotic Attractors", Technical Report CCSR-92-14, *Proceedings of the Intenational Symposium on the Auditory Display of Data (ICAD92)*, Santa Fe, NM Oct. 1992, in press

[8] G. Mayer-Kress, I. Choi, N. Weber, R. Bargar, A. Hübler, "Musical Signals from Chua's Circuit", IEEE Transactions on Circuits and Systems, special issue on *Chaos in Nonlinear Electric Circuits*, in press

[9] I. Choi, "Shadowing Lemma: $r \in [3.9, 3.905706]$ where period 5 cycle occurs, $x_o = 0.7435897435897437$", Composers Forum, Urbana, Il. 4/19/93

[10] I. Choi, "Anti-Odysseus - The Irreversibility of Time", World Expo, Taejon and Seoul, Korea, 10/20-23/1993

[11] L. O. Chua, "A Simple ODE with more than 20 Strange Attractors", preprint UCB/ERL M92/141, UC Berkeley, Aug. 1992, to app. also in *Proc. World Congress of Nonlinear Analysts*,Tampa, Florida, Aug. 19-26, 1992

[12] L.O. Chua, "Global unfolding of Chua's circuits", IEICE Trans. Fundamentals of Electronics, Communications and Computer Sciences, vol. E76-A, no. 5, 704-734, May 1993

[13] P. Deregal,"Chua's Oscillator: A Zoo of Attractors", J. of Circuits, Systems, and Computers, Vol.3, No. 2, 309-359, 1993

[14] K. Pyragas,"Continuous Control of Chaos by Self-Controlling Feedback", Phys. Let. **A170**, 421-428, 1992

[15] M.Lee, D.Wessel, "Connection Models for Real-Time Control of Synthesis and Compositional Algorithms", Proc. of the ICMC 1992, San Jose, CA.,277-280, 1992

[16] X. Rodet, "Nonlinear Oscillator Models of Musical Instrument Excitation", Proc. of the ICMC 1992, San Jose, CA., 412-413, 1992

[17] R. Mettin, G. Mayer-Kress, to appear

[18] A. Hübler, "Modeling and Control of Complex Systems: Paradigms and Applications", in *Modeling Complex Phenomena*, edited by L. Lam (Springer, New York 1992)

[19] E.A. Jackson,"Controls of Dynamic Flows with Attractors", Phys.Rev. **A 44**, 4839-4853, 1991

[20] E.A. Jackson, Private communication

1993 International Symposium on Nonlinear
Theory and Its Applications (NOLTA '93)
Hawaii, U.S.A., December 5-10, 1993

Chua's Circuit: Rigorous Results and Future Problems

Leonid P. Shil'nikov[1]

Research Institute for Applied Mathematics & Cybernetics
10 Ul'janov str., Nizhny Novgorod 603005, RUSSIA

One of the most remarkable achievements of science in the $20th$ century is the discovery of dynamical chaos. Using this paradigm, many of the problems in modern science and engineering which can be modelled via the language of nonlinear dynamics, have attained an adequate mathematical description. However, the explanation of a number of phenomena of dynamical chaos has required the creation of new mathematical techniques. The reason for this is that the classical theory of nonlinear oscillations developed by Van der Pol, Andronov, Pontryagin, Krylov, Bogolyubov et al, was based on Poincare's theory of periodic orbits and Lyapunov's stability theory, i.e., on methods for studying mainly *quasi-linear* systems.

Problems associated with systems involving high energies, powers, velocities, etc., must be modelled by multi-dimensional and *strongly nonlinear* differential equations (ordinary, partial, etc.). The study of such systems has generated numerous new concepts and terminology: hyperbolic sets, symbolic dynamics, homo- and heteroclinic orbits, global bifurcations, entropy (topological and metric), Lyapunov exponents, fractal dimension, etc.. We note the possibility of describing dynamical chaos via statistical tools as well; e.g., correlation function, power spectrum, etc. They are widely used in numerical simulations and in experiments.

Here, an important role should be noted on which concrete phenomena and models play in establishing dynamical chaos in different fields of knowledge. It is *Lorenz model* in hydrodynamics and in the theory of lasers, the *Belousov-Zhabotinsky reaction* in chemistry, *Chua's circuit* in radiophysics, etc.

Chua's circuit has become very popular since the middle of the 80's [1, 2]. Being, in its physical nature, a rather simple electronic generator of chaos (it consists of four linear elements and one nonlinear circuit element, as shown in Fig.1).

Chua's circuit is an ideal paradigm for research on chaos by means of both laboratory experiments and computer simulations, because it admits an adequate modelling via the language of differential equations. In the simplest case these equations are written in the dimensionless form:

$$\begin{aligned} \dot{x} &= \alpha(y - h(x)) \\ \dot{y} &= x - y + z \\ \dot{z} &= -\beta y \end{aligned} \tag{1}$$

where the nonlinear function $h(x)$ has the form

$$h(x) = m_1 x + (m_0 - m_1)\frac{|x+1| - |x-1|}{2}$$

The main reason why Chua's circuit is a subject of not only engineering interest is the following:

[1]Supported by the Russian Foundation of Fundamental Researchers 93-011-1787.

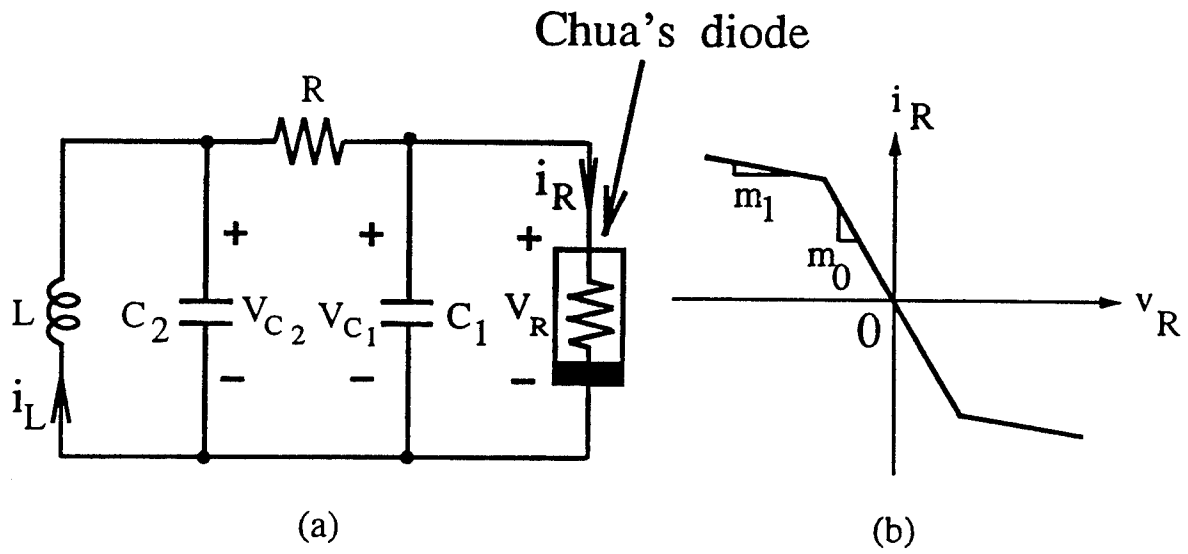

Figure 1: (a) Chua's circuit (b) The voltage versus current characteristic of the Chua's diode may be *any* nonlinear function; e.g., a polynomial, a "cubic" $f(x) = c_0 x + c_1 x^3$, a "sigmoid" $f(x) = \frac{exp(\gamma x)-1.0}{exp(\gamma x)+1.0}$, etc.[2]. Here, we show the most commonly chosen piecewise-linear characteristic.

1. Chua's circuit exhibits a number of different scenarios of appearance of chaos, namely, transition to chaos through the period-doubling cascade, through the breakdown of an invariant torus, etc., which makes the study of Chua's circuits a rather universal problem.

2. Chua's circuit exhibits a chaotic attractor called the "double scroll Chua's attractor". It appears at a conjunction of a pair of non-symmetric spiral attractors. Three equilibrium states of a saddle-focus type are visible in this attractor, which indicates that the double-scroll Chua's attractor is *multi-structural*, in distinction with other known attractors of three-dimensional systems.

3. Chua's equations (1) are rather "close" (in the sense that the bifurcation portraits are "close") to the equations defining a three-dimensional normal form for bifurcations of an *equilibrium state* with *three zero characteristic exponents* (in the case of additional symmetry), and that of a *periodic orbit* with *three multipliers* equal to -1.

4. In their mathematical nature, the attractors which occur in Chua's circuit are new and essentially more complicated objects than it seemed before. This is based on new subtle results on systems with homoclinic tangencies and homoclinic loops of a saddle-focus [3, 4].

The chaotic nature of the double-scroll Chua's attractor was proved in Ref. [5] by establishing the existence of homoclinic loop of the saddle-focus in the origin, and by applying the Shil'nikov theorem. Another proof of the chaotic nature of Chua's circuit, which also makes use of the Shil'nikov theorem is given by Silva [6]. This theorem asserts that if the three-dimensional system

$$\dot{x} = \rho x - \omega y + P(x, y, z)$$

$$\dot{y} = \omega x + \rho y + Q(x,y,z)$$
$$\dot{z} = \lambda z + R(x,y,z)$$

(where P.Q,R are smooth functions vanishing in the origin along with their derivatives, $\rho < 0, \lambda > 0, \omega \neq 0$) has a *homoclinic loop*, then provided that

$$\rho + \lambda > 0 \tag{2}$$

the Poincare map on a cross-section transverse to the loop has an infinite number of Smale's horseshoes. It is also important that under small variations of the system a large number of the horseshoes are preserved.

The nonwandering sets lying near the homoclinic loop of a saddle-focus are locally unstable. So, these structures must belong to the attractor in order for the system to exhibit chaotic behaviors. In Ref. [5, 6] regions in the parameter space of equations were found where this indeed takes place. Actually, the presence of a saddle-focus homoclinic loop in Chua's circuit does *not* guarantee that the double-scroll Chua's attractor is a classical strange attractor having well-understood properties, e.g., sensitive dependence on initial conditions, transitivity, and so on. In fact, the above homoclinic loop can not take place for such typical strange attractors: It was shown in Ref. [3], that if condition (2) and the following condition

$$2\rho + \lambda < 0$$

are satisfied, then there exist an infinite number of stable periodic orbits which are dense on the bifurcation surfaces of three-dimensional systems with saddle-focus homoclinic loops. Furthermore, in any neighborhood of such a surface the so-called Newhouse regions exist where systems with infinitely many stable periodic orbits are dense.

For the Chua's equations (1), this corresponds to the possibility of parameter values for which infinitely many stability windows exist, which implies a sensitive dependence of the structure of the attractor on small variations of parameters. Besides, as it was shown in Ref [4], systems with infinitely many structurally unstable periodic orbits of any degree of degeneracy are dense in the Newhouse regions. Therefore a "complete description" of the dynamics and bifurcations in the Chua's equations is impossible as it is for many other models.

The main reason for such a complicated behavior of orbits in the attractors observed in Chua's circuits is connected with the fact that either the attractor itself, or an attractor of a nearby system, contains structurally unstable Poincare homoclinic orbits, i.e., orbits which arise from the tangency of the stable and the unstable manifolds of some saddle periodic orbit(cycle). If the inequality $|\lambda\gamma| < 1$ is fulfilled where λ and γ are multipliers of the cycle, then the attractor contains stable periodic orbits , as a rule. Such an attractor differs essentially from the hyperbolic and the Lorenz attractors. The latter admits the introduction of reasonable ("physical") invariant measures. This makes it possible to study its chaotic behavior by means of statistical methods. In particular, it provides a rigorous foundation for studying such characteristic of the attractors as Lyapunov exponents. Therefore, hyperbolic and Lorenz attractors are called *stochastic*. On the other hand, the attractors we discuss here hardly admits the introduction of an invariant measure. We called such attractors *quasistochastic* or *quasiattractor* [7, 8]. In our opinion, the reasons formulated above make it natural for us to add the hypothesis of small noise in studying quasiattractors. It is well known that noise is unavoidable both in physical experiments and in computer simulations (due to round-off errors). An explicit introduction of noise could spread stable periodic orbits with long

periods and thin basins, as well as structurally unstable periodic orbits.

Being closely related to the study of homoclinic tangencies, an extension of the results pointed out above for the multi-dimensional case appears to be rather non-trivial and provides us with opportunities for discovering many essentially new effects. Concerning those generalizations of Chua's circuits which are described by equations of dimension greater than three, the multi-dimensional theory predicts the following phenomenon: together with a "large" attractor, stability windows can exist which exhibit not only periodic and quasiperiodic orbits but also "small" strange attractors [9, 10]. These can be attractors of a very different nature, for instance, attractors similar to the Lorenz attractor and to the double-scroll Chua's attractor. Finally, we remark that there are still many unsolved mathematical problems associated not only with Chua's circuit but also with its globally unfolded canonical circuit [11] and its higher-dimensional generalizations; e.g., one-dimensional chains and two or three-dimensional arrays of such circuits.

References

[1] L. O. Chua. The Genesis of Chua's Circuit. *Archiv fur Elektronik und Ubertragungstechnik*, 46(4):250–257, 1992.

[2] R. N. Madan (Guest Editor). *Special Issue on Chua's Circuit: A Paradigm for Chaos*, volume 3 of *Journal of Circuits, Systems, and Computers*. 1993.

[3] I. M. Ovsyannikov and L. P. Shil'nikov. Systems with homoclinic curve of the multi-dimensional saddle-focus and spiral chaos. *Mathem.Sbornik*, 182:1043–1073, 1991.

[4] S. V. Gonchenko, L. P. Shil'nikov, and D. V. Turaev. On models with non-rough Poincare homoclinic curves. *Physica D*, 62:1–14, 1993.

[5] L. O. Chua, M. Komuro, and T. Matsumoto. The Double Scroll Family, Parts I and II. *IEEE Transactions on Circuits and Systems*, 33(11):1073–1118, 1986.

[6] C. P. Silva. The double hook attractor in Chua's circuit: Some analytical results. In R. N. Madan, editor, *in Chua's circuit: A paradigm for chaos*, pages 671–710. World Scientific, Singapore, 1993.

[7] V. S. Afraimovich and L. P. Shil'nikov. Strange attractors and quasiattractors. *in Dynamics and Turbulence, Pitman, NY*, 1983.

[8] L. P. Shilnikov. Strange attractors and dynamical models. *Journal of Circuits, Systems, and Computers*, 3(1):1–10, March 1993.

[9] S. V. Gonchenko, L. P. Shil'nikov, and D. V. Turaev. Chaos. to appear.

[10] S. V. Shil'nikov, A. L. Shil'nikov, and D. V. Turaev. Normal forms and Lorenz attractor. *International Journal of Bifurcation and Chaos*, 3(5), 1993.

[11] L. O. Chua. Global unfolding of Chua's circuits. *IEICE Transactions on Fundamentals of Electronics, Communications and Computer Sciences*, E76-A:704–734, 1993.

1993 International Symposium on Nonlinear
Theory and Its Applications (NOLTA '93)
Hawaii, U.S.A., December 5-10, 1993

A CMOS Monolithic Chua's Circuit Array

M. Delgado-Restituto and A. Rodríguez-Vázquez

Centro Nacional de Microelectrónica-Universidad de Sevilla
Edificio CICA, C/Tarfia s/n, 41012-Sevilla, SPAIN

This paper presents design considerations for monolithic implementation of a monolithic Chua's circuit array. The paper proposes a new design for a CMOS integrated Chua's circuit, that instead of based on the original mathematical model, it follows that of a canonical system in the Chua's family. The purpose is to reduce the number of biasing lines driven each circuit in the array, and to minimize the spread of the parameters. The GmC approach, combining quasi-linear VCCSs, PWL VCCSs, and capacitors is then explored regarding the implementation of this model. CMOS basic building blocks for the realization of the quasi-linear VCCSs and PWL VCCSs are presented and applied to design an isolated Chua's circuit IC. The HSPICE electrical simulation results from the design show bifurcation towards a double-scroll Chua's attractor by changing a bias current. The manufacturability of the prototype has been confirmed by Monte Carlo analysis.

1. INTRODUCTION

Since its appearance in 1988 [1], *cellular neural networks* (CNN) have deserved considerable interest, experimenting continuous generalizations that have broaden their application fields. The CNN universal machine constitutes the last and most sophisticated expression of the CNN paradigm, which represents the first algorithmically programmable analog array computer [2]. An interesting property of such machine is its ability to solve many types of partial differential equations by using processing cells slightly more complex than the traditional sigmoidal neurons. In particular, it has been demonstrated that when the Chua's circuit [3] is used as the basic cell in a two-dimensional CNN array with resistive coupling, the whole system is able to reproduce the *autowave* phenomenon in the same way as accounts in many physical, chemical and biological systems [4]. From an engineering point of view, this phenomenon is of interest since it can be exploited for image processing in operations such as contrast regulation, restoration of a broken contour, and edge detection [5].

The purpose of this paper is to present a new monolithic design of the Chua's circuit that is well-suited for the implementation of a VLSI array such as that reported in [4]. The circuit has been designed in a 2.4μm CMOS technology for a time constant of 1μs, and displays different chaotic attractors, including the double scroll, by simply changing a bias current. Manufacturability of the prototype has been assessed by Monte Carlo analysis.

2. VLSI DESIGN OF A CHUA'S CIRCUIT

The monolithic implementation of a Chua's circuit array forces a series of conditions concerning the physical realization of each basic cell, summarized in the following:

a) Robustness. Adequate operation of all the Chua's circuits in the array should be guaranteed, in spite of the inevitable deviations with respect to the nominal design point, principally caused by variations in the technological parameters and mismatching.

b) Reduced number of input/output pins. This implies that each cell should be as self-contained as possible, in such a way that involves a minimum number of bias sources. In sum, an attempt must be made to reduce the area consumed due to routing lines.

c) Modularity. Interconnection with the adjacent cells must be simple, with no affect on the compactness of the whole array. In addition, the degree of coupling must be programmable and easily controlled from the outside.

d) Low area and power consumption. This infers that the different components of the monolithic Chua's circuit have low spread, and that current levels are of a few μA's.

Authors have reported of the monolithic realization of an isolated Chua's circuit, based on the state-variable methods [6]. This implementation uses Gmc techniques, amply accepted by the scientific community in analog filter design. The designed circuit meets all the above cited conditions to serve as a base cell within an array, with the exception of b): it requires a large number of biasing lines.

We have developed a new integrated design of the Chua's circuit to solve this problem and improve the system performance under the remaining conditions. This design presents an important modification with respect to that presented in [6], in that its mathematical model is obtained after an exhaustive search among the Chua's family *canonical* systems, to determine which configuration has the same qualitative behavior as the original system, and presents a minimum spread in the parameter values. The resulting model is described by the following set of equations:

$$\begin{aligned} \frac{dx}{dt} &= f(x) + \alpha y \\ \frac{dy}{dt} &= \alpha (x - z) \\ \frac{dz}{dt} &= x - z + \beta y \end{aligned} \tag{1}$$

where

$$f(x) = bx + \frac{a-b}{2}\{|x + B_p| - |x - B_p|\} \tag{2}$$

and the parameter values that give rise to the well-known *double scroll* Chua's attractor are:

$$(\alpha, \beta, a, b) = (3, \frac{14}{3}, -\frac{5}{4}, \frac{5}{2}) \tag{3}$$

whose spread is three times less than the model used in [6]. Regarding the robustness of the model, Monte Carlo analysis with uncorrelated relative variations of up to 7% from the nominal values in (3), show that 100% of the obtained trajectories evolve towards a double scroll.

Fig.1 shows a schematic of the circuit associated to system (1), consisting of only capacitors, transconductance amplifiers, and a nonlinear resistor. To ensure that real transconductors share the same biasing line and to reduce relative errors between the gains of the VCCSs, we have made a preliminary scaling of the model in (1), so that all the parameter values are integers. The new values of the parameters used in Fig. 1 are:

$$(\alpha, \beta, a, b) = (3, 2, -2, 2) \tag{4}$$

and the following relation between capacitors must be verified:

$$\frac{C_x}{2} = 2C_y = C_z \equiv C \tag{5}$$

The design of Fig. 1 is completed by the choice of the time constant, τ, defined as:

$$\tau = 2\pi \frac{C}{g_{mu}} \tag{6}$$

where g_{mu} is the transconductance unit on which all the gains of the VCCSs shown in Fig.1 are scaled. If we make $\tau = 1\mu s$ and assume that $C = 5$ pF (usual value in analog integrated circuit design), we obtain $g_{mu} = 31.416\ \mu A/v$.

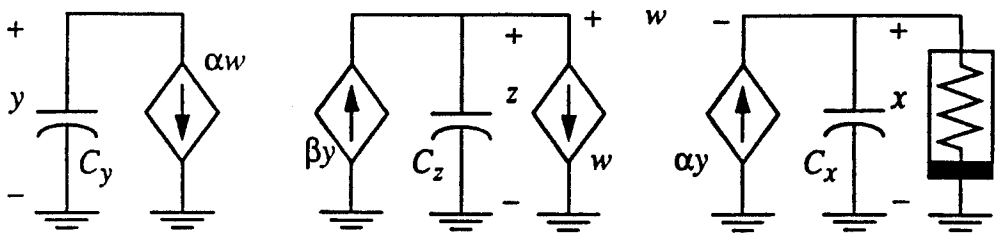

Figure 1. Conceptual transconductance-mode Chua's circuit.

Thus, the design of the monolithic Chua's circuit is reduced to the implementation at a transistor level of one single transconductance amplifier of g_{mu} gain (the remaining transconductors are realized by the parallel connection of as many amplifiers of g_{mu} gain as necessary) and a nonlinear resistor. Fig. 2(a) shows the schematic used for the transconductor unit. It is a folded-cascode structure, whose input stage presents a linearization scheme through source degeneration [7] characterized by an ample range of linearity in the voltage-current conversion, low systematic offset, and very high output resistance. The design was developed in a 2.4 μm double-poly double-metal CMOS technology. Fig. 2(b) shows the corresponding driving-point characteristic, with less than 2% error in the input voltage ranging from -1.25v to 1.25v, assuming symmetrical biasing of ± 2.5v. Obviously, proper operation of the circuit implies that the chaotic attractor be comprised inside this range.

The nonlinear resistor can be implemented as the parallel connection of two circuits like that shown in Fig.3(a) (bear in mind the values of a and b in (4)). The only difference with respect to Fig.2(a) is the inclusion of a differential pair (M_{3A}, M_{3B}) with their corresponding current source, I_B; and the feedback between the transconductor's input and output nodes. Fig. 3(b) presents the resistor's characteristics for B_p = 0.3 V. Note that said characteristic is not exactly piecewise linear; however, this is not a major problem since other

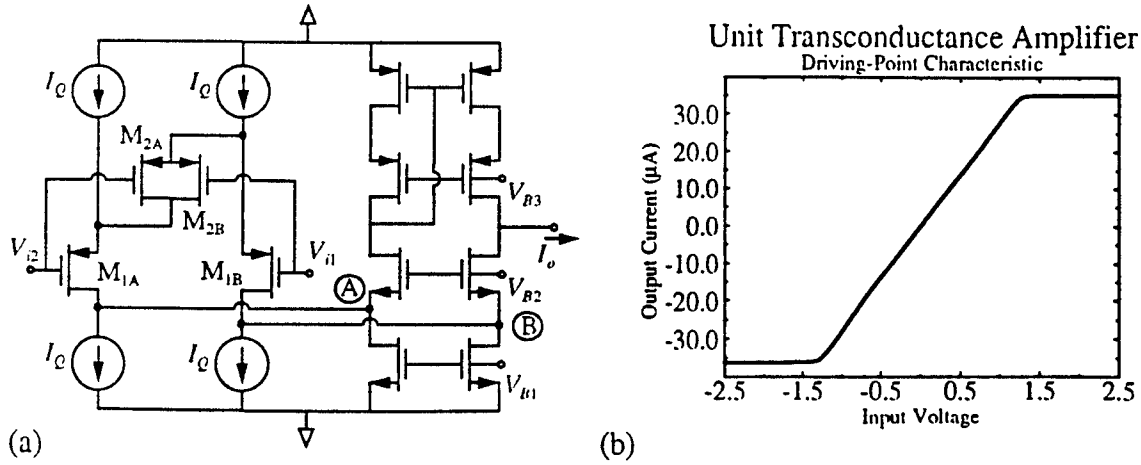

Figure 2. Unit transconductance amplifier: (a) Schematic; (b) Driving-point characteristic.

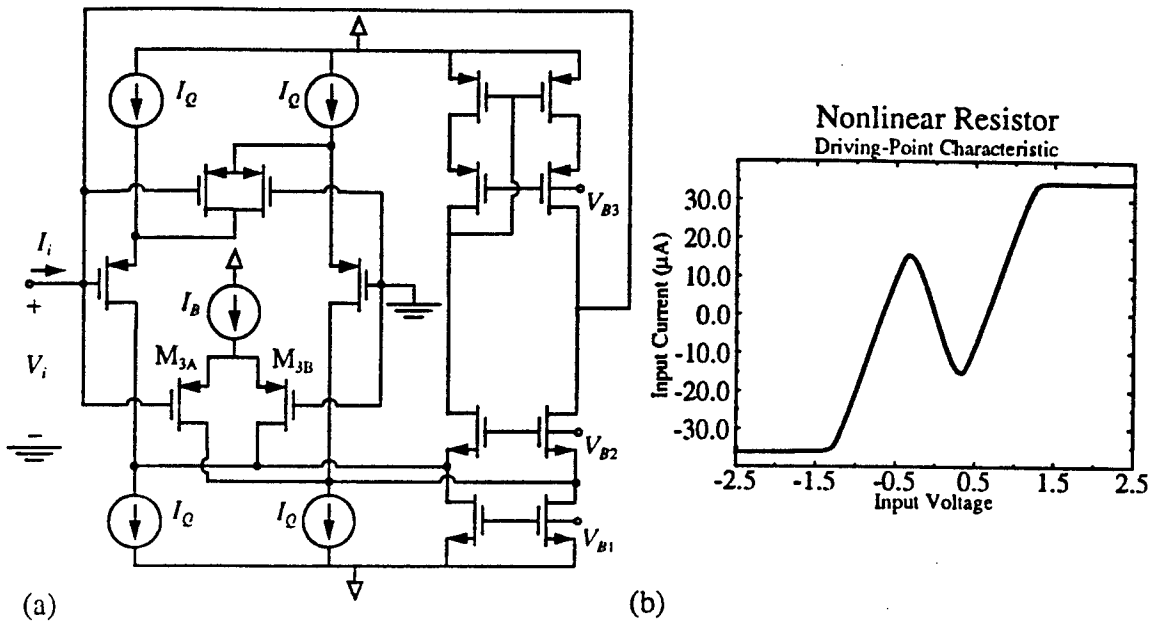

Figure 3. Nonlinear resistor: (a) Schematic; (b) Driving-point characteristic.

smoother nonlinearities also qualify for the resistor.

Fig. 4 presents the results of the electrical simulation of the whole circuit, where the double scroll is clearly apparent. Monte Carlo analysis has been also performed to assess the manufacturability of the circuit. Random global variations of up to 20% and simultaneous

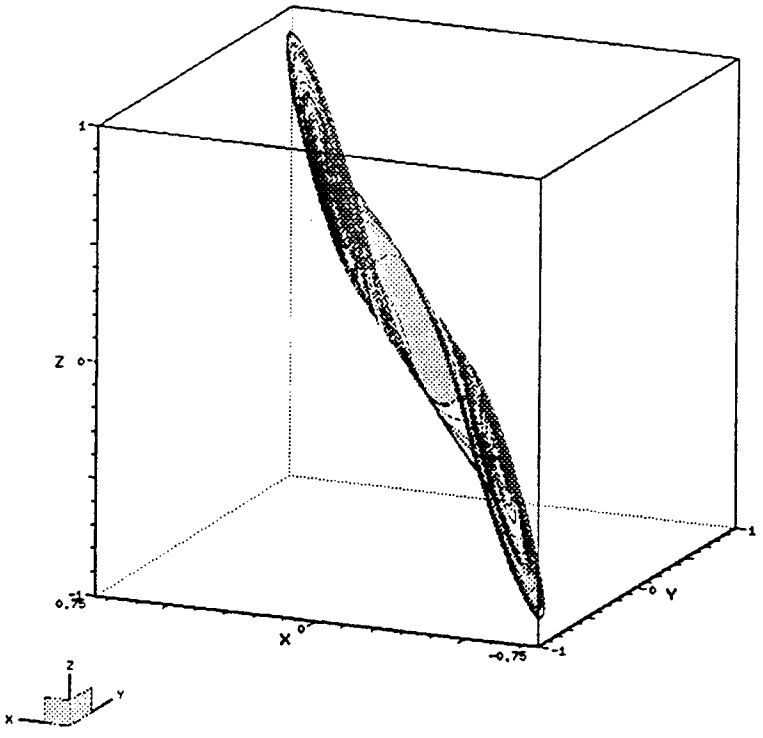

Figure 4. Chaotic attractor form the monolithic Chua's circuit.

statistically independent local variations of up to 2% are considered. Under these rather pessimistic conditions, the circuit performed correctly (despite changes in the time scale) for all the Monte Carlo instances.

Once the design of an isolated Chua's circuit is accomplished, the implementation of an analog array is straightforward: it is about to design a simple resistive grid template that interconnect the corresponding nodes of each Chua's circuit cell. In [4], these interconnections reduce to the four nearest cells in the two-dimensional array, and so, easily feasible for VLSI realizations. A 10x10 Chua's circuit array is now being designed by the authors to explore the capabilities of the Chua's circuit in an image processing context. Details will be reported in a separate paper.

3. REFERENCES

[1] L. O. Chua and L. Yang: "Cellular Neural Networks: Theory". *IEEE Transactions on Circuits and Systems*, Vol.35, No.10, pp. 1257-1272, Oct. 1988.
————: "Cellular Neural Networks: Applications", *ibid.*, pp. 1273-1290.

[2] T. Roska and L. O. Chua: "The CNN Universal Machine: An Analogic Array Computer". *IEEE Transactions on Circuits and Systems* - II: *Analog and Digital Signal Processing*, Vol.40, No.3, pp. 163-173, Mar. 1993.

[3] T. Matsumoto, L. O. Chua and M. Komuro: "The Double Scroll". *IEEE Transactions on Circuits and Systems*, Vol.32, No.8, pp. 797-818, Aug. 1985.

[4] V. Pérez-Muñuzuri, V. Pérez-Villar and L. O. Chua: "Autowaves for Image Processing on a Two-Dimensional CNN Array of Excitable Nonlinear Circuits: Flat and Wrinkled Labyrinths". *IEEE Transactions on Circuits and Systems* - I: *Fundamental Theory and Applications*, Vol.40, No.3, pp. 174-181, Mar. 1993.

[5] V. I. Krinsky, V. N. Biktashev and I. R. Efimov: "Autowaves Principles for Parallel Image Processing". *Physica D*, Vol.49, pp. 247-253, 1991.

[6] M. Delgado-Restituto and A. Rodríguez-Vázquez: "A CMOS Monolithic Chua's Circuit". Journal of Circuits, Systems and Computers, Vol.3, No.2, pp. 259-268, Jun. 1993.

[7] F. Krummenacher and N. Joehl: "A 4MHz CMOS Continuous-Time Filter with On-Chip Automatic Tuning". IEEE Journal of Solid-State Circuits, Vol. SC-23, pp. 750-758, Jun. 1988.

1993 International Symposium on Nonlinear
Theory and Its Applications (NOLTA '93)
Hawaii, U.S.A., December 5-10, 1993

Synchronization and stochastic resonance in Chua's circuit

V.S. Anishchenko, M.A. Safonova, O. V. Sosnovtseva

Physical Department, Saratov State University
Astrakhanskaya, 83, Saratov 410071, Russia

Abstract

The phenomena of chaos synchronization are investigated in the nonautonomous and in two coupled Chua's circuits. The occurence of stochastic resonance (SR) effect in cases of amplitude and frequency modulation is shown.

1 INTRODUCTION

The phenomena of periodic oscillation synchronization and resonance are well known in the classical theory of oscillations. It is natural to attempt to generalize these phenomena to more complicated oscillations which arise in dynamical system with chaotic behavior.

Two well-known dynamical systems possessing the above mentioned property were chosen for our investigation of the phenomenon of chaotic oscillation synchronization. A basic model in our consideration is a Chua's circuit [1]. For comparison we use an Anishchenko-Astachov oscillator (modified oscillator with inertial nonlinearity (OIN)) [2].

The classical phenomenon of stochastic resonance (SR) is observed in bistable nonlinear systems driven simultaneously by external noise and a sinusoidal force [3]. In the presence of an external modulation a coherence between the modulation frequency ω_0 and the mean switching frequency ω_s emerges. As a result, a part of the noise energy is transformed into energy of the periodic modulation signal so that the signal-to-noise ratio (SNR) increases.

We generalize this classical SR-phenomenon to the class of quasi- hyperbolic systems [4, 5]. Many regular and chaotic attractors can coexist and interact in the state space of such systems. The most general example of such interaction is a "chaos-chaos" type intermittency. Two chaotic attractors separated in state space by a hypersurface separatrix can merge into one chaotic attractor. The phenomenon of this "chaos-chaos"type intermittency is observed in a small range of some control parameters greater than some critical parameter value where the merging of the attractors takes place. Since the statistical properties of this kind of intermittency is identical to that observed from classical bistable systems, it can be considered as a generalized form of bistable behavior. If the control parameter value is less than critical, the transition can be induced by a noise source.

The second generalization which we make in this work is to extend the class of signals for inducing the SR- phenomenon. In most studies that deal with the SR the signal is considered as monochromatic: $f(t) = A\cos(\omega_0 t)$. However it is more important to investigate the SR with information-like (multi-frequency) signals. As a first step, we consider amplitude modulated: $f(t) = A[1 + m\cos(\omega_m t)]\cos(\omega_0 t)$ and frequency modulated: $f(t) = A\cos[(1 + m\cos(\omega_m t))(\omega_0 t)]$ signals.

2 FORCED SYNCHRONIZATION OF CHAOS

Chua's circuit with external forcing is described by the following equations:

$$\dot{x} = \alpha[y - h(x)], \qquad \dot{y} = x - (1+\gamma)y + z + \gamma E \sin(pt), \qquad \dot{z} = -\beta y, \tag{1}$$

where $h(x) = bx + 0.5(a-b)(|x+1| - |x-1|)$, γ is the coefficient of coupling between autonomous Chua's circuit and external sinusoidal voltage source, E is the forcing amplitude and $p = 2\pi f_1$ is the forcing frequency. Parameters of the three-segment piecewise-linear function $h(x)$ were fixed: $a = -0.143, b = 0.286$. We denote the frequency of the initial limit cycle of the autonomous Chua's circuit by f_0.

The neighborhood of the main resonance region ($f_0 : f_1 = 1 : 1$) was investigated.

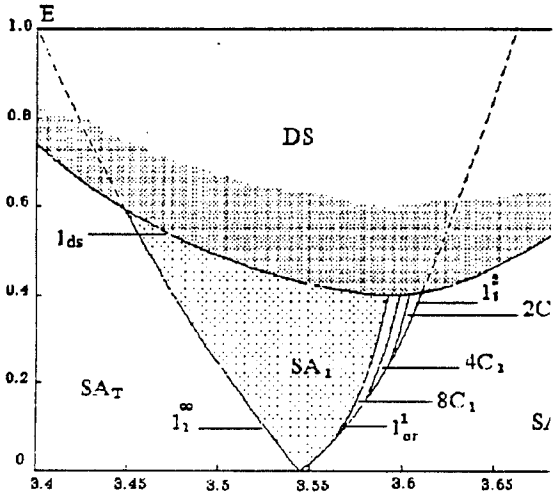

Figure 1: Main synchronization region for system (1).

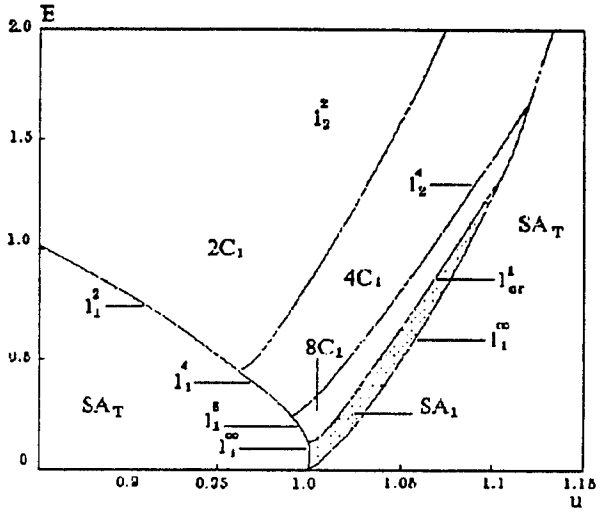

Figure 2: Main synchronization region for system (2).

Fig.1 illustrates the main synchronization region in the case of the weak spiral chaos ($\alpha = 11.98, \beta = 22.0, \gamma = 0.1$). This region arises due to locking of the basic frequency. The left boundary l_1^∞ corresponds to the transition "chaotic torus-attractor $SA_T \Rightarrow$ chaotic spiral Chua's attractor SA_1". In the right side of the region, narrow zones of regular oscillation kC_1 with periods $kT_1, T_1 = 1/f_1$ exist ($k = 2, 4, 8, ...$) The boundary is formed by the lines of tangent bifurcations l_1^k here. The line l_1^∞ has a very complicated structure and we conjecture that the accumulation of the lines l_1^k for the saddle cycles kC_1 corresponds to the transition "nonsynchronous chaos $\Rightarrow$ synchronous chaos" through frequency locking [2].

Numerical investigation of forced synchronization in Chua's circuit was supplemented by experiments with real Chua's circuits. Our experimental results agree qualitatively with the computer generated ones.

Let us consider next the forced synchronization of OIN, described by the following equations:

$$\dot{x} = mx + y - xz + \frac{\gamma E}{u}(\sin(ut) - \cos(ut)), \qquad \dot{y} = -x, \qquad \dot{z} = g(z - F(x)), \tag{2}$$

where $F(x) = x$ if $x \geq 0$ and $F(x) = 0$ if $x < 0$, E and u are forcing amplitude and frequency, respectively, and γ is the coupling coefficient. Fig.2 shows the main synchronization region for the regime of weak spiral-type chaos in the autonomous system (2) ($m = 1.52, g = 0.2, \gamma = 0.1$). The fundamental difference between the behavior of the forced Chua's circuit and the OIN is that upon increasing the synchronous forcing amplitude, the weak chaos in the Chua's circuit is transformed into the "stronger" chaotic double-scroll DS regime. It does not allow us to realize a synchronous suppression of chaos, which can be simply observed in the OIN, where the synchronous chaotic region is bounded from above by the sequence of lines of period-doubling bifurcations l_2^k, $k = 1, 2, 4, \ldots$. For the forced OIN we have succeeded in verifying with high precision our above hypothesis concerning the complicated structure of the line l_1^∞.

3 MUTUAL SYNCHRONIZATION OF CHAOS

Consider next two resistively-coupled Chua's circuits with detuning between basic frequencies:

$$\begin{aligned} \dot{x}_1 &= \alpha[y_1 - h(x_1)], & \dot{y}_1 &= x_1 - y_1 + z_1 + \gamma(y_2 - y_1), & \dot{z}_1 &= -\beta y_1, \\ \dot{x}_2/p &= \alpha[y_2 - h(x_2)], & \dot{y}_2/p &= x_2 - y_2 + z_2 + \gamma(y_1 - y_2), & \dot{z}_2/p &= -\beta y_2. \end{aligned} \tag{3}$$

Here γ characterizes the degree of coupling and $p = f_1/f_2$ determines the detuning. If $p = 1$, equations (3) describe the dynamics of two coupled completely identical Chua's circuits.

Let us fix the parameter values: $\beta = 22.0, a = -0.143, b = 0.286$. When $p = 1$ and $0 < \alpha < 8.78$, there are four stable equilibrium states P_i, $i = 1, 2, 3, 4$. When $\alpha = 8.78$, limit cycles C_i are born from the point P_i via Hopf bifurcations. As the parameter α increases, each of these cycles undergoes some sequence of bifurcations, and resulting in the increase of a number of multistable states. As detuning is introduced ($p \neq 1$), all oscillatory regimes observed at $p = 1$ continue to exist in some interval of values of the parameter p. These regimes evolve in some manner with the variation of p and undergo various bifurcations.

The main synchronization region and its neighborhood ($p \approx 1$) were investigated. Fig.3 shows the main synchronization region on the $(p-\gamma)$ plane for attractors placed in the neighborhood of the point P_1 at $\alpha = 11.6$, when the regime of spiral chaos SA_1 is realized in partial subsystems without coupling. Here kC_1^1 is the limit cycle with k loops around P_1, T_1^1 is the two-dimensional torus, SA_1^1 is the spiral chaos, SAT_1^1 is the torus-chaos, l_{cr}^2 is the line of torus collapse and torus-attractor emerging. In Fig.3, the synchronization region is determined by the lines of tangent bifurcation l_1^1 and the lines of torus birth l_1^0.

The investigation of the structure of the main synchronization region in the two coupled OIN's in the regime of weak spiral chaos was conducted in [2]. In contrast to Chua's circuit, the OIN circuit does not possess the symmetry property and its multistability is connected with the existence

of several fixed points in the phase space. A comparison of the bifurcation structure of the main synchronization region for the coupled Chua's circuit and the coupled OIN circuit reveals both similarities and essential differences, which can be explained both by individual peculiarities of the partial systems, and by the different character of coupling.

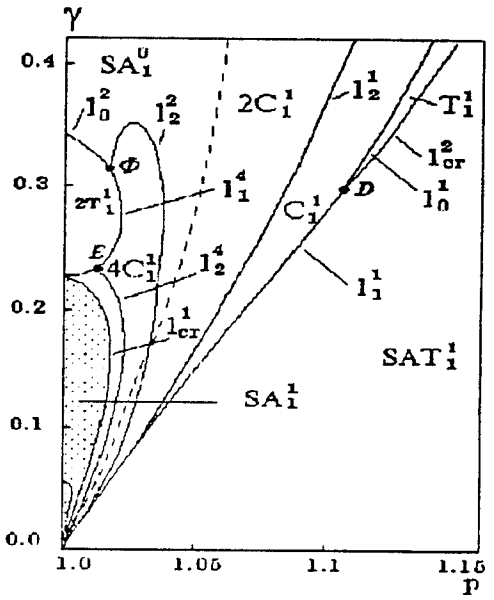

Figure 3: Main synchronization region in system (3).

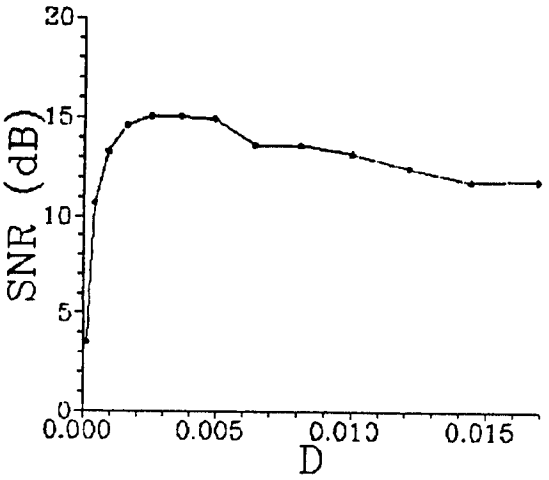

Figure 4: SNR versus D in the Chua's circuit driven by periodic signal and noise.

4 STOCHASTIC RESONANCE

We now turn our attention to the investigation of multi-frequency SR-phenomenon in the nonautonomous Chua's circuit:

$$\dot{x} = \alpha[y - h(x)], \qquad \dot{y} = x - y + z, \qquad \dot{z} = -\beta y + f(t) + \xi(t). \tag{4}$$

Let us fix the parameter values $a = -1/7, b = 2/7$. There is a bifurcation line l_{ds} separating regions of existence of two different types of chaotic attractors on the $(\alpha - \beta)$ parameter plane of the autonomous Chua's circuit. A pair of symmetrical spiral Chua's attractors take place to the right of the l_{ds}. Hence, Chua's circuit can be interpreted as a bistable nonlinear chaotic oscillator in this region. Any interactions between the two attractors can be induced only by external perturbations. These two attractors merge on the curve l_{ds} thereby giving rise to the birth of the double-scroll Chua's attractor, which exists to the left of this curve. In the vicinity of the bifurcation curve, the phase trajectory resides in each of the merged attractors for a long time and makes relatively few

transition between them. The mean switching frequency ω_s is very small here and we can identify a dynamical "chaos-chaos" intermittency phenomenon.

Let us fix $\beta = 14.286$ and consider the monochromatic signal $f(t)$ with $\omega_0 = 0.5652, A = 0.1$. Fig. 4 illustrates the case of noise induced intermittency and demonstrates the SR-phenomenon at $\alpha = 8.55$. Similar results were obtained for dynamical "chaos-chaos" intermittency at $\alpha = 8.85$, but a stronger SR-phenomenon take place in this case.

Consider now the amplitude modulated signal $f(t)$ with $m = 0.5, \omega_m = 0.1256$. In Figs. 5 and 6, we can observe an obvious SR-phenomenon both for a noise-induced and for a dynamical type of intermittency for all three basic frequencies of the signal. However, these results show rather strong nonlinear distortions of this signal, especially in the presence of noise. Probability density of the residence times for amplitude modulated signal was computed as well. Its structure reflects the presence of all three mentioned characteristic time constants and must contain the information about the fourth time constant $T_m = 2\pi/\omega_m$. However, more detailed calculation have to be conducted to reveal it.

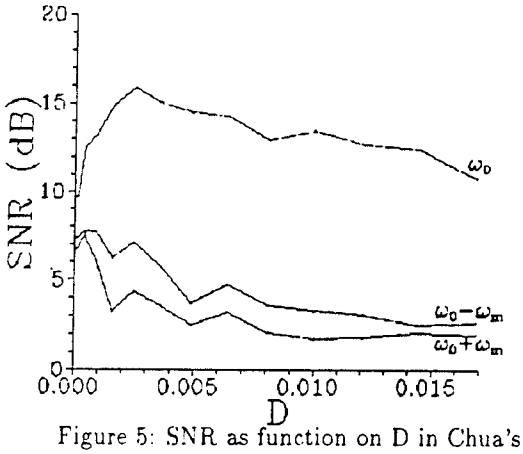

Figure 5: SNR as function on D in Chua's circuit with amplitude modulated signal.

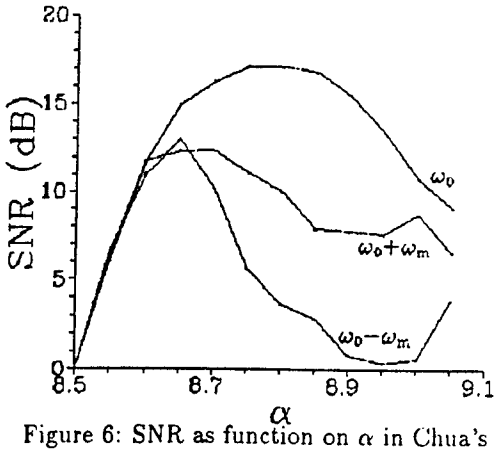

Figure 6: SNR as function on α in Chua's circuit with amplitude modulated signal.

Our examination of the SR-phenomenon induced by the frequency modulated signal $f(t)$ allows us to obtain qualitatively similar results. The SR-phenomenon takes place for all three basic frequencies in this case too and nonlinear distortions are a little less in this case.

5 CONCLUSIONS

Both non-autonomous Chua's circuit and system of two coupled Chua's circuits possess a rich set of all possible distinct dynamical regimes and their bifurcations. All currently known types of quasihyperbolic chaotic sets, scenarios of their birth, and bifurcations into chaos are present in these systems. These properties make Chua's circuit an ideal model for the investigation of the phenomenon of synchronization of chaos.

Investigations of forced synchronization in Chua's circuit in the spiral chaotic regime confirmed that both classical mechanisms of synchronization (frequency locking and frequency suppression) are realized in the case of chaotic behavior. Two resistively coupled identical Chua's circuits demonstrate the phenomenon of multistability of the regimes, which is connected with the existence of four potential wells in the neighborhood of four saddle equilibrium points. Our computer simulation gives evidence that the bifurcation scenario of multistability development has some universal character determined by the type of coupling between partial systems.

In the system of coupled Chua's circuits with detuning between basic frequencies, the frequency synchronization of the spiral chaos can be observed, as a result of mutual locking of basic frequencies of partial systems.

Our numerical data confirms that the SR-phenomenon in quasi-hyperbolic systems with chaotic dynamics can be realized. The interaction between chaotic attractors having a "chaos-chaos" type intermittency includes more possibilities. In particular, an increase in the SNR can take place by tuning the system parameters without external noise. In this case, the intrinsic chaotic dynamics plays the role of "deterministic" noise.

It is shown that the SR-phenomenon takes place in the case of amplitude and frequency modulated signals. The numerical simulation demonstrates that for the case of weak signals, some nonlinear distortions in the output take place. In this connection it is interesting to look for conditions where nonlinear distortion is minimized.

References

[1] L.O.Chua, M.Komuro, T.Matsumoto. "The double scroll family", *IEEE Trans. Circuits and Systems*, **33** (1986) 1073-1118.

[2] V.S.Anishchenko, T.E.Vadivasova, D.E.Postnov, M.A.Safonova. "Synchronization of chaos", *Int. J. Bif. and Chaos*, **2** (1992) 633-644.

[3] F.Moss. "Stochastic Resonance: From the Ice Ages to the Monkey's Ear", Dept. of Phys. of University of Missoury at Saint Louis, St.Louis, MO63121, USA, January 1992.

[4] V.S.Anishchenko, A.B.Neiman, A.M.Safonova. "Stochastic resonance in chaotic systems", *J. Stat. Phys.*, **70** (1993) 183-196.

[5] V.S.Anishchenko, M.A.Safonova, L.O.Chua. "Stochastic resonance in Chua's circuit", *Int. J. Bif. and Chaos*, **2** (1992) 397-402.

1993 International Symposium on Nonlinear
Theory and Its Applications (NOLTA '93)
Hawaii, U.S.A., December 5-10, 1993

Secure Communication via Chua's Circuit

M. Hasler*, H. Dedieu*, M. P. Kennedy**, J. Schweizer**
* Department of Electrical Engineering,
Swiss Federal Institute of Technology, 1015 Lausanne, Switzerland
** Department of Electrical and Electronic Engineering
University College Dublin, Dublin 4, Ireland

ABSTRACT

The various methods of synchronizing chaotic circuits and transmitting information hidden in a chaotic signal are presented in a systematic manner. Different realizations of such systems using Chua's circuit, and a limiting version proposed by Saito, are discussed.

1. INTRODUCTION

Since Pecora and Caroll [1, 2] have shown that it is possible to synchronize chaotic systems, various authors [3–6, 8–10, 13] have proposed schemes for using a chaotic signal for secure communications. The various approaches differ in the way synchronization is obtained, and in the way the information carrying signal is hidden in the chaotic signal. We shall give a short overview over these two subjects that is inspired by [7].

Chua's circuit has been a good vehicle for laboratory implementations of such communication systems [4–6, 8–10] but other circuits have also been used [3, 13]. In this paper we report on various realizations we have accomplished by simulation and hardware implementations using Chua's circuit and a limiting case of Chua's circuit family proposed by Saito.

It should be stressed that by far not all aspects of a secure communication system are addressed in this work nor have they been addressed in the other papers that are referenced here. At this stage we simply show that it is possible to hide useful information in a chaotic signal and retrieve it subsequently. Problems like finite channel bandwidth have not been studied.

2. SYNCHRONIZATION PRINCIPLES

Basically, three different methods have been proposed for the synchronization of chaotic systems, synchronization by decomposition into subsystems [1, 2], synchronization by error feedback [5, 11] and synchronization using the inverse system [8, 9]. The first method amounts to representing a chaotic system as a connection of two subsystems (Fig. 1). Under certain circumstances, opening the loop in Figure 1 leads to a system whose asymptotic input-output function is the identity (Fig. 2). In this case, a 'master' system can drive a 'slave' system such that asymptotically all variables in the slave system are identical to those at the master system, even if the waveforms have a chaotic aspect. This method is studied systematically in [12]. The second method is a classical control approach by error feedback shown in Fig. 4. Finally the last method uses as the 'slave' system an inverse of the 'master' system. A system is called an inverse here, if it produces the input signal of the original system when it is excited by the output of the original system and when the initial conditions of the two systems are identical. Of course, we have in general no control over

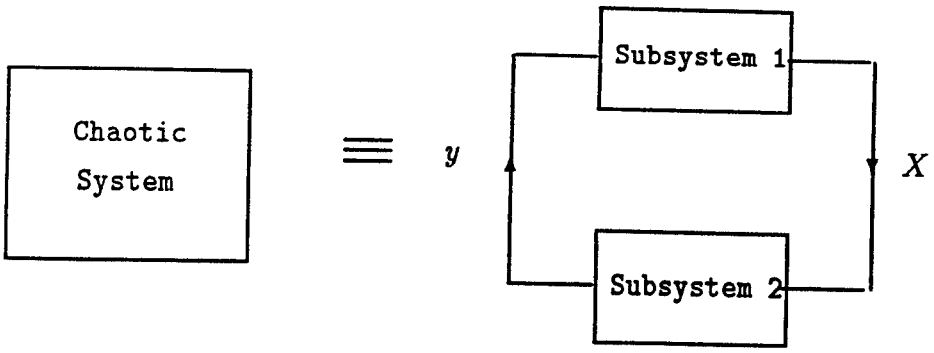

Figure 1. Decomposition of a chaotic system as a loop made of two subsystems

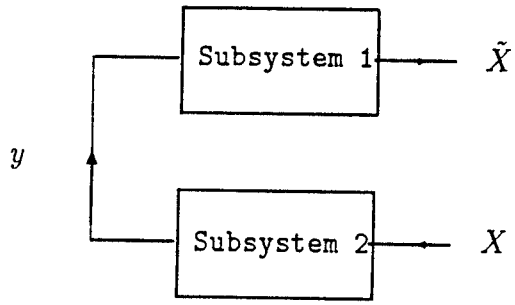

$$|\tilde{X}(t) - X(t)| \rightarrow 0 \quad for \quad t \rightarrow \infty$$

Figure 2. Breaking the loop and forcing one subsystem may result in a system asymptotically equivalent to the system of Fig. 1

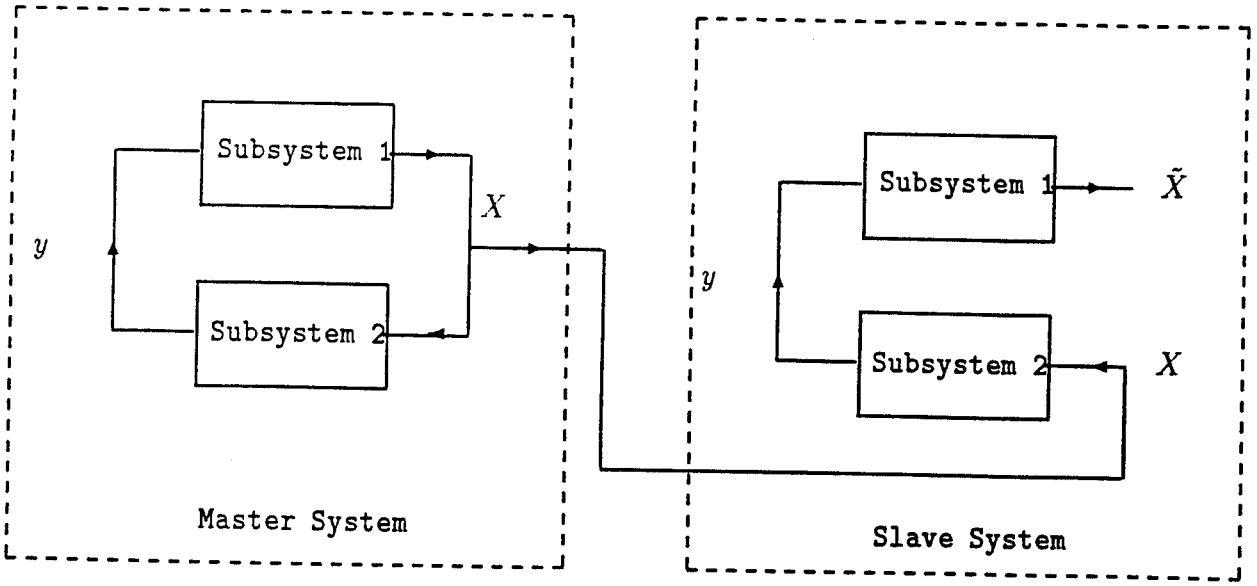

Figure 3. Basic configuration scheme for the synchronization by decomposition into subsystems

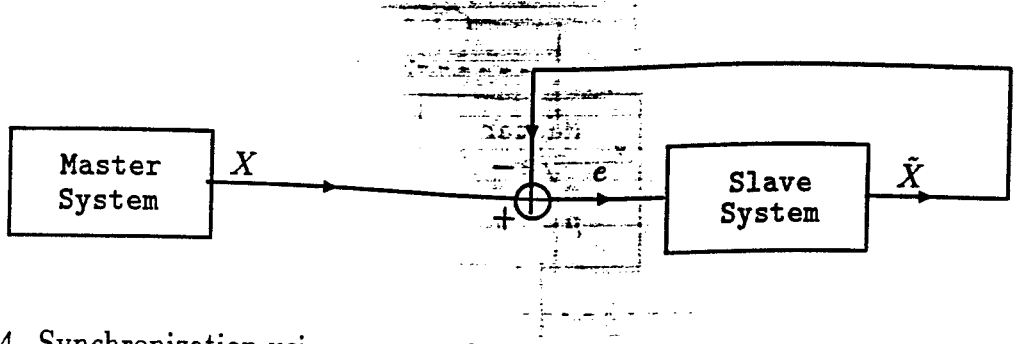

Figure 4. Synchronization using an error feedback scheme

Figure 5. Syncronization using a slave system that is the 'inverse' of the master system

the initial conditions and therefore for synchronization we need the asymptotic convergence to the input of the original system when the inverse system starts from an arbitrary initial condition. Note that in the first two methods the master system is autonomous, whereas in the third method it is driven by an external signal. This difference is important in the context of secure communications. It might appear hopeless to find a chaotic system with a globally asymptotically stable inverse. However in the context of circuits, this is not so strange. In fact, the voltage of a one-port can be interpreted as the input variable and the current as the output variable or *vice versa* (Fig. 6). Usually, the two corresponding systems are the inverse of each other.

3. TRANSMISSION PRINCIPLES

Again, three different methods for transmitting an information signal $S(t)$ via a chaotic carrier $X(t)$ can be distinguished.

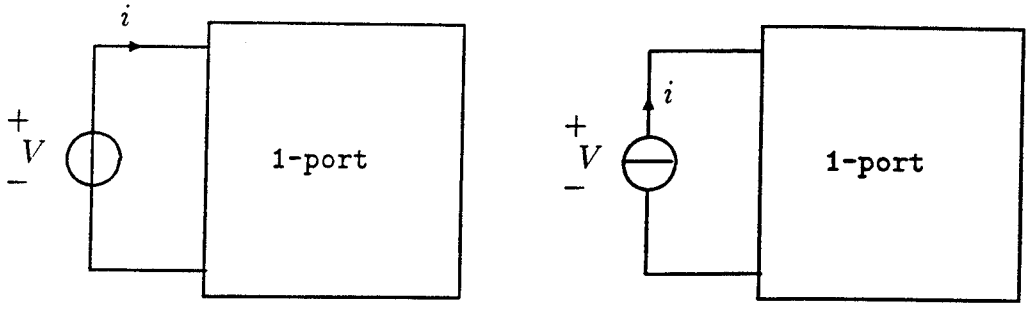

Figure 6. Master system and inverse system circuit design

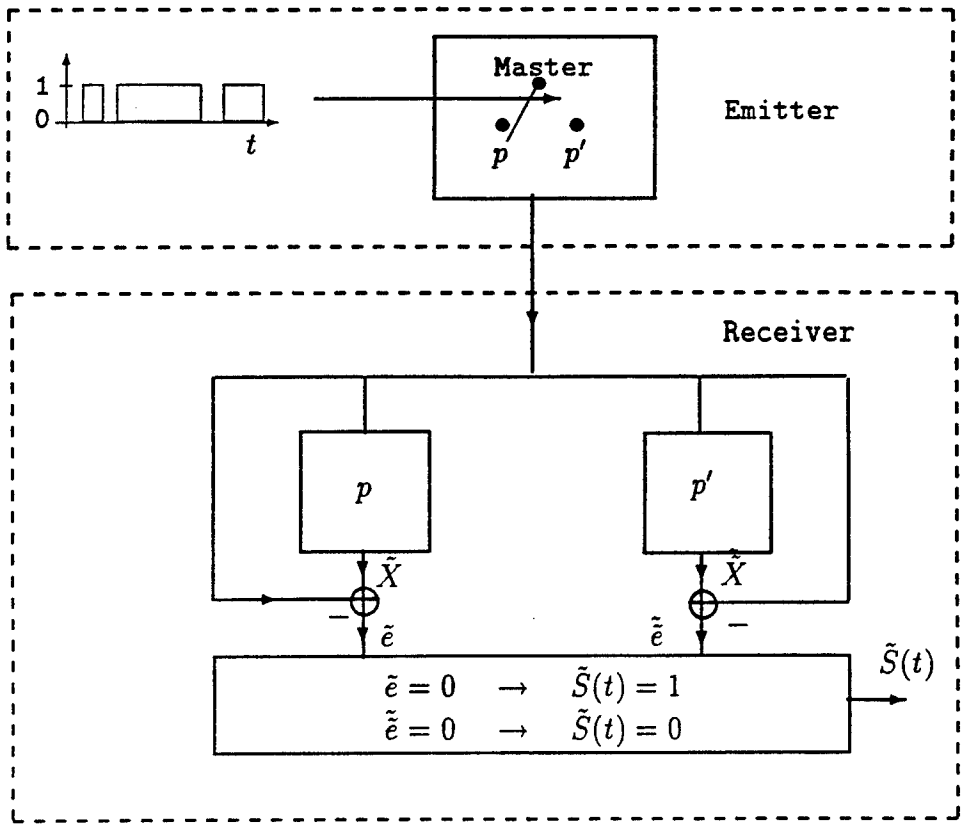

Figure 7. Basic scheme for chaotic switching

The first, *chaotic masking* consists simply of adding $S(t)$ to the chaotic signal $X(t)$ [3]. In the second, *chaotic switching* [4–6, 10, 13], a binary signal drives a switch between two parameters values of the master system, which is the emitter. On the receiver side, two slave systems, one for each parameter value, try to synchronize to the transmitted (chaotic) signal $X(t)$. The one who succeeds determines the received bit (Fig. 7) Finally, *chaotic modulation* [8, 9] uses directly the synchronization method of Fig. 5. In this case, the information signal $S(t)$ is usually analog, but a digitally modulated signal $S(t)$ can also be used, as will be shown in the last example of this paper.

4. EXAMPLES

As a first approach we have divided Chua's circuit into two subcircuits for synchronization according to the Pecora-Caroll method. The binary input signal switches a linear resistor in parallel to the nonlinear resistor in Chua's circuit. The experimental and simulation results are reported in [4], together with a proof of synchronization under a certain hypothesis on the transmitted (chaotic) signal.

A second approach uses feedback and chaotic switching. Simulations and laboratory experiments have shown the viability of the approach [5] and for certain sets of parameters synchronization has been shown by a Lyapunov function.

The last approach we have tried uses the circuit proposed by Saito with chaotic modulation (Fig. 8). The nonlinear element is a voltage controlled voltage source with the nonlinear

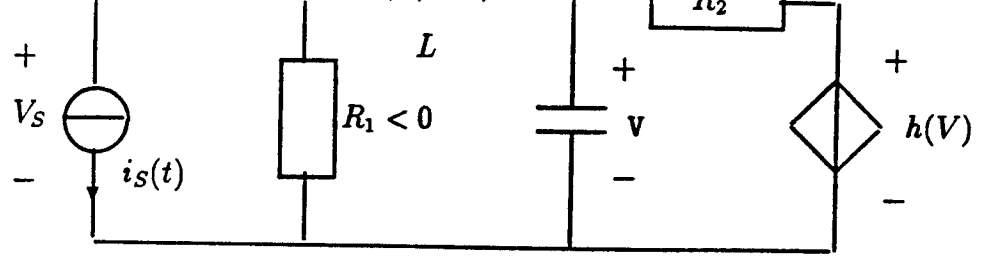

Figure 8. The Saito's circuit

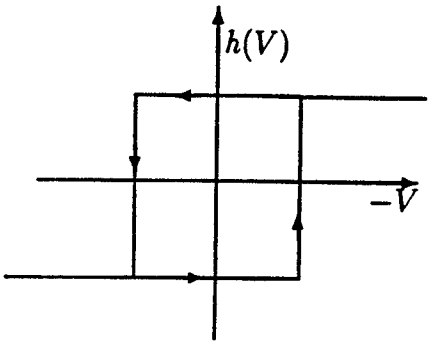

Figure 9. Nonlinear characteristic of the voltage controlled source of the Saito's circuit

that instead of the current source with signal $i_s(t)$ a voltage source imposes $v_s(t)$ transmitted by the emitter. The current in this source is $\tilde{i}_s(t)$ that asymptotically equals $i_s(t)$, the information carrying signal. We have used 180° phase-shift keying for transmitting binary information on the analog signal $i_s(t)$. In Fig. 10 both $i_s(t)$ (in bold) and $\tilde{i}_s(t)$ are shown. Clearly the circuit is able to follow perfectly the sign inversions of the sinusoid. Finally, in Fig. 11 the transmitted and the detected baseband signal are shown when 0 and 1's alternate regurlarly. It can be seen that there is no obvious way to detect the transmitted bit from the transmitted signal without any additional knowledge.

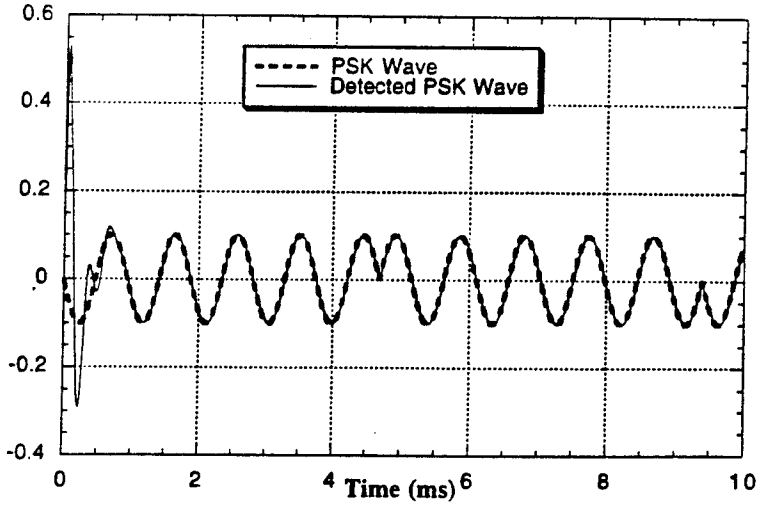

Figure 10. Recovery of the phase-shift keyed sinusoid

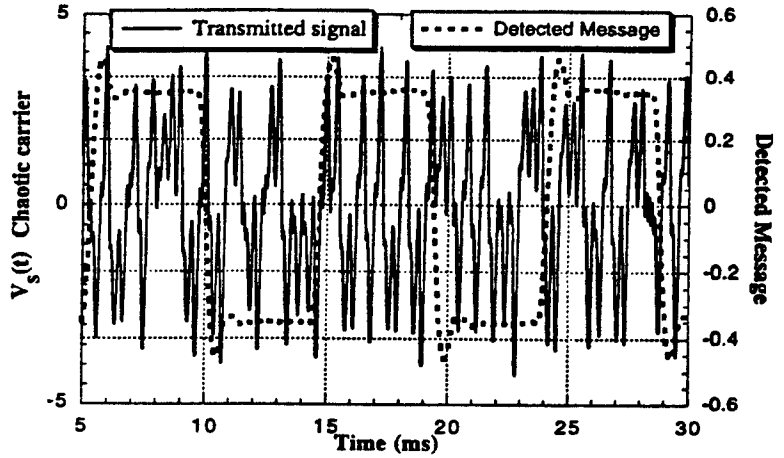

Figure 11. Detected signal versus transmitted (chaotic) signal

5. CONCLUSION

We have given a classification of synchronization methods and of transmission methods using a chaotic carrier signal. Three prototype circuits have been shown to work in principle, each one using a different synchronization method.

REFERENCES

1. L. M. Pecora, T. L. Carroll, *Synchronization in Chaotic Systems.* Physical Review Letters, Vol 64, Number 8, pp. 821-824, February 1990.
2. L. M. Pecora, T. L. Carroll, *Driving Systems with Chaotic Signals.* Physical Review A, Vol 44, Number 4, pp. 821-824, August 1991.
3. A. V. Oppenheim, G. W. Wornell, S. H. Isabelle, K. M. Cuomo, *Signal Processing in the Context of Chaotic Signals.* Proceedings of the 1992 IEEE ICASSP, pp. IV-117-IV-120
4. H. Dedieu, M.P. Kennedy, M. Hasler, *Chaos Shift Keying: Modulation and Demodulation of a Chaotic Carrier using Self-synchronising Chua's Circuits.* IEEE Trans. Circuits Systems, vol.40, No.10, 1993 (in press).
5. M. Hasler, H. Dedieu, J. Schweizer, M.P. Kennedy *Synchronization of Chaotic Signals.* Worshop on Nonlinear Dynamics of Electronics Systems, Dresden, July 1993.
6. M.P. Kennedy, H. Dedieu, *Experimental Demonstration of Binary Chaos-Shift-Keying using Self-Synchronising Chua's Circuits.* Worshop on Nonlinear Dynamics of Electronics Systems, Dresden, July 1993.
7. M.J. Ogorzałek, *Taming chaos: Part I - Synchronisation.* IEEE Trans, Circuits Systems, vol.40, No.10, 1993 (in press)
8. K. Sean Halle, Chai Wah Wu, Makoto Itoh and L. O. Chua *Spread Spectrum Communication Through Modulation of Chaos* Int. Journal of Bifurcation and Chaos, Vol. 3, No. 2, 1993.
9. M. Itoh, H. Murakami, K. S. Halle, L. O. Chua *Communication Systems via Chaos Synchronization.* 1993 Joint Technical Conference on Circuits/ Systems, Computers and Communications, Nara, Japan.
10. Lj. Kocarev, K. S. Halle, K. Eckert, L. O. Chua and U. Parlitz *Experimental Demonstration of Secure Communications via Chaotic Synchronization.* International Journal of Bifurcation and Chaos, Vol. 2, Number 3, September 1992, pp. 709-713.
11. X. Dong, G. Chen, *On Feedback Control of Chaotic Continuous-Time Systems.* IEEE Trans. on Circuits and Systems, in press.
12. A. Tesi, A. De Angeli, R. Genesio *On the System Decomposition for Synchronizing Chaos.* Technical Report, RT 12/93, Universitá di Firenze.
13. K. M. Cuomo, A. V. Oppenheim *Circuit Implementation of Synchronized Chaos with Applications to Communications.* Physical Review Letters, Vol. 71, pp. 65-68, 1993
14. T. Saito, K. Mitsubori *Hyperchaos and Related Phenomena from Odd-Dimensional Hysteresis System.*Worshop on Nonlinear Dynamics of Electronics Systems, Dresden, July 1993.
15. T. Saito *An Approach toward Higher-dimensional Hysteresis Chaos Generator.* IEEE Trans., CAS-37, 3 (1990), p. 399.

1993 International Symposium on Nonlinear
Theory and Its Applications (NOLTA '93)
Hawaii, U.S.A., December 5-10, 1993

Trajectory Recognition in an Array of Chaotic Systems Using Chua's Circuit

Edward J. Altman
ATR Communication Systems Research Laboratories,
2-2 Hikari-dai, Seika-cho, Soraku-gun, Kyoto 619-02, Japan

ABSTRACT

This paper presents a formulation of the problem of human hand gesture recognition in terms spatial pattern formation induced within an array of dynamical systems. The primary problem of gesture recognition for real-time human-computer interaction is the rapid acquisition and classification of motion trajectories. The design of a multi-attractor array is presented which uses Chua's circuit as a simplified abstraction of the model dynamics. Temporal trajectories are used to drive the array of modified Chua's circuits into spatial patterns of synchronous behavior.

1 Introduction

The system of hand gestures developed in American Sign Language constitutes a richly expressive visual language. The real-time recognition of temporal trajectories arising from hand gestures is an inherently parallel task for which it is argued that nonlinear dynamical systems are particularly well matched. A simple subset of these signed expressions has important applications for human-computer interaction in virtual reality applications[1].

The parallel recognition of a large repertoire of trajectories is a nonlinear phenomena for which chaotic systems provide the potential for considerable simplification. Synchronization to the input signal optimizes the correspondence with the input signal. Rapid convergence onto an attractor on a center manifold surface enables real-time recognition. The formation of spatial patterns of synchronized activity in the array enables recognition of multiple gestures. Rapid transitions between attracting surfaces enable the tracking of smooth transitions of hand motion between sign language expressions. The full utilization of these interdependent phenomena for the recognition of complex motion trajectories requires new methods for the design of nonlinear dynamical systems.

A paradigm for the study of nonlinear systems has recently emerged with the introduction of Chua's circuit[2] and its associated canonical circuit family[3]. The relative simplicity of Chua's circuit provides a convenient model of the dynamics and bifurcation phenomena for the design of more complex systems. A coupled array of Chua's circuits is an example of a complex, massively parallel system synthesized from simpler elements. In order to simplify the design of the gesture recognition system, each dynamical system in the array is constrained to have the same normal form as Chua's circuit, therefore the detailed knowledge

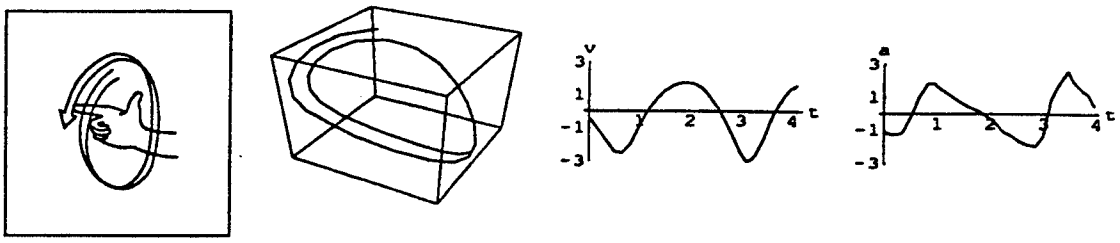

(a) (b) (c) (d)

Figure 1: Hand trajectory for a simple gesture. (a) Hand motion. (b) Position. (c) Velocity in the x direction. (d) Acceleration in the x direction.

of a single system suffices for all elements in the array. The introduction of local coupling and external driving signals creates new phenomena, not present in the original circuit, which are particularly useful for temporal pattern recognition. In particular, the problem of trajectory recognition is transformed into the simpler task of pattern formation through the design of multiple, simple systems, each of which is broadly responsive to many inputs, while exhibiting a collective behavior which is quite selective.

2 Formulation of the Recognition Problem

A simplified hand gesture is characterized by the following attributes. (1) A space curve followed by the moving hand. (2) The position of the hand along this space curve as a function of time. (3) The configuration of the hand as a function of position along the curve. Additionally, the recognition of gestures is strongly influenced by velocity and acceleration profiles[4] which are illustrated in Fig. 1. In this paper, the recognition of trajectories formed by the moving hand with a fixed hand configuration is formulated using chaotic systems. The role of chaos is to facilitate the transition between attractors for motion trajectories from two successive gestures.

One possible formulation of the gesture recognition problem is to assume a direct mapping between the hand motion trajectory and a trajectory on a center manifold surface of a dynamical system. Such a one-to-one correspondence leads to severe demands on the detailed design of nonlinear dynamics and unnecessary specialization. A more general recognition problem can be solved by making a weaker assumption concerning the mapping between input trajectories and dynamics. The design of the more general system is based upon global synchronization to the input signal and the formation of spatial patterns.

The design of the recognition system begins with a large array of identical dynamical systems. A core set of dynamical systems within the array can be modified to recognize specific input signals. This corresponds to a traditional winner-take-all network in which the response of the dominant system is used to identify the input signal. However, the ability of simple nonlinear circuits to synchronize to a broad class of inputs means that many systems in the array will respond to a large class of signals. This gives rise to the emergence of spatial patterns of synchronized activity reflecting the global behavior of the array similar to a Freeman type network[5].

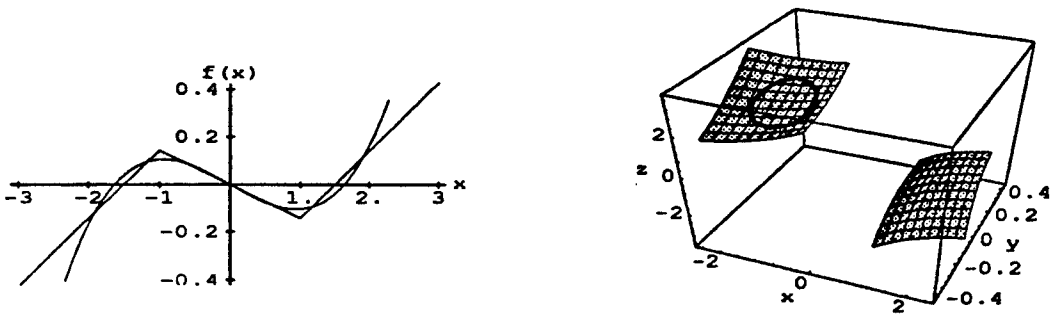

(a) (b)

Figure 2: Nonlinear dynamics. (a) Cubic nonlinearity of Chua's circuit equations. (b) Center manifolds at the equilibria with limit cycle oscillations on the manifold surface.

3 Normal Form of Chua's Circuit

The hand motion associated with a particular gesture may be partially described by a trajectory on a 3D surface and modeled by a dynamical system. The model dynamics is based upon the dimensionless form of Chua's circuit equations[2],

$$\begin{aligned} \dot{x} &= \alpha\,[y - f(x)] \\ \dot{y} &= x - y + z \\ \dot{z} &= -\beta y \end{aligned} \tag{1}$$

where the piece-wise linear function is replaced with the cubic nonlinearity $f(x) = c_0 x + c_1 x^3$ with $c_0 = -\frac{1}{6}$ and $c_1 = \frac{1}{16}$. The shape of $f(x)$ and the corresponding piece-wise linear function are illustrated in Fig. 2(a).

Chua's circuit has three equilibria at $P_0 = (0,0,0)$ and $P_\pm = \left(\pm\sqrt{-\frac{1+c_0}{c_1}}, 0, \mp\sqrt{-\frac{1+c_0}{c_1}}\right)$. Near the equilibrium P_+, we have the linearization

$$M = Df|_{P_+} = \begin{bmatrix} \alpha c_0 - 3(c_0+1) & \alpha & 0 \\ 1 & -1 & 1 \\ 0 & -\beta & 0 \end{bmatrix}. \tag{2}$$

If α and β are chosen such that (2) has a pair of complex conjugate eigenvalues $\sigma \pm i\omega_0$ and a real eigenvalue γ, then the augmented Jordan form[6]

$$\begin{bmatrix} \dot{u} \\ \dot{v} \\ \dot{\sigma} \\ \dot{w} \end{bmatrix} = \begin{bmatrix} 0 & -\omega_0 & 0 & 0 \\ \omega_0 & 0 & 0 & 0 \\ 0 & 0 & 0 & 0 \\ 0 & 0 & 0 & \gamma \end{bmatrix} \begin{bmatrix} u \\ v \\ \sigma \\ w \end{bmatrix} + \begin{bmatrix} \sigma u \\ \sigma v \\ 0 \\ 0 \end{bmatrix} + \begin{bmatrix} f(u,v,w) \\ g(u,v,w) \\ 0 \\ h(u,v,w) \end{bmatrix} \tag{3}$$

has the linear part in block diagonal form and the higher order nonlinear terms are expressed by the functions $f(\cdot)$, $g(\cdot)$, and $h(\cdot)$. This system is augmented by treating σ as an additional variable with the condition $\dot{\sigma} = 0$. The term σ will later serve as a bifurcation parameter which determines the amplitude of limit cycle oscillations in the normal form.

In the study of the local behavior of solutions of nonlinear differential equations, the choice of coordinate systems plays a major role in identifying the qualitative properties of the flows. The *normal form* is considered as the simplest member of an equivalence class of

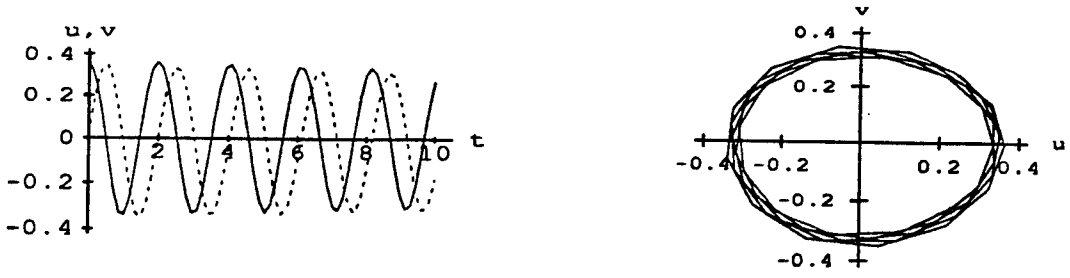

(a) (b)

Figure 3: Limit cycle oscillations of Chua's circuit on the center manifold. (a) Temporal profiles of the center manifold variables u (solid) and v (dashed). (b) Phase plot in the uv-space.

vector fields, all exhibiting the same qualitative behavior near the equilibria of the system. The basic approach to constructing the normal form equations for a dynamical system is based upon the computation of nonlinear transformations which systematically reduce the coupling among low order terms in the original system. The normal form computations of Takens[6] and Ushiki[7] systematically simplify the form of the dynamical system using Lie bracket operators to make coordinate transformations in the complementary space. Takens' method assumes that the coefficients in the transformation are fixed, then uses rescaling to simplify the normal form coefficients. In Ushiki's method, the coefficients are parameterized so that a particularly simple form can be obtained for certain parameter values.

The normal form transformations are based upon diffeomorphisms, therefore the local dynamics near the equilibria of the original system is topologically equivalent to the dynamics on the center manifold. The center manifold provides a geometric method for modifying the vector field to optimize the response of the system to the input trajectory to be recognized.

The normal form computation requires that the dynamics be projected onto a reduced dimensional space called the *center manifold* which is an invariant manifold tangent to the center eigenspace at the equilibrium of the system[6]. The surface of the center manifold is described locally by the nonlinear graph $w = S(u, v, \sigma)$. A view of the two center manifolds associated with P_+ and P_- projected back into the xyz-coordinates of Chua's circuit is illustrated in Fig. 2(b). The limit cycle oscillations of Chua's circuit in the uv-coordinates of the center manifold in Fig. 3, show that the complex limit cycle trajectories in the xyz-space have a simple form in the uv-coordinate space of the center manifold.

The third order normal form of Chua's circuit on the center manifold is given by[8]

$$\begin{bmatrix} \dot{u}' \\ \dot{v}' \\ \dot{\sigma}' \end{bmatrix} = \begin{bmatrix} 0 & -\omega_0 & 0 \\ \omega_0 & 0 & 0 \\ 0 & 0 & 0 \end{bmatrix} \begin{bmatrix} u' \\ v' \\ \sigma' \end{bmatrix} + \begin{bmatrix} s_1 u'\sigma' - a_2 v'\sigma' \\ a_2 u'\sigma' + s_1 v'\sigma' \\ s_2(u'^2 + v'^2) + b_2 \sigma'^2 \end{bmatrix} + \begin{bmatrix} a_3(u'^2 + v'^2)u' - a_4(u'^2 + v'^2)v' \\ a_4(u'^2 + v'^2)u' + a_3(u'^2 + v'^2)v' \\ b_4 \sigma'^3 \end{bmatrix}. \quad (4)$$

This normal form has a particularly simple form when expressed in cylindrical coordinates

$$\begin{aligned} \dot{\rho} &= s_1 \rho \sigma' + a_3 \rho^3 + \mathcal{O}\left(|\rho, \theta, \sigma'|^4\right) \\ \dot{\theta} &= \omega_0 + a_2 \sigma' + a_4 \rho^2 + \mathcal{O}\left(|\rho, \theta, \sigma'|^4\right) \end{aligned} \quad (5)$$

$$\dot{\sigma}' = s_2\rho^2 + b_2\sigma'^2 + b_4\sigma'^3 + \mathcal{O}\left(|\rho, \theta, \sigma'|^4\right)$$

evaluated up to order three. The value of ρ corresponds to the radius of the limit cycle on the uv-surface of the center manifold, θ is the phase angle, and σ' corresponds to the bifurcation parameter σ in the augmented system in (3). The design of new dynamics based upon the normal form is facilitated by the use of closed form expressions relating the normal form coefficients to the dynamics on the center manifold surface[6, 8].

4 Pattern Formation and Global Synchrony

A restricted set of trajectories consisting of circular motions in various regions in the physical space are initially used. This initial set of trajectories is chosen to allow the direct mapping between the core set of modified Chua's circuits and the space coordinates of the input trajectory. This forms a base set of dynamical systems having the same normal form, thus the qualitative behavior of each autonomous system is known. The general form of the nonautonomous dynamics for the diffusively coupled array is

$$\begin{aligned} \dot{x}_{ij} &= f(x_{ij}, y_{ij}, z_{ij}) \\ \dot{y}_{ij} &= g(x_{ij}, y_{ij}, z_{ij}) + \gamma(y_{ij} - \sum_{W} y_{lm}) \\ \dot{z}_{ij} &= h(x_{ij}, y_{ij}, z_{ij}) \end{aligned} \tag{6}$$

where γ is the diffusive coupling among systems within the window of size W. Considerable simplification is achieved when (6) is divided into an x-subsystem (called the *drive system*) and a yz-subsystem (called the *response system*) following the formulation of Pecora and Carroll[9, 10]. Each x_{ij} term in the yz-system is subsequently replaced by the input trajectory $x'(t)$ to be recognized to form a *drive-response system.*

The interpretation of the state of each dynamical system in the array may be as difficult to achieve as the original recognition task. This problem is greatly simplified by the partial entrainment of each dynamical system to the input trajectory. The perturbation to the dynamics in the yz-subsystem is minimized when $x'(t)$, corresponds to a trajectory on the center manifold surface, thus leading to the synchronization of the y and z-components to the corresponding components of the input. The global entrainment of the array is illustrated in Fig. 4(a) with a 3×3 subsample of the y component from a 12×12 array of modified Chua's circuits. The spatial pattern formed by measuring the distance between the y and z components of each driven system in the array and the corresponding components of the input signal is shown in Fig. 4(b). A small subset of the elements, indicated by the dark regions, synchronize in both phase and amplitude to the input. The remaining elements synchronize in phase but not amplitude as indicated by the light regions of Fig. 4(b).

5 Conclusion

The proposed recognition system begins with the specialized design of a few dynamical systems responsive to particular input signals. Subsequent changes to the dynamics are based upon the optimization of pattern formation in the array. The global synchrony and formation of spatial patterns then constitutes a generalization of the system to the recognition of a potentially large number of input signals depending upon the size of the array and the capacity for pattern formation by the array. This evolution of dynamics enables the eventual decoupling of the specific characteristics of the input signal from the details of the dynamics.

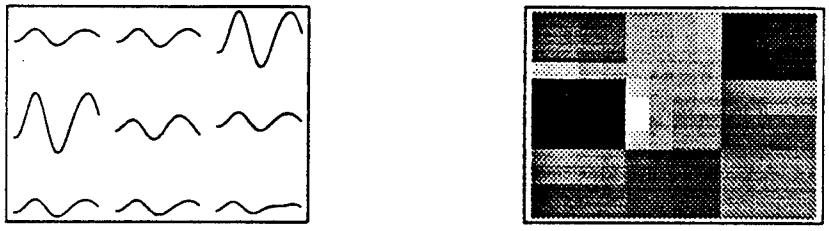

(a) (b)

Figure 4: An array of Chua's circuits driven by a nonperiodic function. (a) Global coherence of the y-component. (b) Spatial pattern of activity in the array.

References

[1] M. Krueger, *Artificial Reality II.* Reading, Mass.: Addison-Wesley, 1991.

[2] L. O. Chua, M. Komuro, and T. Matsumoto, "The double scroll family," *IEEE Trans. Circuits Syst.*, vol. CAS-33, no. 11, pp. 1073–1118, 1986.

[3] L. O. Chua and G.-N. Lin, "Canonical realization of Chua's circuit family," *IEEE Trans. Circuits Syst.*, vol. CAS-37, no. 7, pp. 885–902, 1990.

[4] H. Poizner, E. S. Klima, and U. Bellugi, *What the Hands Reveal about the Brain.* Cambridge, Mass.: The MIT Press, 1987.

[5] Y. Yao and W. J. Freeman, "Model of biological pattern recognition with spatially chaotic dynamics," *Neural Networks*, vol. 3, pp. 153–170, 1990.

[6] J. Guckenheimer and P. Holmes, *Nonlinear Oscillations, Dynamical Systems, and Bifurcations of Vector Fields.* New York: Springer-Verlag, 1983.

[7] L. O. Chua and H. Kokubu, "Normal forms for nonlinear vector fields–Part I: Theory and algorithm," *IEEE Trans. Circuits Syst.*, vol. CAS-35, no. 7, pp. 863–880, 1988.

[8] E. J. Altman, "Normal form analysis of Chua's circuit with applications for trajectory recognition," *IEEE Trans. Circuits Syst.—I*, vol. 40, Oct. 1993.

[9] L. M. Pecora and T. L.Carroll, "Synchronization in chaotic systems," *Phys. Rev. Lett.*, vol. 64, pp. 821–824, 1990.

[10] L. O. Chua, M. Itoh, L. Kocarev, and K. Eckert, "Chaos synchronization in Chua's circuit," *J. Circuits, Systems, and Computers*, vol. 3, no. 1, pp. 93–108, 1993.

Theory and its Applications (NOLTA'93)
Hawaii, U.S.A., December 5-10, 1993

Real-time Horseshoe Visualization in Chua's Circuit

Fan Zou, J. Pletl and Josef A. Nossek
Institute for Network Theory and Circuit Design
Technical University of Munich, Germany

Abstract

This paper describes a set up for the visualization of Poincaré return maps of dynamic systems. Previously, this circuit has been successfully applied to a nonautonomous electrical circuit, which exhibits chaos. It is shown in this paper, that the circuit can be also successfully applied to the famous Chua's circuit.

1 Introduction

It is well known that horseshoe map can be often found in a chaotic system [1]. However, the visualization of a horseshoe map in a real circuit has not been reported. In this paper, a method is proposed for this purpose. Let the initial conditions be set subsequently to the points of a square on a plane in phase space, and let's trace trials to the points of the first Poincaré map. If the circuit is fast enough, we are able to show both the initial square and the distorted (expanded, stretched and folded in chaotic case) map of this square. Because the size and position of this initial square can be easily adjusted, the circuit can be used as a fast searching tool for horseshoe map in nonlinear electrical systems.

2 Circuit Description

At first, we have chosen the two-cell nonautonomous CNN (Lady's Shoe Attractor) [2] as our target circuit under investigation. The circuit for visualization of horseshoe map is depicted in the Fig. 1. The sinusoidal signal, needed for the Lady's shoe attractor as the periodic forcing signal, is used here to synchronize the timing of the circuit. The Phase-shifter forms a pulse signal from the sinusoidal signal at the given phase lag. An adjustable counter is connected to the output of the Phase-shifter. It gives a reset signal by the set value and switches at the same time in the run or load mode. This reset signal is directly connected to the z-input of the oscilloscope in order to sample the state variably in the discrete time. To ensure the right timing of the initial points or their Poincaré maps, we have added a time-delay unit between the adjustable counter and the Run/Load input of the CNN circuit. The initial conditions are formed in steps with the 4-bit counter and with the D-A converter. Each step corresponds with a point of the initial square in the voltage phase plane. The square consist of 16*16 dots. The 1/16 divider is used for providing rowwise

scanning properly. The initial conditions are inverted for the projection, because the CNN inverts the input conditions too. The analog switches finally choose the initial conditions or the output of the CNN in the right time.

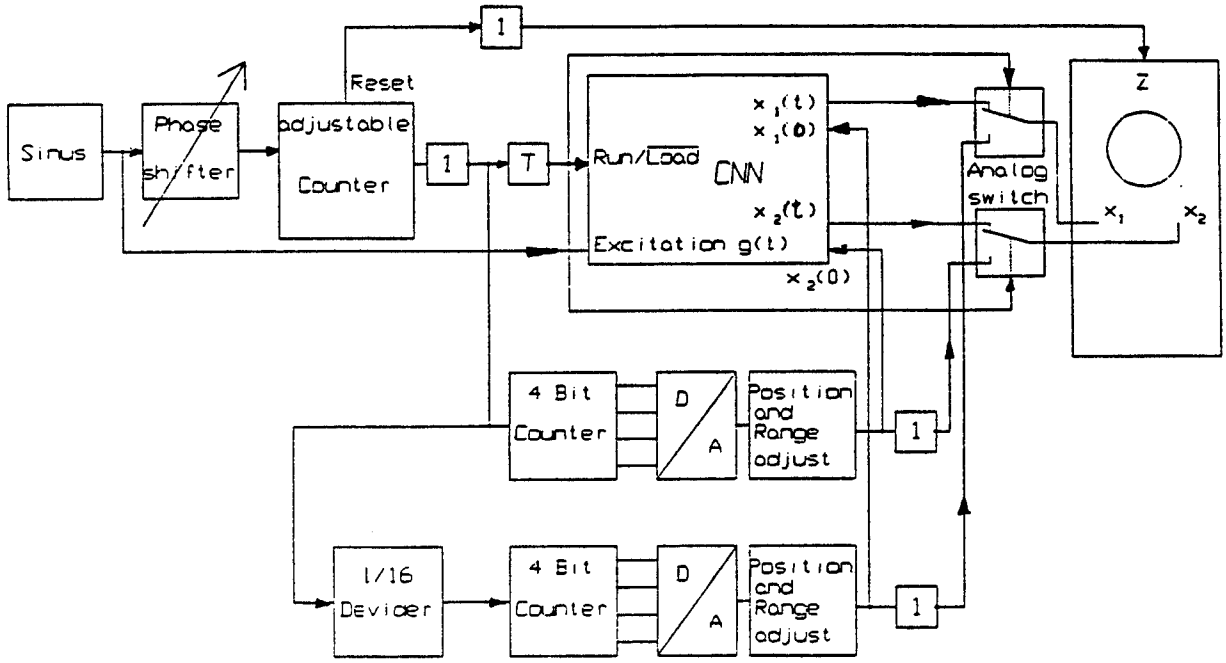

Fig. 1. Circuit in block diagram

Experimental results with the nonautonomous CNN circuit can be find in [3].

3 Showing Horseshoe Map in Chua's Circuit

The real-time visualization of horseshoe map in an autonomous circuit is a much more difficult job. For the purpose of experiments, we have chosen the Chua's circuit as our target circuit under investigation. The circuit for visualization of horseshoe map is depicted in the Fig. 2. Because the Chua's circuit is autonomous, we have no external periodic exciting signal to synchronize the timing of Poincaré maps. The signal of the third dimension in the system (called $x_3(t)$), be either u_{C1}, u_{C2} or i_L, is used here to synchronize the timing of the circuit. A level crossing detector forms pulse signal from $x_3(t)$ at the given voltage level and the positive transition direction. An adjustable counter is connected to the output of the level-shifter. It gives a reset signal by the set value and switches at the same time in the run or load mode. The reset signal and other signals (e.g. signals for initial condition settings) can be generated using the same circuitry above. Note that the pulses of these signals have an irregular timing now. For setting initial conditions conveniently, the inductor used in

Chua's circuit is replaced by a capacitor with a gyrator. The circuit with its control switches are depicted in great detail in Fig. 5 at the end of this paper.

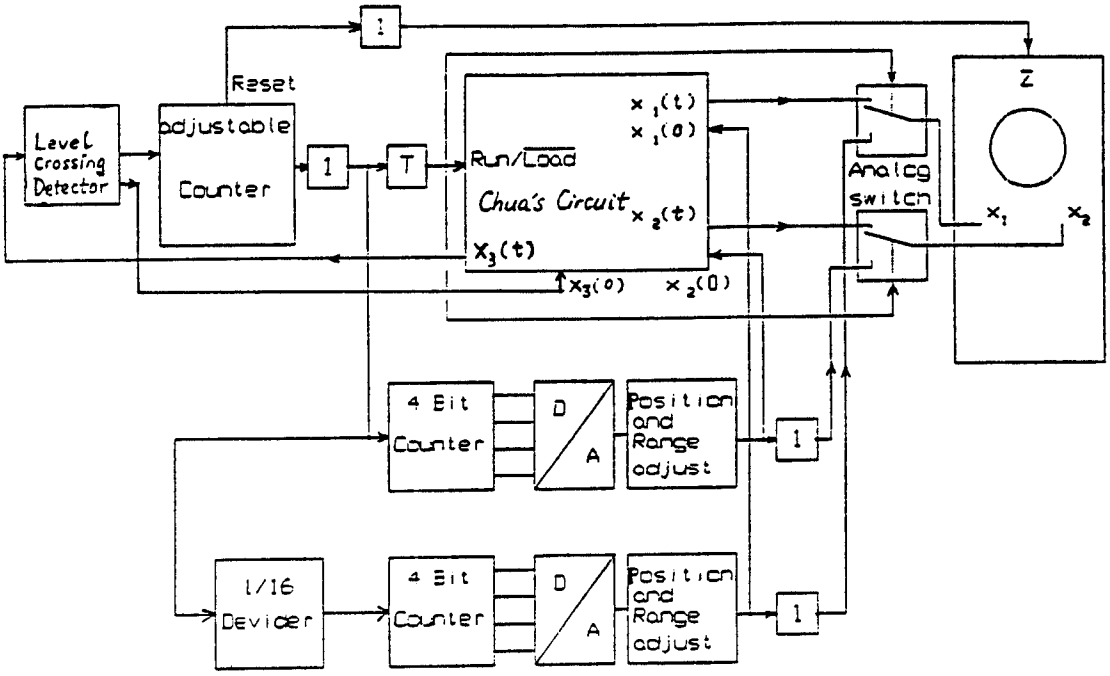

Fig. 2. Circuit for showing horseshoe map in Chua's circuit

4 Experimental Results

The experiments with the Chua's circuit and the circuit in Fig. 2 show that it is easy to find horseshoe maps. Fig. 3 shows an initial rectangle within the attractor area.

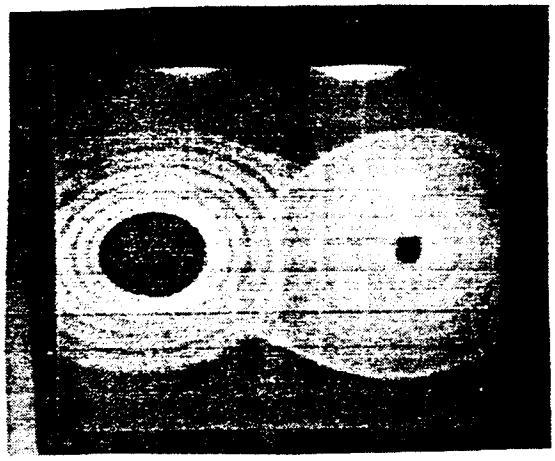

Fig. 3. An initial rectangle in the double scroll attactor

Fig. 4.(a)-(f) display the development of the first, second, $\cdots$, sixth return maps of that initial rectangle. In the sixth return map we see a clear horseshoe map.

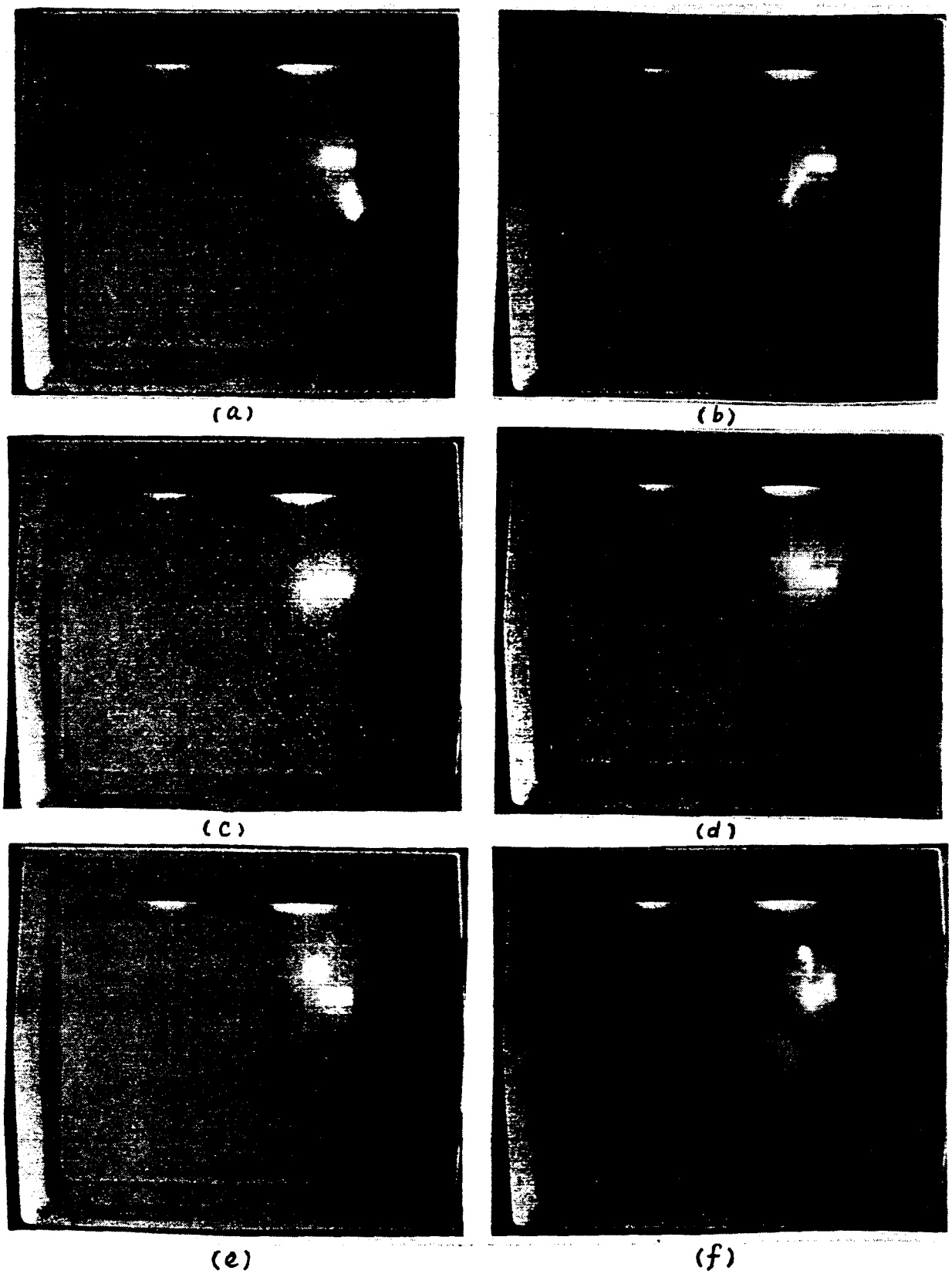

Fig. 4. Experimental results: Initial square and first (a) to sixth (f) return map

5 Conclusion

With this circuit it is possible to visualize the horseshoe map in nonlinear nonautonomous circuits having analog switches in order to load the initial voltages and then start the transient. The principle can also be applied to autonomous circuits. Experimental results show that visualization of horseshoe maps has been demonstrated with Chua's circuit successfully.

References

[1] A. Mees and C. Sparrow, "Some Tools for Analyzing Chaos", Proceedings of the IEEE, vol. 75, pp 1058-1070, Aug.1987.

[2] F. Zou and J. A. Nossek, "A chaotic attractor with cellular neural networks", IEEE Trans. Circuits Syst., vol. 38, July 1991.

[3] F. Zou, Pletl and J. A. Nossek, "A Circuit for Real-time Horseshoe Visualization", to appear in IEEE Trans. Circuits Syst.

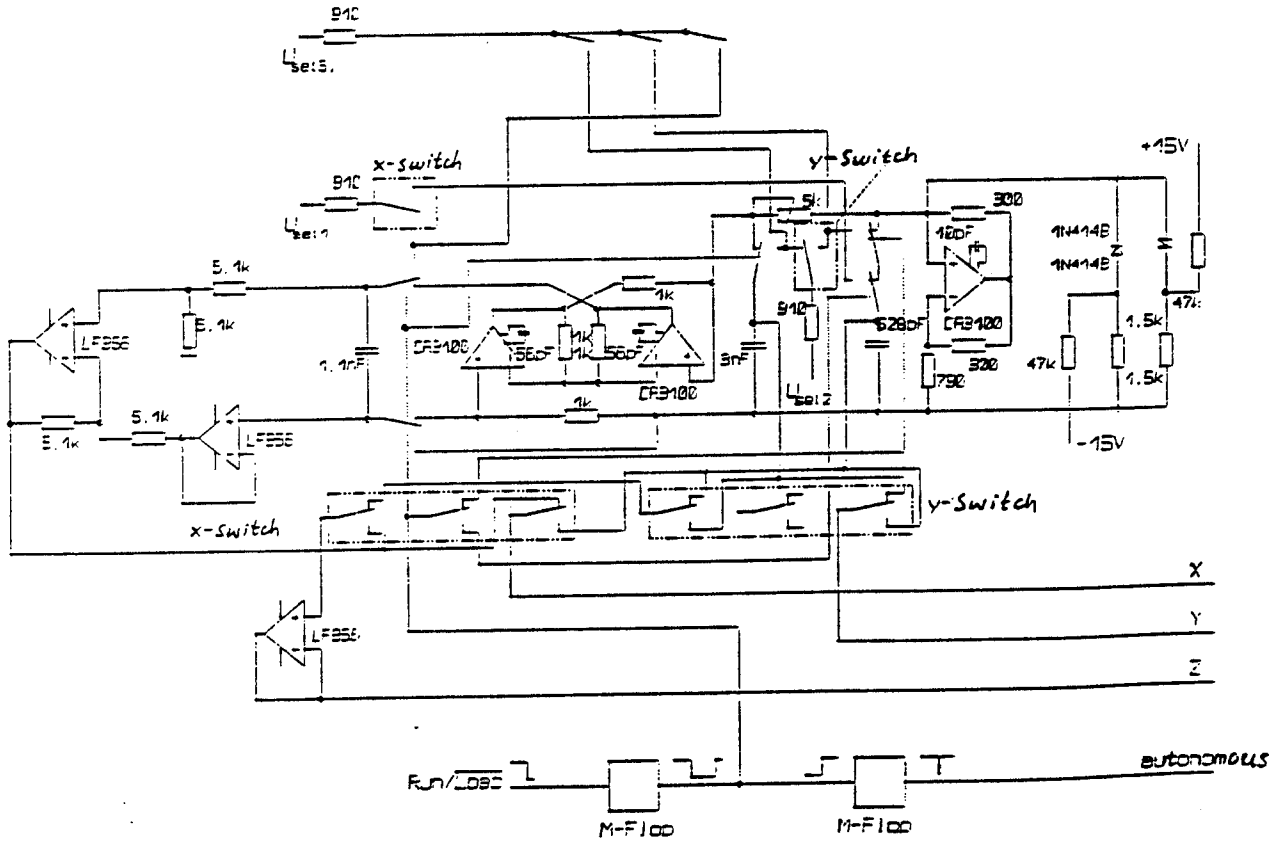

Fig. 5. The Chua's circuit in gyrator realization

1993 International Symposium on Nonlinear
Theory and Its Applications (NOLTA '93)
Hawaii, U.S.A., December 5-10, 1993

APPLICATIONS OF CHUA'S CIRCUIT TO SOUND, MUSIC AND MUSICAL INSTRUMENTS

Xavier Rodet[1], IRCAM, 31 r. St- Merri, 75004 Paris, France
tel: (1) 44 78 48 68, fax: (1) 42 77 29 47, email: rod@ircam.fr

Abstract

Models of the excitation mechanism of sutained musical instruments are studied in terms of nonlinear dynamics. We focus on passive linear systems coupled to nonlinear oscillators. A clarinet-like model is proposed and recognized as similar to the time delayed Chua's circuit. Results are given concerning the role of the memoryless nonlinearity and of the linear element in single feedback loop systems. Implementations, real-time simulations and sound results are discussed.

1. Introduction

We examine here models of the excitation mechanism of sutained musical instruments, such as strings, brass, reeds, flutes and voice [1], [2] in terms of nonlinear dynamics. One of the goals of our work is sound synthesis by computers for musical applications. Beyond the strict imitation of a specific instrument, the aim is to provide new *simulated instruments* with extended properties, such as a broader range of sounds, improved playability and other properties sought by musicians. For a musical use of instrument models, typical problems are stability, periodic trajectories, transient behavior, ease of control (according to the relations between control parameter values and sound characteristics) and influence of the linear and nonlinear components. Finally we look for a rather general model of several instruments with good behavioral and control characteristics.

2. Passive Linear Systems Coupled to Nonlinear Oscillators

Seen from the mouthpiece, the bore of a clarinet appears roughly as a delay line with a sign inversion reflection at the other extremity, and some low pass filtering with impulse response h. The corresponding delay τ or some related period is responsible for the pitch played by the instrument. The basis of the oscillatory behavior is to be found in the coupling of the passive linear part with the nonlinear reed. For string instruments the main delay comes from transverse waves travelling back and forth along the string. The bow-string interaction is represented by the nonlinear velocity-force function. Let $x, \gamma, h: R \rightarrow R$, $\tau \in R$, γ be nonlinear and * be the convolution operator. These instruments can be described by autonomous retarded functional equations such as:

$$x(t) = h * \gamma(x(t-\tau)) \qquad (1)$$

3. Example: the reed of a clarinet-like instrument coupled to the bore

Following [3], let us call q_o and q_i the outgoing and incoming pressure waves in the bore respectively, p the pressure in the player's mouth and z the characteristic impedance of the bore. The system can be described in a simplified way by the equations:

$$q_o(t) - q_i(t) = zF(q_i(t) + q_o(t) - p(t)),$$

$$q_i(t) = r(t)*q_o(t) = h(t)*q_o(t-\tau)$$

where $h(t-\tau)=r(t)$ is the *reflection function* of the bore. The most important assumption here is that the reed has no mass, leading to a *memoryless* nonlinearity F. In the case where this system has a

[1] Research done partly at CNMAT, University of California, Berkeley, CA 94709

unique solution, we obtain a very simple model to explain the basic oscillatory behavior of the reed in a clarinet-like instrument (Fig. 1):

$$q_0 = \gamma(h*q_0(t-\tau)).$$

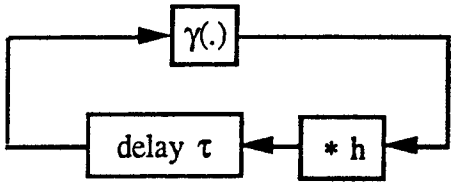

Fig. 1. The simplest clarinet-like model

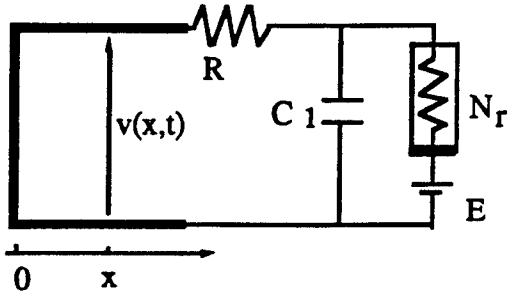

Fig. 2. Time delayed Chua's circuit

4. Chua's circuits

The time-delayed Chua's circuit [4] is shown in Fig. 2. In a first simplification, the slopes m_0 and m_2 of the characteristic of N_r (Fig. 3) are set equal to each other. With $C_1=0$, the solution consists of the sum of an incident wave a(t-x/v) and a reflected wave b(t+x/v) such that:

$$a(t-x/v) = -b(t-x/v) = u(t-x/v),$$

$$u(t) = \gamma(u(t-2T)),$$

where T is the time delay in the transmission line and γ is a piecewise linear 1-D function. This is the same delay-equation that we have obtained for the basic clarinet model, except for the filter h which we will examine later.

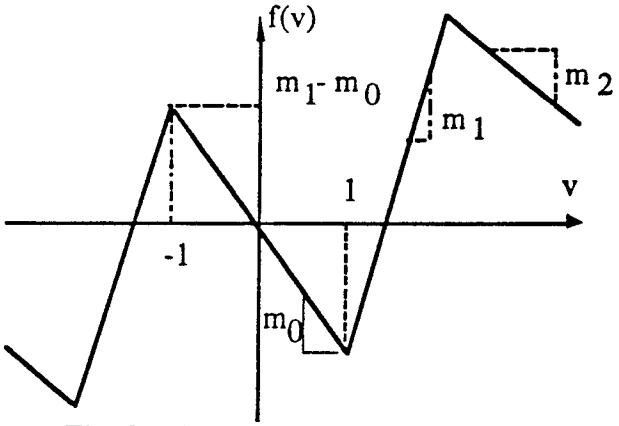

Fig. 3: Chua's diode characteristic

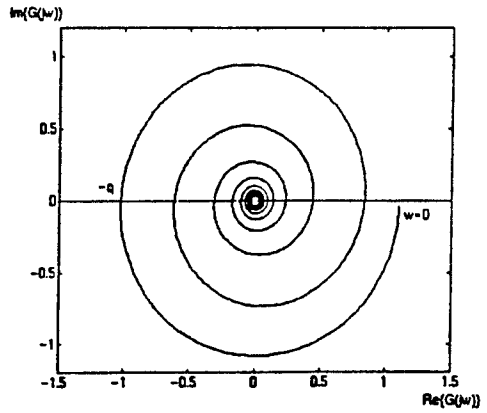

Fig. 4: Nyquist plot of G(jω).

By a proper affine change of variable, for certain parameter values, the function γ is composed of two segments only in the invariant interval with slopes s_1 and s_2. In this case the time-delayed Chua's circuit exhibits a remarkable period-adding and chaos phenomenon (see Figure 11 of [4]). In the (s_1, s_2) space, regions are found where the system has either stable limit cycles with period equal respectively to 2, 3, 4, etc.... or chaotic behavior. From the point of view of sound synthesis, this is very interesting [5]. Period adding corresponds to successively lowering the pitch. In the case of chaos, the signal sounds like noise added to a periodic tone of the instrument but with a relation between partials and noise.

The existence of several stable solutions, as in natural instruments can be a serious inconvenience for an electronic instrument. We look for a system which would model the usual playing behavior of an instrument but could avoid other solutions if requested to do so. The requirement of a low pass filter *above the oscillation frequency* appears in the describing function method [6] and in the Hopf Theorem (see section 5) which gives sufficient conditions for oscillation and *unicity* of the solution. The linear part of Chua's circuit [7], [8], [9], for some parameters values at least, can be viewed as a low pass filter above the frequency of a pair of conjuguate poles. This frequency is approximately equal to the oscillation frequency. Chua's circuit also appears as a model of an acoustic instrument where the feedback loop is limited to the first mode or the dominant mode. It is an example of a model of the behavior in the normal playing of an instrument which can easily be constrained to have a unique periodic solution.

5. Single feedback loop systems with a memoryless nonlinearity

We define the class of single feedback loop systems of which we can easily determine stability and some oscillatory properties. Such a system is composed of a unique memoryless nonlinearity and a linear feedback loop which can include delays. The only restriction on the linear element G(s) is that its impulse response be *stable* [10], which is natural for physical instruments. Many musical models can be redesigned to fall into this class. Assume there is a fixed point at the origin where the slope of the nonlinearity $\gamma(.)$ is s_1. Since G(s) has no poles in the closed right half plane C_+, the *Graphical Stability Test* [10] is simplified: Consider the intersection points of the Nyquist plot of $G(j\omega)$ with the real axis. Let -q+j0 denote the point with the smallest value and let ω_q be such that $G(j\omega_q) = -q$ (Fig. 4). Then the system becomes unstable when $s_1 < -1/q$, indicating that the system could oscillate. A proof is provided by the following method.

The Graphical Hopf Theorem and its algebraic version [11] apply to a nonlinear multiple feedback loop system where the nonlinearity γ is C^4. It applies to rather sophisticated physical models of instruments [2], [12]. Even though it is straightforward, we will not state this theorem in detail since it is rather lengthy. We merely emphasize that it provides the existence, uniqueness and stability test of the periodic solution required for our application. However, other stable solutions may appear under more general playing conditions. For other instruments such as the trumpet, the nonlinearity seems to be *with memory*, and the previous reasoning does not apply.

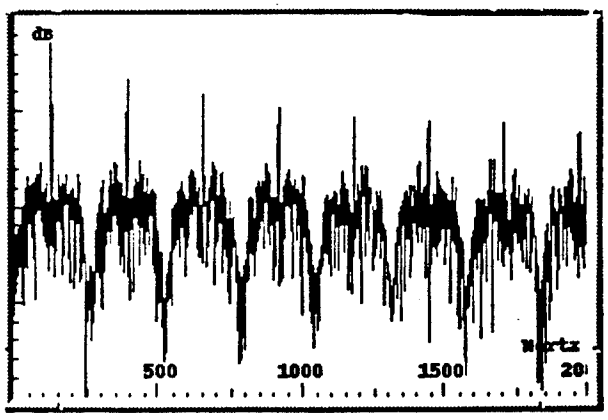

Fig. 5: Spectrum showing the simultaneous presence of sinusoidal components and noise.

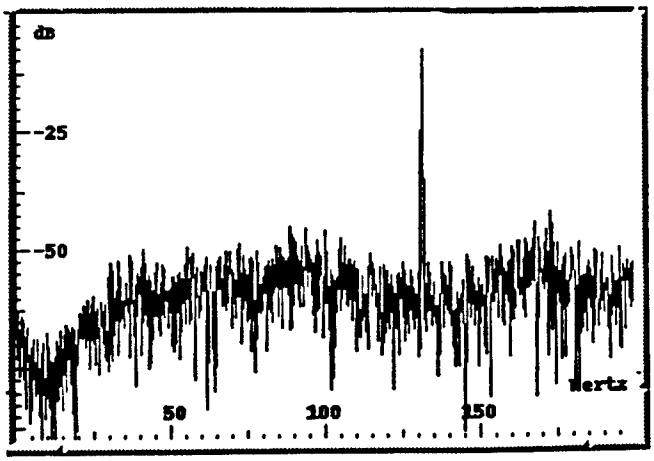

Fig. 6: Detail of Fig. 2 up to 200 Hz.

6. Some results on the role of the memoryless nonlinearity

Results of the time-delayed circuit with a piecewise-linear function γ without the filter h, and short-time spectra of signals are given in [5]. We observe the simultaneous presence of sinusoidal components and chaotic components (heard as *noise*) in the signal as displayed on Fig. 5 and 6.

The slope $|s_1|$ of the nonlinearity $\gamma(.)$ at the origin controls the *transient onset velocity*: the greater $|s_1|$, the faster the onset. If $h(t)=\delta$ the signal is a square wave. If h(t) is a low pass kernel, the signal may be *rounded*. The closer $|s_1|$ and $|s_2|$ are from 1, the less high the frequencies are in the signal. Therefore, two important characteristics of the sound, transient onset velocity and richness are controlled by $|s_1|$ and $|s_2|$. We have been led to the s_1-s_2 nonlinearity by considering the control of the basic instrument. It is the same nonlinearity as in the Time Delayed Chua's circuit [4]. But the piecewise-linear function has a drawback. At the onset of the signal, i.e. in the transient from zero, before a certain amplitude is reached, only a linear part of γ is used. There is no change in the short time spectrum of the signal other than amplitude growth. On the contrary, the nonlinearity of a real reed can be more realistically approximated by a quadratic function [13]. During the transient there is a constant transfer of energy between frequency components. As a consequence, we may as well use another one, e.g. a quadratic or cubic nonlinearity such as $\gamma(x)= ax^2+s_1x$.

Without the filter h, when the system has a limit cycle with period-2, the limit cycle x(t) has the symmetry $x(t+\tau) = -x(t)$, i.e. has no even harmonics. This result generalizes to any region with period k=3, 4, etc. In such a region the system has a limit cycle x(t) the harmonics (k, 2k, 3k etc...) of which are absent [14]. This is also a rather interesting result from a musical point of view.

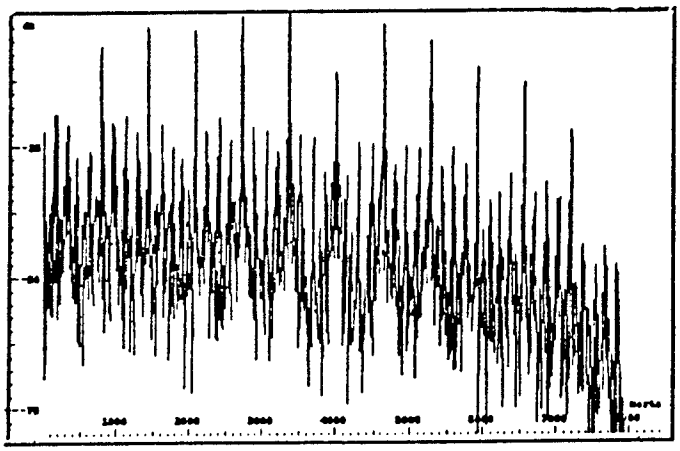

Fig. 7: Spectrum of signal with complicated structure.

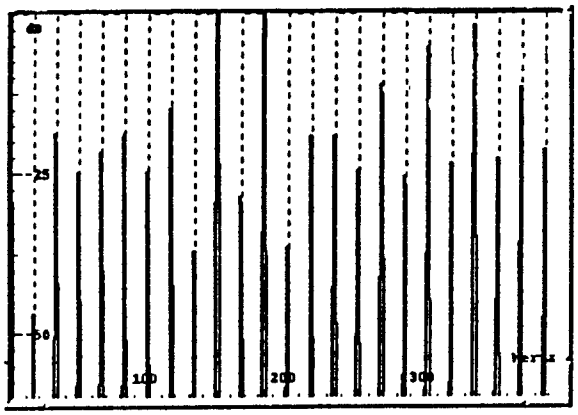

Fig. 8: Detail of Fig. 16 up to 400 Hz

7. First results in presence of the linear element

With the linear element h in the loop, the solutions to equation (1) and their stability are known only partially and in restricted cases (see for example [15], [16], and [17]). Chow et al. [15] consider a particular h and particular odd functions $\gamma \in C^2$. They prove that the equation (1) has a stable period-2 solution composed of odd harmonics only. This is an interesting result since it corresponds to the usual playing periodic solution of a clarinet. However we feel the need for a more general result since we show in section 8 that the odd nature of γ and the odd-harmonicity of the solution are in some way *non-generic*. Ivanov and Sharkovsky [16] consider the solutions to a singularly perturbed delay equation which is somehow a special case of equation (1):

$$ax'(t) + x(t) = \gamma(x(t-\tau)) \qquad (2)$$

Ivanov and Sharkovsky give very interesting results for (2), but the term x'(t) is a rather severe limitation compared to the filtering by a more general impulse response h.

8. Role of the linear element in single feedback loop systems

Let the open-loop transfer function be $G(j\omega)=H(j\omega)\, e^{-j\omega\tau}$. Suppose for the moment that $H(j\omega)$ is real positive. Then the intersection of $G(j\omega)$ with the negative real axis occurs for $\omega_k\tau=\pi+2k\pi$, i.e. for the modes of the instrument. The frequency $f_0 = 1/2\tau$ corresponds to the delay 2τ necessary for a sound wave to propagate from the reed to the end of the bore and back. Therefore, $G(j\omega_q)$ and $\omega_q/2\pi$ can be simply interpreted as the amplitude and the frequency of the strongest mode of the instrument[2]. The frequencies f_k are the odd harmonic partials of the fundamental f_0, but the oscillation frequency may be different from f_0. Assume now that the argument of $G(j2k\omega_q)$ is different from zero. Then the modes can be moved away from harmonic positions.

In our experiments we have observed that when simultaneously γ is not odd symmetric and there is a filter h, then even partials can appear. A very slight breaking of the symmetry of γ is sufficient. Therefore the results of Chow et al. [15] are of little applicability in our case, since natural instruments will not have perfectly odd-symmetric nonlinearities. Finally, it seems also that when γ is close to odd symmetry, the even harmonic partials are of small amplitude (such as with the clarinet) if the argument of $G(j2k\omega_q)$ is zero, and can be of large amplitude (such as with the saxophone) when the argument of $G(j2k\omega_q)$ is different from zero. Surprising results can occur in this latter case: Fig. 7 and 8 display the spectrum of such a signal and show that a very low fundamental frequency (17 Hz) has been obtained even though the delay τ corresponds to a relatively high frequency (200 Hz.).

9. Some open questions concerning equation (1)

- How do we explore the behavior of the time-delayed circuit when a filter is introduced?
- With a finite dimensional dynamical system, we could modify the vector field out of the region used for *normal playing* in order to exclude other stable solutions. How can we obtain a similar result with an infinite dimensional system?
- What are the necessary and/or sufficient conditions for getting sinusoidal components and noise simultaneously as presented in section 6, and how do we control the ratio between them? The correlation between both components is also of interest.
- Can we find some caracteristics of the linear and nonlinear parts which would provide better control of the spectral content of the solution?
- Can we extend our result to systems *with memory*?

10. Digital simulation

For more flexibility, we have simulated the time-delayed Chua's circuit on a SGI workstation running in real-time using HTM [18]. Various graphs are displayed in real-time. The possibility of looking at the Short Time Fourier Transform in real-time is very useful for a better understanding of the system and of the role of the various parameters [5]. The structure of the periodic and chaotic regions in the (s_0, s_1) space, as displayed in Figure 11 of [4], is interesting from a sonic point of view. By listening to the sound of the circuit, one can determine these regions and their frontiers. This audification of the local properties of the space allows an easy determination of very complex structures which could eventually not be determined analitically.

---

[2] In the case of the trumpet for instance, the mouthpiece acts as a resonator wich boosts some modes with number greater than 1, thereby allowing an easy oscillation at the frequency of one of these modes [13].

11. Conclusion

In our study of the excitation of musical instruments from the point of view of a nonlinear oscillators, we have found a retarded functional equation (1) as the model of a large class of instruments. We have obtained precise conditions of oscillation, good control parameters, period stability and values, and the properties of the generated waveforms. We have implemented nonlinear oscillators in real time on a workstation with a graphic user interface allowing for an easy experimention of their properties and behaviors. However, many open questions remain concerning the very interesting solutions of the functional equation (1). This is due to the combination of the rich dynamics of the nonlinear map together with the number of states represented by the delay line

References

1. P. Cook, "A meta-wind-instrument physical model", *Proc. International Computer Music Conference*, San Jose, pp. 273-276, Oct. 1992.
2. X. Rodet & P. Depalle, "A physical model of lips and trumpet", *Proc. International Computer Music Conference*, San Jose, pp. 132-135, Oct. 1992.
3. M.E. McIntyre et al., "On the Oscillations of Musical Instruments", *JASA* 74 (5), Nov. 83
4. A.N. Sharkovsky, Yu. Mastrenko, Ph. Deregel, and L.O.Chua, "Dry Turbulence from a time-delayed Chua's Circuit", to appear in *Journal of Circuits, Systems and Computers*, Special Issue on Chua's Circuit: a Paradigm for Chaos, Vol. 3, No. 2, June 1993.
5. X. Rodet, "Sound and Music from Chua's Circuit",*Journal of Circuits, Syst. and Computers*, Special Issue on Chua's Circuit: a Paradigm for Chaos, Vol. 3, No. 1, pp. 49-61, March 1993.
6. A. R. Bergen & R. L. Franks, "Justification of the Describing Function Method", SIAM J. Control, Vol. 9, No. 4, pp. 568-589, Nov. 71.
7. L. O. Chua, M. Komuro and T. Matsumoto, "The Double Scroll Family", *IEEE trans. Circuits & Syst.*, Vol. CAS-33 (Nov. 1986) No. 11, pp 1073-1118.
8. L. O. Chua and G.-N. Lin, "Canonical Realization of Chua's Circuit Family", *IEEE trans. Circuits & Syst.*, Vol. CAS-37 (July. 1990) No. 7, pp 885-902.
9. L.O. Chua, "A zoo of strange attractors from the Chua's circuit", *Proc. 35th Midwest Symposium on Circuits and Systems*, Washington, D.C., August 9-12, 1992, pp. 916-926.
10. M. Vidyasagar, "Nonlinear System Analysis", Prentice Hall, 1978.
11. A. Mees & L. Chua, "The Hopf Bifurcation Theorem and Its Applications to Nonlinear Oscillations in Circuits and Systems", *IEEE Transactions on Circuits and Systems*, Vol. Cas-26, No. 4, April 1979, pp. 235-254.
12. D. Keefe, "Physical Modeling of Wind Instruments", *Computer Music Journal*, MIT Press, Vol 16 No. 4, pp. 57-73, Winter 1992.
13. N.H. Fletcher, T. D. Rossing, "The Physics of Musical Instruments", Springer Verlag, 1991.
14. X. Rodet, "Models of Musical Instruments from Chua's Circuit with Time Delay", to appear in IEEE Trans. on Circ. and Syst., Special Issue on Chaos in nonlinear electr. circts, Sept. 1993.
15. S. N. Chow & D. Green Jr., "Stability, Multiplicity and Global Continuation of Symmetric Periodic Solutions of a Nonlinear Volterra Integral Equation", Japan Journal of Applied Mathematics, Vol. 2, No. 2, pp. 433-469, Dec. 85.
16. A.F. Ivanov & A.N. Sharkovsky, "Oscillations in Singularly Perturbed Delay Equations", in *Dynamics Reported*, C.K.R.T. Jones, U. Kirchgraber & H.O. Walther editors, Springer Verlag, pp. 164-224, 1992.
17. J.K. Hale, "Dynamics and Delays", in Delay Diff. Equations and Dynamical Syst., Proc., 1990, S. Busenberg & M. Martelli (Eds.), Lect. Notes in Math. 1475, Springer Verlag, 1991.
18. A. Freed, "Tools for rapid prototyping of Musical Sound Synthesis Algorithms", *Proc. International Computer Music Conference*, San Jose, pp. 178-181, Oct. 1992.